

# **Tricycloquinazoline (TCQ) based electron deficient discotics and conjugated polymers with indenofluorene and bisfluorenylidene units**

Dissertation

zur Erlangung des akademischen Grades  
Doktor der Naturwissenschaften  
(Dr. rer. nat.)

in der Wissenschaftsdisziplin Makromolekulare Chemie

eingereicht im  
Fachbereich Chemie  
der Bergischen Universität Wuppertal

**Jitendra S. Kadam**

geb. am 09.07.1974  
in Tasgaon, India

Wuppertal, im Januar 2004

Die vorliegende Arbeit wurde in der Zeit von Oktober 1999 bis Januar 2004 am Max-Planck-Institut für Polymerforschung in Mainz, an der Universität Potsdam und an der Bergischen Universität Wuppertal unter der Anleitung von Herrn Prof. Dr. U. Scherf angefertigt.

Ich bedanke mich bei Herrn Prof. Dr. U. Scherf für die Überlassung des interessanten Themas dieser Arbeit, für seine stete Diskussionsbereitschaft sowie für seine persönliche Unterstützung.

*For my parents  
&  
Swapna*

*Jitendra*



*The Heights of Great men,  
Reached and kept,  
Were not attained by the sudden flight,  
But they,  
When their companions slept,  
Were toiling upwards in the night.*

*.....Napolean Hill*

# Contents

|          |  |           |
|----------|--|-----------|
| <b>1</b> | <b>MOTIVATION &amp; OBJECTIVE .....</b>  | <b>1</b>  |
| 1.1      | MOTIVATION .....   | 1         |
| 1.2      | OBJECTIVE .....  | 2         |
| <b>2</b> | <b>INTRODUCTION.....</b>   | <b>4</b>  |
| 2.1      | TRICYCLOQUINAZOLINE (TCQ) BASED ELECTRON-DEFICIENT DISCOTICS .....   | 4         |
| 2.2      | DISCOTIC LIQUID CRYSTALS .....   | 5         |
| 2.3      | TRICYCLOQUINAZOLINE (TCQ) BASED DISCOTIC LIQUID CRYSTALS .....   | 8         |
| 2.4      | APPLICATIONS OF DISCOTIC LIQUID CRYSTALS .....   | 9         |
| 2.5      | INDENOFUORENE AND 9,9'-BISFLUORENYLIDENE BASED CONJUGATED POLYMERS .   | 10        |
| 2.5.1    | <i>Poly(indeno[1,2-b] fluorene) PIF:</i> .....   | 10        |
| 2.5.2    | <i>9,9'-Bisfluorenylidene</i> .....  | 12        |
| 2.6      | ORGANIC FIELD-EFFECT TRANSISTORS (OFETs) .....   | 14        |
| 2.6.1    | <i>Thin-Film Transistors (TFTs)</i> .....  | 15        |
| 2.6.2    | <i>Operation of the Thin-film field-effect transistor</i> .....  | 16        |
| <b>3</b> | <b>RESULTS AND DISCUSSION.....</b>   | <b>18</b> |
| 3.1      | SYNTHESIS OF ELECTRON-DEFICIENT TCQ DERIVATIVES .....  | 18        |
| 3.2      | CHARACTERIZATION OF TCQ BASED DISCOTIC MOLECULES .....   | 26        |
| 3.3      | SYNTHESIS OF INDENOFUORENE AND BISFLUORENYLIDENE-BASED<br>CONJUGATED POLYMERS .....  | 34        |
| 3.3.1    | <i>Low Bandgap Conducting Polymers</i> .....   | 34        |
| 3.3.2    | <i>Poly(indeno[1,2-b-]fluorene) PIF</i> .....  | 36        |
| 3.3.3    | <i>Fluorenylene-endcapped poly(indeno[1,2-b]fluorene) PIF</i> .....  | 43        |
| 3.3.4    | <i>Absorption properties of fluorenylene-endcapped<br/>poly-(indeno[1,2-b]fluorene)</i> .....  | 45        |
| 3.3.5    | <i>Fluorenylene-endcapped PIF as active layer in ambipolar organic<br/>field effect transistors and inverters</i> .....              | 47        |
| 3.3.6    | <i>Synthesis of poly(indeno[1,2-b]fluorene) PIF / poly(para-phenylene-<br/>diphenylvinylene) DP-PPV statistical copolymers</i> ..... | 53        |
| 3.3.7    | <i>Absorption properties of PIF/DP-PPV statistical copolymer</i> .....   | 54        |
| 3.3.8    | <i>Novel conjugated polymers with the bisfluorenylidene (BFD) unit</i> .....   | 55        |
| <b>4</b> | <b>EXPERIMENTAL .....</b>  | <b>64</b> |
| 4.1      | INSTRUMENTAL DETAILS .....   | 64        |
| 4.2      | MONOMERS AND POLYMERS .....  | 66        |
| 4.2.1    | <i>2-Nitro-4,5-dimethoxybenzaldehyde 12</i> .....  | 66        |
| 4.2.2    | <i>5, 6-Dimethoxyanthranil 13</i> .....  | 67        |

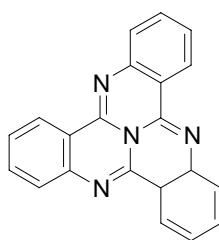
|           |   |            |
|-----------|---|------------|
| 4.2.3     | 2,3,7,8,12,13-Hexamethoxytricycloquinazoline 14.....  | 68         |
| 4.2.4     | 2,3,7,8,12,13-Hexaacetoxycycloquinazoline 16.....   | 68         |
| 4.2.5     | 2,3,7,8,12,13-Hexaalkoxytricycloquinazolines 17a-d.....   | 69         |
| 4.2.6     | 2,3,7,8,12,13-hexa-[(S)-3,7-dimethyloctyloxy]tricycloquinazoline 17a (S).....                                       | 70         |
| 4.2.7     | Racemic 2,3,7,8,12,13-Hexaalkoxytricycloquinazolines TCQ 17b.....   | 71         |
| 4.2.8     | 3,7-Dimethyl-1-octanol 37.....  | 72         |
| 4.2.9     | 3,7,11-trimethyl-1-dodecanol 38.....  | 72         |
| 4.2.10    | 1-Bromo-3,7-dimethyloctane 39.....  | 73         |
| 4.2.11    | (S)-3,7-dimethyloctylbromide 40.....  | 73         |
| 4.2.12    | 1-Bromo-3, 7,11-trimethyldodecane 41.....   | 74         |
| 4.2.13    | 2-Bromo-9-fluorenone 32.....  | 75         |
| 4.2.14    | 2,2'-Dibromo-9,9'-bisfluorenylidene (cis/trans-mixture) 33.....   | 76         |
| 4.2.15    | 2,5-Dibromo-4-methylbenzoic acid 18.....  | 76         |
| 4.2.16    | 2,5-Dibromo-terephthalic acid 19.....   | 77         |
| 4.2.17    | 1,4-Dibromo-2,5-bis(4-tert-butylbenzoyl)benzene 22.....   | 78         |
| 4.2.18    | 3,9-Di-tert-butyl-indeno[1,2-b]fluorene-6,12-dion 23.....   | 79         |
| 4.2.19    | 3,9-Di-tert-butyl-6,6,12,12-tetrachloro-6,12-dihydro<br>indeno[1,2-b]-fluorene 24.....                              | 80         |
| 4.2.20    | 1,4-Bis(phenyldichloromethyl)benzene 29.....  | 81         |
| 4.2.21    | Poly[9,9'-bisfluorenylidene-2,2'-diyl] 34.....  | 82         |
| 4.2.22    | Poly(1,4-phenylene-co-9,9'-bifluorenylidene-2,2'-diyl) 35.....  | 85         |
| 4.2.23    | Poly(2,5-dihexyl-1,4-phenylene-co-9,9'-bifluorenylidene-2,2'-diyl) 36.....  | 86         |
| 4.2.24    | Poly(3,9-di-tert-butylindeno[1,2-b]fluorene) 25.....  | 87         |
| 4.2.25    | Fluorenylene-end-capped poly(indeno[1,2-b]fluorene) PIF 27.....   | 88         |
| 4.2.26    | Statistical copolymers PIF/DP-PPV composed of indeno[1,2-b]fluorene<br>and phenylene-diphenylvinylene units 30..... | 89         |
| <b>5</b>  | <b>SUMMARY.....</b>   | <b>91</b>  |
| <b>6</b>  | <b>FUTURE RESEARCH.....</b>   | <b>95</b>  |
| <b>7</b>  | <b>LITERATURE.....</b>  | <b>96</b>  |
| <b>8</b>  | <b>LIST OF PUBLICATIONS.....</b>  | <b>103</b> |
| <b>9</b>  | <b>CURRICULUM VITAE.....</b>  | <b>104</b> |
| <b>10</b> | <b>ACKNOWLEDGEMENT.....</b>   | <b>105</b> |

# 1 Motivation & Objective

---

## 1.1 Motivation

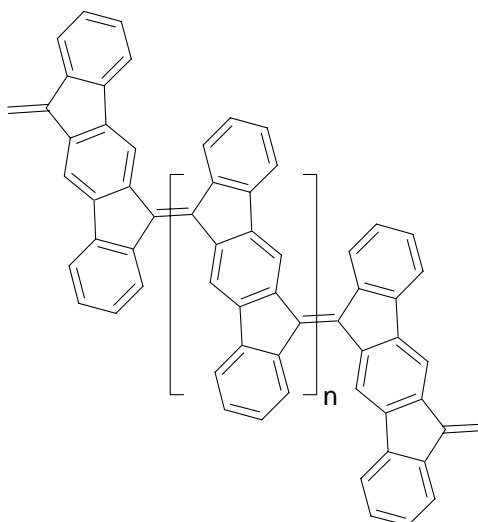
(a). TCQ based discotic liquid crystals are known to be attractive materials for potential applications in optical data storage and light emitting devices. Therefore, one starts thinking of easy and low cost methods to synthesize the compounds. It becomes relevant to synthesize derivatives with enhanced chemical stability as well as tailored electronic properties. Improved synthetic routes and enhanced materials properties may make these compounds suitable for commercial applications in optoelectronics and photovoltaics.



*Structure of Tricycloquinazoline (TCQ)*

(b) The study of novel low band-gap polyhydrocarbons, for example poly(indeno[1,2-b]fluorene) (PIF) is gaining high importance in the field of polymer science. Research has been done on various aspects, such as easy synthetic approaches, characterisation, applications etc. For studying these aspects the most important thing is to check the chemical stability. Low-band-gap polymers (e.g. PIF) often possess only limited stability against atmospheric influences like air, moisture and sunlight <sup>[1]</sup>. Efforts are being made to synthesize new derivatives of PIF with improved stability. Such polymers should be useful in designing novel active materials for organic field effect transistors (OFETs).





*Structure of PIF*

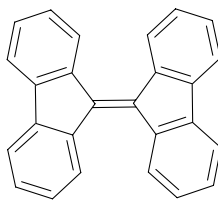
### 1.2 Objective

**Electron deficient discotics:** Literature studies show various routes for synthesis and characterization of TCQ based discotic liquid crystals. The aim of this work was to modify the thermal properties and to allow better processing. Introduction of a chiral side chain in the TCQ molecule was used to gain deeper insight into the solid state aggregation and LC mesophase formation.

**Indenofluorene and bisfluorenylidene (BFD)-based conjugated polymers:**

In our work we tried to synthesize novel “endcapped” poly(indeno[1,2-b]fluorene) derivatives, statistical copolymers containing the indeno[1,2-b]fluorene unit, and novel polymers containing the 9,9'-bisfluorenylidene unit. Our aim was to increase the chemical stability of such polymers, to get an exact molecular weight control, and to modify the optical and electronic properties. Some materials should be tested as active layers in organic field effect transistors (OFETs), especially to obtain ambipolar transistors which allow charge carrier transport both in the *p*- and *n*- channel <sup>[2]</sup>.

The 9,9'-bisfluorenylidene (BFD) unit is the main structural motif of poly(indeno[1,2-b]fluorene). BFD is an electron deficient moiety and can be easily reduced (n-type character).



*Structure of BFD*

It was therefore interesting to synthesize novel conjugated polymers containing the 9,9'-bisfluorenylidene unit.

## 2 Introduction

---

### 2.1 Tricycloquinazoline (TCQ) based electron-deficient discotics

The development of materials and devices such as tools or machines has been one of the most important driving forces for humanity and mankind. The development process, from the actual invention to the real application, often took centuries. In 1839, the French experimental physicist *Edmund Becquerel*, discovered the photovoltaic effect while experimenting with an electrolytic cell made up of two metal electrodes placed in an electrically conducting solution; the current increased when exposed to light <sup>[3]</sup>. In 1905, *Albert Einstein* speculated that light could penetrate atoms. The collision of photons and atoms could force electrons to leave their orbit. This would allow for the creation of an electric current. Nevertheless, it was not until 1954 when scientists at Bell Labs developed the first solar cell in the USA <sup>[4]</sup>. It was the development of smaller and smaller growing integrated circuits that, *for example* made it possible to build faster and more compact computers. *Shockley, Brattain*, and *Bardeen* were awarded the Nobel Prize in 1956 for their research on Field Effect Transistors (FETs) <sup>[5-7]</sup>. Many of today's leading scientists agree, that the invention of the transistor is probably one of the most important achievements of the 20 th century. The raw material that is most often used for building these devices, *i.e.*, photovoltaic cells and Field Effect Transistor is silicon. Silicon does not occur in its pure state in nature. Therefore, extensive efforts have to be made in order to obtain the material in its crystalline form. Within the last two decades, research interest has focused more and more also on electronic devices built from polymers or other organic materials. Around 1980, *Cohen* and co-workers reported the first solar cell using conducting polymers <sup>[6-8]</sup> and it was in 1989 that few groups reported the utilization of such polymers in FETs <sup>[9,10]</sup>. In addition, organic materials have found a number of other potential applications such as sensors, batteries, switching devices, and optical data storage. Unlike inorganic materials that consist of covalent or ionic

lattices in three dimensions, organic materials are based on individual molecules, which are linked together via weak intermolecular forces such as *van der Waals* and hydrogen bonds, or  $\pi$ - $\pi$  interactions. Moreover mesophase forming (self-assembling) molecules show great promise since they may be easier to process and may possess self-healing properties. It is because of these advantages that organic materials have led to so much research interest in the past. Due to the nature of self assembly, the design of the material can be made on the level of the individual molecule. Therefore, the amount of synthetic work can be considerably lower than in the case of inorganic materials such as crystalline silicon based materials. When organic materials are used in electronic or optoelectronic devices, they are usually in the form of thin films, due to which mesophase forming liquid crystals are being intensively studied.

### 2.2 Discotic liquid crystals

Liquid crystals represent a state between crystalline solids and isotropic liquids. Liquid crystal phases generally exhibit orientational, and can additionally show some positional order. However because they are less ordered than solids, liquid crystals also show properties like fluids.

On the basis of their appearance, liquid crystals are divided into two different classes,

- Calamitic mesogens characterized by rod like shape of the molecules which allow closer packing in a mesophase.
- Discotic mesogens characterized by disc like core of the molecules.

An important subclass of liquid crystals are **discotic liquid crystals** (discotic mesogens). The disc-shaped molecules that comprise these phases are capable of stacking on top of one another to form so called **columnar mesophases** (shown schematically below in Figure 1) While the molecules within each column can be ordered with respect to one another, there is no positional correlation between the molecules in different columns.



**Fig. 1:** *Stacking of columnar mesophases*

The cores which are aligned in columns are surrounded by side chains. These columns can be arranged in various ways, e.g. in a hexagonal ( $\text{Col}_h$ ), rectangular ( $\text{Col}_r$ ), or oblique lattice ( $\text{Col}_{ob}$ ), etc. (Figure 5).

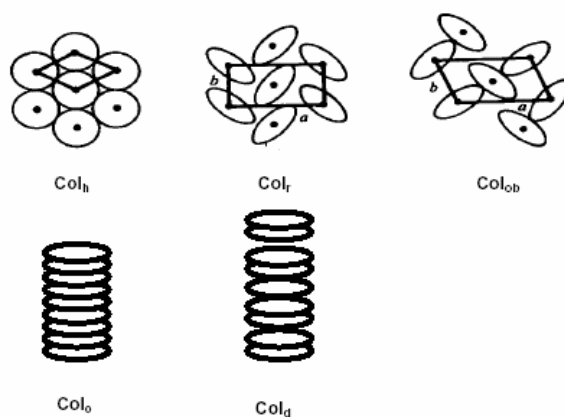


**Fig. 2:** *Structures of columnar mesophases*

Additionally, the suffix “o”  $\text{Col}_o$  (for ordered) and “d”  $\text{Col}_d$  (for disordered) can indicate the degree of organisation in the individual column (figure 1). Apart from a few exceptions, these discotic mesogens are built of a flat or nearly flat core, which is surrounded by four, six, or eight flexible side chains. In figure 2, some of the most prominent core fragments which form discotic liquid crystals are displayed. These range from the first reported discotic liquid crystals forming compound hexaacyloxybenzene **1**, to octaalkylphthalocyanines <sup>[12, 13]</sup> **2**, perylene tetracarboxydimides <sup>[14-16]</sup> **3**, triphenylenes <sup>[17-21]</sup> **4**, hexa(thioalkoxy)tricycloquinazoline <sup>[35]</sup> **5**, and hexaalkoxydibenzopyrenes <sup>[19]</sup>,

22, 23] **6**. The later two (**4** and **6**) belong to the class of polyaromatic hydrocarbons (PAHs) [38].

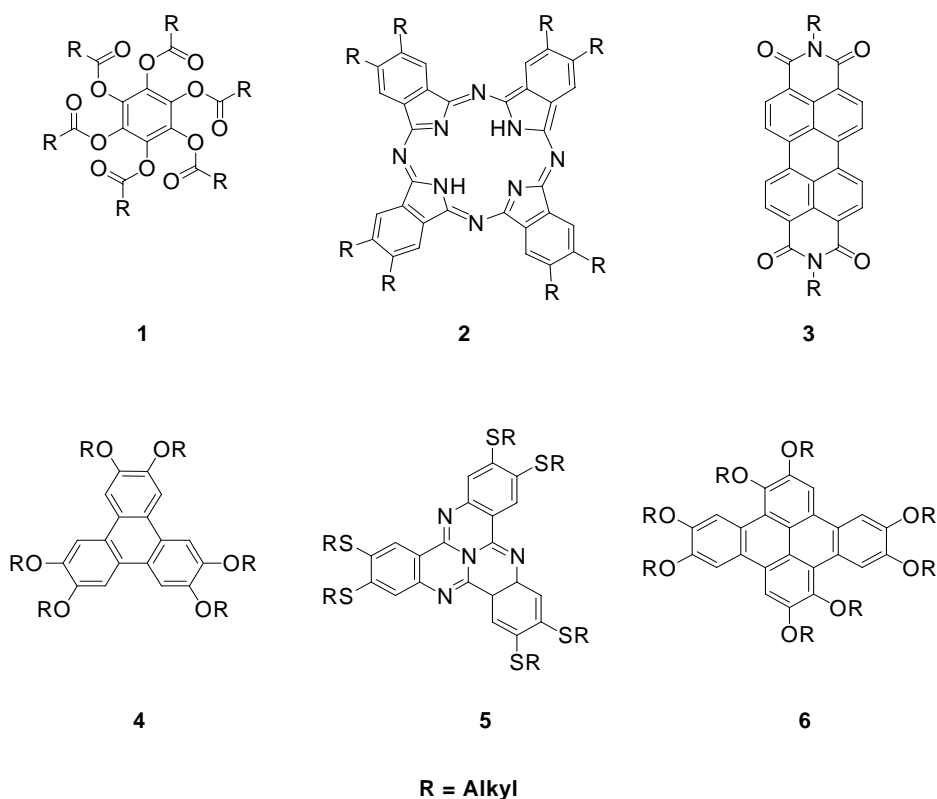


**Fig. 3:** Formula of some of the most prominent compounds which forms discotic liquid crystals

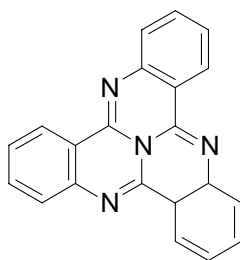
Perylene tetracarboxydimides **3** are well-known chromophores, which combine high extinction coefficients, and nearly quantitative fluorescence quantum yields with outstanding photochemical and thermal stability [15-16]. However, the unsubstituted core suffers from its low processability. This was partially solved with the introduction of solubilizing side groups at the imide nitrogens, yielding perylene derivatives that exhibit discotic liquid crystallinity over temperature ranges of up to 200°C [15]. These materials combine several attractive properties:

- i) stable mesophases over large temperature ranges,
- ii) high thermal and photochemical stability and
- iii) intense absorption at long wavelengths [15].

Among the above mentioned liquid-crystalline PAHs, triphenylenes **4** are the ones that have been studied most extensively in view of the mechanism of charge transport <sup>[39-41]</sup>, one-dimensional energy transport <sup>[42-43]</sup>, photoconductivity <sup>[44-49]</sup>, ordering in multilayers (generated by the Langmuir-Blodgett technique) <sup>[50]</sup> and, orientation of two-dimensional crystals <sup>[51-52]</sup>

### 2.3 Tricycloquinazoline (TCQ) based discotic liquid crystals

In the last decades there has been an enormous development in utilizing liquid crystals (LCs) in different display devices <sup>[27]</sup>. More recently, discotic liquid crystals <sup>[28]</sup> have also been considered as new materials for one dimensional transport of charge and energy. Their potential applications in conducting, photoconducting, optical data storage, light emitting, and photovoltaic devices have been sought <sup>[29]</sup>.



**7**

**Fig. 4:** *Tricycloquinazoline (TCQ)*

TCQ **7** is a discotic molecule of both biological and physical interest which has been found to function as a core fragment for new family of discotic mesogens. It is formed in cyclization reactions of a number of anthranilic acid derivatives for example methyl anthranilate <sup>[30-31]</sup>. The wide occurrence of the later in plant materials and the ease of TCQ production from them by combustion have boosted an extensive study of the carcinogenic activity of TCQ <sup>[32]</sup>. The high carcinogenicity of TCQ is probably due to its ability to intercalate into DNA <sup>[32]</sup>, and points to a strong tendency to stacking and aggregation This may be

suggested by its high melting point and its columnar crystal structure. The heterocyclic TCQ molecule is attractive for many reasons: a) it possess  $C_3$  symmetry, b) its derivatives are coloured, c) it shows extraordinary thermal and chemical stability, d) it sublimates without decomposition under atmospheric pressure at very high temperatures, e) it tolerates strong oxidants such as chromic anhydride in concentrated sulphuric acid, f) it is highly resistant to biological oxidation and, g) it does not couple with diazotised aryl amines<sup>[30, 33]</sup>. The molecule exhibits intriguing physical characteristics, such as a low ionisation potential and interesting spectroscopic and electronic properties<sup>[34, 35]</sup>. Most of the known discotic liquid crystals are electron-rich systems, and therefore show a p-type charge transport within the columns. The electron-deficient nature of TCQ derivatives makes them suitable for an application as n-type semiconductors and for doping with electron donors. The first organic one-dimensional n-type semiconducting discotic LC based on TCQ has been recently reported by *Bushby et al.*<sup>[36]</sup>.

### 2.4 Applications of Discotic Liquid Crystals

Liquid crystals are nowadays very common in everyday life. The most important use as of today is in display devices (LCD). These are produced in huge numbers and used for various applications such as calculators, watches, mobile phones, or computer displays. These common LCDs are usually built of calamitic liquid crystals. A relatively small amount of research has so far been committed to the application of discotic liquid crystals, which were lately discovered in 1977. Discotic liquid crystals have some unique properties, which are starting to get exploited for commercial use. The most important aspect is the columnar, rather rigid stacking of the (aromatic) cores of the discs, surrounded by the flexible side chains. This geometry enables one-dimensional transport of charge within the columns. There is a huge anisotropy in conductivity between the dimension parallel to the column axis and those perpendicular to that, caused by the insulating effect of the alkyl or alkoxy side chains. The ratio of the conductivities (anisotropy) in these two directions is typically about  $10^3:1$ , but with special design this value can be increased up to



10<sup>9</sup>:1. At the moment there are two main commercial applications based on these properties. *Fuji* uses discotic liquid crystals to produce optical compensation films, which help to improve the viewing angle properties of LCDs. Discotic liquid crystals are also used by *Sanyo* to focus electron beams in electron beam lithographic processes. Another possible application could be a gas sensor. In a columnar liquid crystal phase (with homeotropic alignment), the conductivity in a direction perpendicular to the columnar axis is very low. (*“Homeotropic alignment is characterized by the director lying everywhere perpendicular to the liquid crystal cell walls.”*) Gas molecules are adsorbed on the surface of such a (free standing) film, some of the discs get tilted to some extent, greatly increasing the conductivity in the direction perpendicular to the columns. Optical data storage is yet another possible use of the discotic liquid crystal materials. A suitable laser beam activates a sample of planarly aligned (oriented) columns within the illuminated regions and induces homeotropic alignment. As the homeotropic areas do not exhibit birefringence when viewed through crossed polarizer filters, they can be distinguished from the birefringent non-illuminated areas, thus making it possible to write and store information using this technique. In order to develop new applications, the physical properties of discotic LCs have to be optimised. This can be done by using different structural patterns of the rigid core, and/or by introduction of different side chains. Ideally, the liquid crystal phases should be stable over a wide temperature range, including the desired temperature of the planned application <sup>[37]</sup>.

### **2.5 Indenofluorene and 9,9'-bisfluorenylidene based conjugated polymers**

#### **2.5.1 Poly(indeno[1,2-b] fluorene) PIF:**

Poly(indeno[1,2-b]fluorene) (PIF) has a main chain structure resembling a picket fence. This polymer has been first described by *Scherf and co-workers* in 1996 <sup>[47]</sup>. The unique cross-conjugated structure leads to a long wavelength absorption peak at a  $\lambda_{\text{max}}$  of ca. 800 nm (PIF, solution in chloroform).

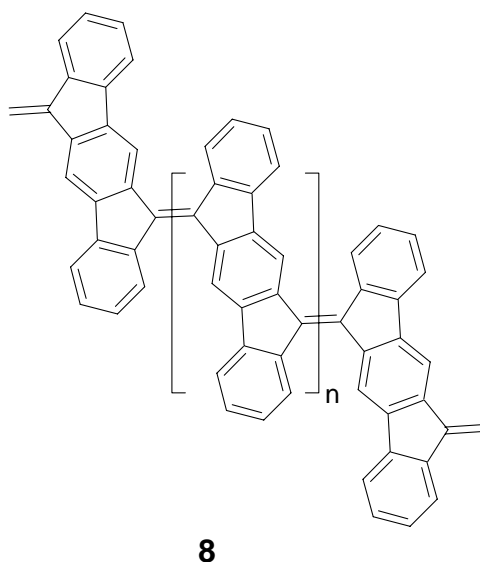
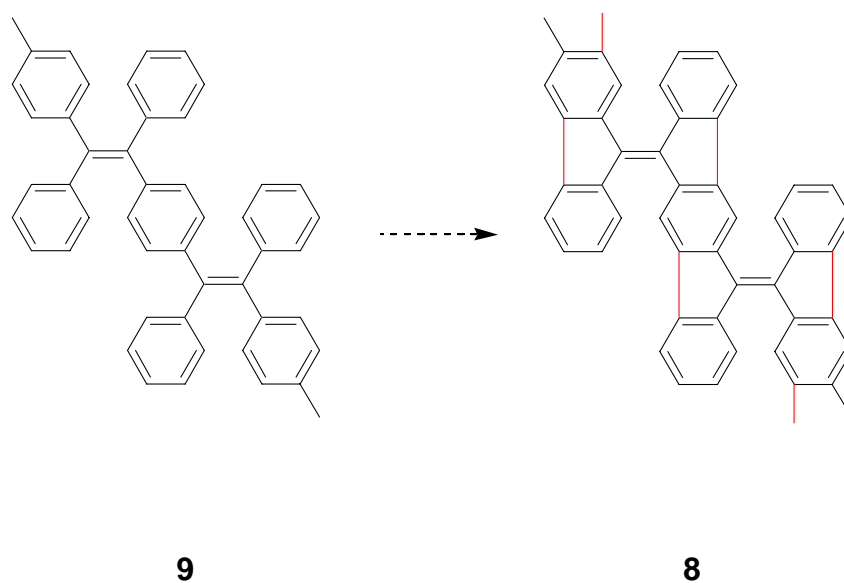


**Fig. 5:** Structure of PIF molecule

In 1977 *Hörhold* first described diphenyl substituted poly(1,4-phenylene vinylene) DP-PPV <sup>[48]</sup>. DP-PPV and its derivatives represent an intensively investigated classes of high bandgap conjugated polymers with intense solid state fluorescence <sup>[48]</sup>.

The introduction of the two additional aryl-aryl bonds (from DP-PPV to PIF, see scheme 1) is accompanied by a dramatic red-shift of the long wavelength absorption band from  $\lambda_{\text{max}} = 366$  nm (DP-PPV) to  $\lambda_{\text{max}} = 797$  nm (PIF)



**Scheme 1:** From DP-PPV to PIF

The geometry of this novel polymer PIF **8** is non-planar <sup>[47]</sup>, since there is a strong steric hindrance at the interring linking positions. 9,9'-Bisfluorenylidene which is a related model system of the interring connection of PIF **8** can form two different conformations, one with a mutual distortion of the planar fluorenylidene building blocks relative to the olefinic double bond, leading to a reduced double-bond character of the BFD molecule, and another with a geometric distortion within fluorenylidene subunits under formation of a “butterfly-like” conformation.

Poly(indeno[1,2-b]fluorene) PIF derivatives with their exocyclic double bonds at the 6- and 12-positions represent deeply colored chromophores. PIF **8** forms intensely blue solutions in halogenated hydrocarbons like methylene chloride, chloroform or tetrachloroethane, and in aromatic solvents.

Nonlinear optical (NLO) properties of oligomeric and polymeric structures containing  $\pi$ -electron conjugated chains have been of continuing interest. *Barry Luther-Davies and co-workers* measured NLO properties of poly(indeno[1,2-b]fluorene), PIF polymer <sup>[93]</sup>. Femtosecond pulses from a Ti-sapphire laser at 800 nm can induce saturation of the long wavelength absorption leading to strong NLO effects. Time resolved degenerate four-wave mixing (DFWM) and pump-probe-measurements on films of PIF show the presence of an oscillatory behaviour <sup>[93]</sup>.

### 2.5.2 9,9'-Bisfluorenylidene

9,9'-Bisfluorenylidene (BFD) was first made by distilling fluorene over lead oxide by *de la Harpe and van Dorp*, 1875 <sup>[49]</sup>. More research was done on various aspects of BFD by different research groups.

As said earlier in chapter 1, BFD is the central moiety, a model chromophore of poly(indeno[1,2-b]fluorene) PIF <sup>[50]</sup>.

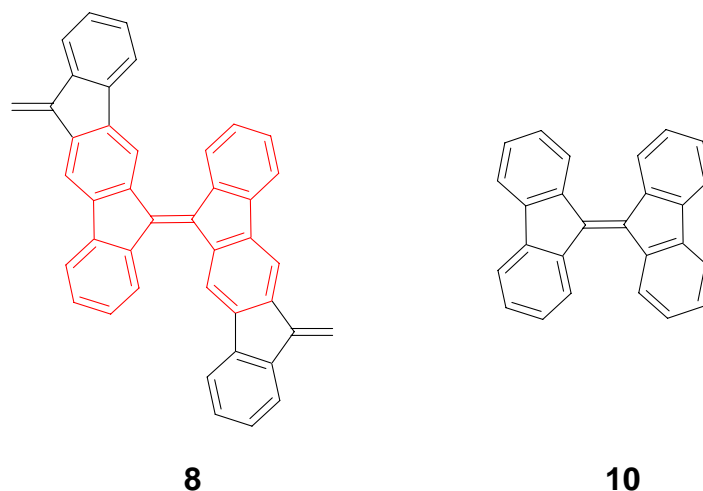


**Fig. 6:** 9,9'-Bisfluorenylidene **10** as a model building block of poly(indeno-[1,2-*b*]fluorene)

The 9,9'-bisfluorenylidene (BFD) chromophore is a highly overcrowded olefin and exists in one of the two possible conformations, the twisted or folded conformation, (as mentioned on page 14) resulting from repulsive interactions around the central double bond.

Planarity in the ground state conformations of overcrowded 9,9'-bisfluorenylidene is prevented by very strong non-bonded hydrogen-hydrogen interactions in the *fjord region* (figure 7) of the molecule. Usually two mechanisms, generally known as *twisting* and *folding*, are responsible for the release of strain in overcrowded alkenes.<sup>[53]</sup>

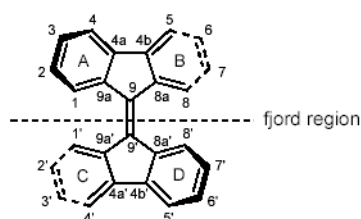


**Fig. 7:** 9,9'-Bisfluorenylidene

In the schematic drawings, depicted in figure 8, the structures are viewed along the central C9=C9' double bond. The lines represent the peripheral benzene

rings of the tricyclic moieties. These schematic projections are different from *Newman projections* of the double bond. In the folded structure the substituents at the central double bond are folded away from the plane defined by the double bond in a point-symmetric manner.

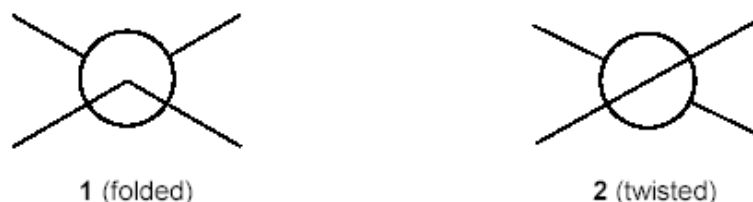


**Fig. 8:** Schematic ground state conformations of 9,9'-bisfluorenylidene. Projection along the central carbon-carbon double bond.

## 2.6 Organic field-effect transistors (OFETs)

The invention of the germanium transistor in 1947<sup>[100, 102]</sup> marked the birth of modern microelectronics, a revolution that has profoundly influenced our current way of life. This early device was actually a *bipolar transistor*, a structure that is mainly used nowadays in amplifiers. However logical circuits, and particularly microprocessors, preferentially use *field-effect transistors* (FETs), the concept of which was first proposed by Lilienfield in 1930<sup>[103]</sup>, but was not used as a practical application until 1960<sup>[104]</sup>. In a FET, the current flowing between two electrodes is controlled by the voltage applied to a third electrode. This operating mode recalls that of vacuum triode, which was the building block of earlier radio and TV sets and of the first electronic computers.

Single-crystalline silicon is the most widely used material in microelectronics. Other inorganic semiconductors are employed in applications where very specific properties are required, for example gallium arsenide in high-speed devices. However, electronic grade silicon is expensive, and is not suitable in devices where large areas are required, such as active matrix liquid crystal displays (LCDs), in which each pixel is monitored by one (three in the case of a color display) FET.

A field-effect in an organic semiconductor was first reported in 1970 <sup>[105]</sup>. However, it is only more recently that organic FETs (OFETs) have been made with attractive performances. The blossoming of OFETs apparently occurred soon after the discovery of conducting polymers (CPs), in the late seventies <sup>[106]</sup>. One of the most exciting properties of CPs is their ability to acquire a high conductivity upon doping and for many years CPs have been mainly investigated in their doped form as *synthetic metals*. However it appeared later that under their non-intentionally doped (often called *undoped*) form, CPs have semiconducting properties that could be potentially used in electronic devices (for this reason, the acronym CP now stands for either *conjugated* polymer or *conducting* polymer). The first polyacetylene OFET was reported in 1983 <sup>[107]</sup>, but the issue was really launched just four years later, with a polythiophene-based device <sup>[108]</sup>. Almost simultaneously small molecules <sup>[109]</sup>, and particular conjugated oligomers <sup>[110]</sup>, have also proven to be very promising organic semiconductors.

The basic idea of a field effect transistor (FET) is to modulate the current that flows in a conducting channel between two electrodes, the source and drain, by applying a voltage to third electrode, called the gate. Basically, the device can be viewed as a capacitor, where one plate contributes the conducting channel and other plate the gate.

### 2.6.1 Thin-Film Transistors (TFTs)

As indicated by its name, this architecture uses a very thin semiconducting layer. A TFT is an isolated gate device operating in the *accumulation* regime. The silicon wafers used in conventional microelectronics are fragile, relatively expensive, and their size is limited to that of the single-crystal ingot form which they are cut. In applications where large areas are required, other materials seem more appropriate, namely polycrystalline, amorphous or organic semiconductors, which are all characterized by a carrier mobility much lower than that of the crystalline inorganic semiconductors. The advantage of TFTs is that the semiconductor consists of a very thin layer even thinner than

the insulator. Secondly, source and drain are ohmic contacts directly formed on top of the thin semiconductor film <sup>[111]</sup>.

### 2.6.2 Operation of the Thin-film field-effect transistor

Thin-film field effect transistors (TFTs) can be considered as a parallel plate capacitor, where one conducting electrode, the gate electrode, is electrically insulated *via* an insulating (oxide) layer from the semiconductor layer (see figure 9). Two electrodes, the source and the drain, are contacted to the semiconductor layer. By applying a gate voltage,  $V_g$ , with respect to the source electrode, charge carriers can electrostatically be accumulated or depleted in the semiconductor at the semiconductor-insulator interface. Due to this field-effect the charge carrier density in the semiconductor can be varied. Therefore, the resistivity of the semiconductor, and hence the current through the semiconductor (upon application of a source-drain field), can be varied over orders of magnitude <sup>[99]</sup>. Since the TFT can be switched between a conducting and non-conducting state, it is widely used as the basic building block of binary logic <sup>[84]</sup>.

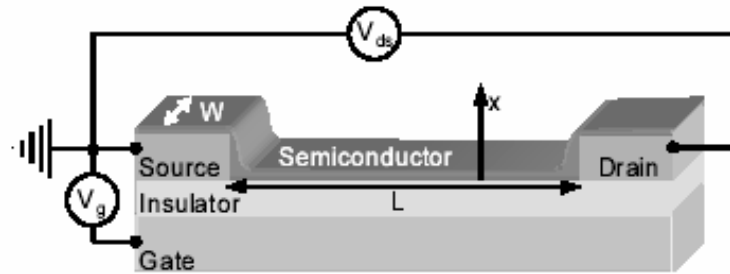


**Fig. 9:** Schematic of a thin-film field effect transistor(TFT)

The band-bending diagrams of a p-type transistor in the different operating regimes are schematically given in figure 10.

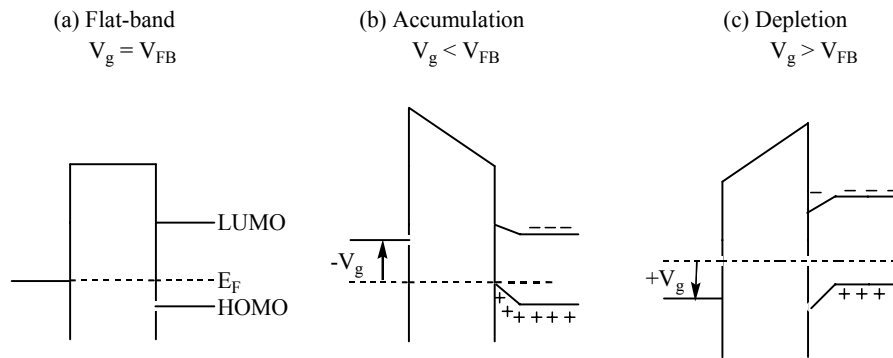


**Fig. 10 :** Energy level band diagram of an ideal metal-insulator-semiconductor device structure with a p-type semiconductor (a) flat band condition, (b) accumulation, (c) depletion.

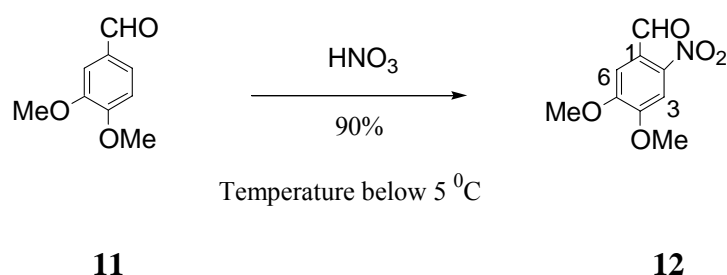
In equilibrium the Fermi levels of the materials align by charge carriers which move to or from the semiconductor-insulator interface. When a bias is applied which is equal to the difference between the Fermi levels of the gate metal and semiconductor, no band bending will occur in the semiconductor at the semiconductor-insulator interface, *i.e.* the energy bands in the semiconductor will be flat (see figure **10a**). This biasing condition is defined as the flat-band voltage. If the Fermi level of the electrode metal and the semiconductor are similar this flat-band voltage will be 0. For a p-type semiconductor, the application of a negative gate voltage will induce charges at the semiconductor-insulator interface (these charges are supplied by the source and drain contacts). In effect the Fermi level of the gate metal is varied with a value of  $qV_g$ , where  $q$  is the elementary charge, causing band bending in the semiconductor layer as schematically represented in figure **10b**. For a positive applied  $V_g$  the energy bands in the p-type semiconductor are bent downwards, and the mobile positive charge carriers are depleted from the semiconductor-insulator interface. In this case the transistor is biased in the depletion mode (see figure **10c**).



### 3 Results and Discussion

#### 3.1 Synthesis of electron-deficient TCQ derivatives

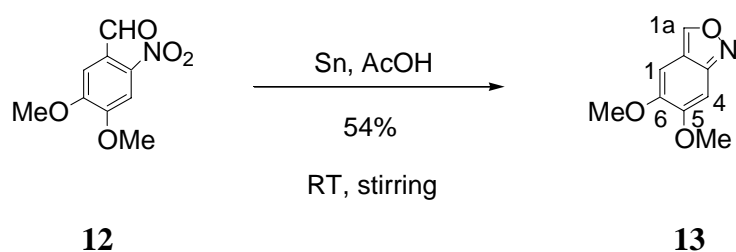
Synthesis of hexaalkoxy TCQ molecules started from the commercially available veratraldehyde (4,5-dimethoxybenzaldehyde). Veratraldehyde was converted to 2-nitroveratraldehyde (2-nitro-4,5-dimethoxybenzaldehyde **12**) in 90% yield by nitration at low temperature (Scheme 2).



**Scheme 2:** Synthesis of 2-nitro-4,5-dimethoxybenzaldehyde

2-nitro-4,5-dimethoxybenzaldehyde **12** was characterized by <sup>1</sup>H NMR-spectroscopy. We could see two aromatic singlet signals at 7.60 ppm (aromatic H3) and 7.41 ppm (aromatic H6) indicating a quantitative nitration of 4,5-dimethoxybenzaldehyde. The deshielded signal at 10.0 ppm shows the presence of an aldehyde group (-CHO). Sharp singlet at 4.01 ppm was seen for six protons of the methoxy groups.

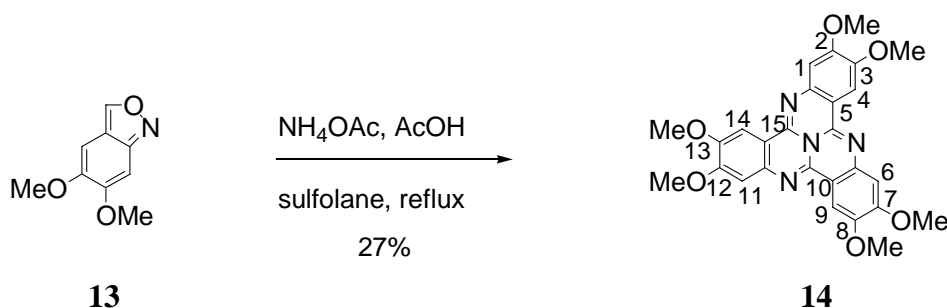
The next step is a partial reduction of 2-nitro-4,5-dimethoxybenzaldehyde using tin foil (in small pieces) in glacial acetic acid at room temperature to produce 5,6-dimethoxyanthranil in about 54% yield (Scheme 3).



**Scheme 3:** Synthesis of 5,6-dimethoxyanthranil

From  $^1\text{H}$  NMR-spectroscopy, 5,6-dimethoxyanthranil **13** shows a deshielded singlet signal at 8.79 ppm for H1a. Aromatic proton H4 and the three protons of –OMe in 5-position show singlets at 6.76 ppm and 3.94 ppm respectively, which are more deshielded than those of the aromatic proton H1 (6.62 ppm) and methoxy protons in 6-position at 3.88 ppm.

Although much less reactive than the more electron-deficient anthranil<sup>[38]</sup>, 5,6-dimethoxyanthranil **13** can be successfully trimerized in the presence of ammonium acetate in refluxing sulfolane to produce hexamethoxytricycloquinazoline **14** in moderate yield of only 27 % (Scheme 4).

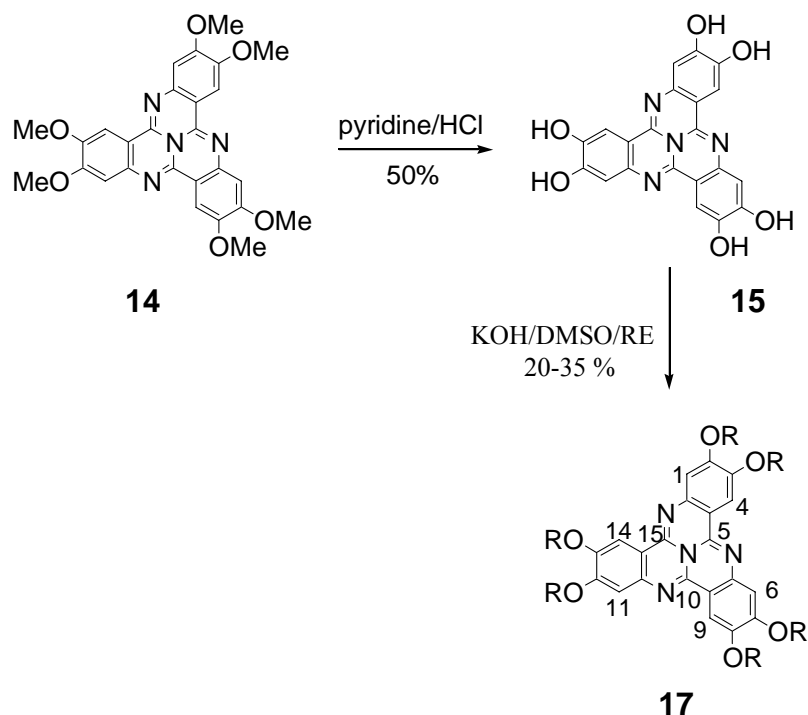


**Scheme 4:** Synthesis of Hexamethoxytricycloquinazoline

Hexamethoxy TCQ **14** shows a downfield proton  $^1\text{H}$  NMR-spectroscopy singlet signal at 7.61 ppm for three aromatic protons (H4, H9, H14). Singlet signal at 6.82 ppm is for the other aromatic protons (H1, H6, H11). 18 protons from –OMe groups show singlets at 3.99 ppm (s, 9H, -OMe) and 3.96 (s, 9H, -OMe), respectively.

$^{13}\text{C}$ -NMR spectroscopy shows 8 signals, 7 of non-equivalent aromatic carbons of the central core ( $\delta$ : 164.4, 150.7, 147.6, 143.9, 119.7, 113.2, 108.7 ppm) and a signal at 58.1 ppm for the 6 –OMe groups.

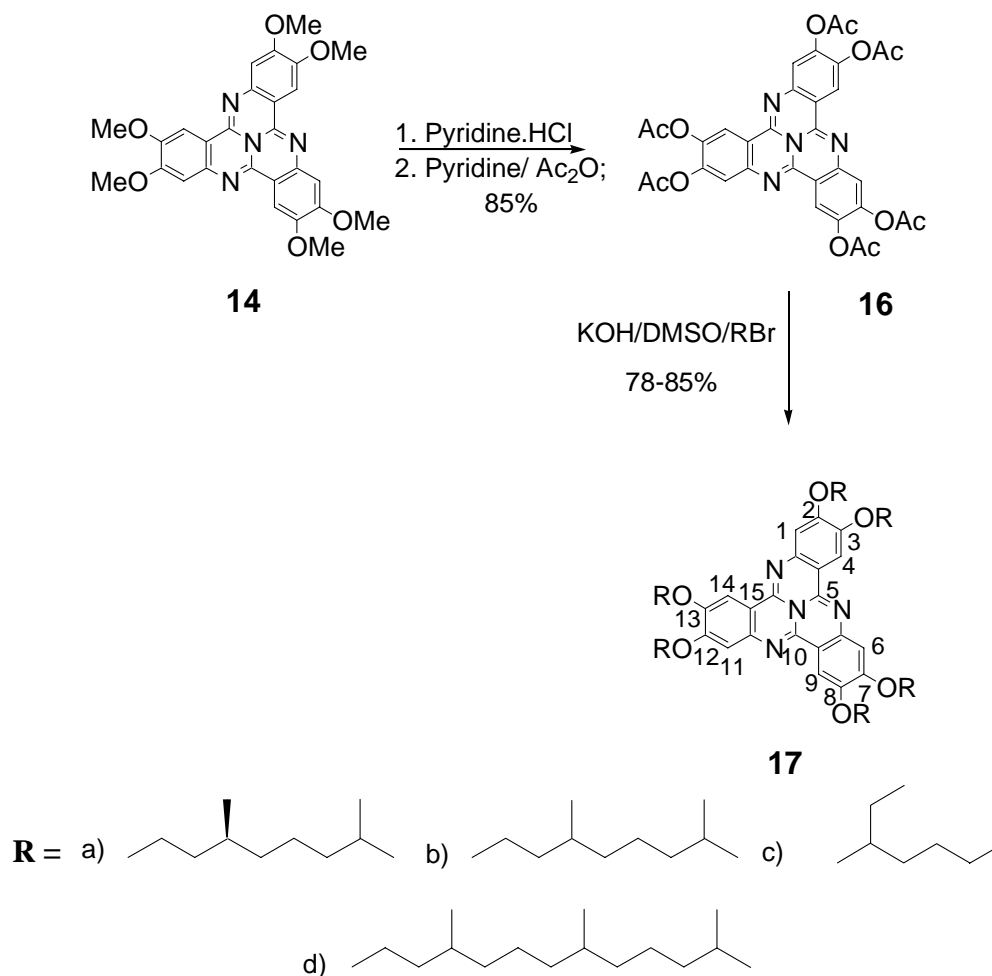
The discotic hexamethoxy TCQ derivative has been commonly used as a precursor for the synthesis of other alkoxy TCQ discogens because aromatic methoxy groups may be easily cleaved to give the corresponding phenolic TCQ, which can be later alkylated with alkyl halides (Scheme 5).



**Scheme 5:** Synthetic route to hexaalkoxy TCQ

Yields of discotic hexaalkoxy TCQ derivatives by this synthetic route (scheme 5) are very low (20-35 %), sometimes less than 5 %. This is because hexaphenols are very sensitive to oxidation in air and cannot be stored for longer time. The yields of aryl hexaethers **17** depend upon the purity of the hexaphenols.

To get higher yields of aryl hexaethers **17** we used another synthetic method involving a one-step preparation of phenyl ethers from phenyl acetates (scheme 6) <sup>[39]</sup>. With this route alkylation is rapid and gives higher yields. Conversions were often more than 90 % with highly reactive halides such as allyl or benzyl halides. With “normal” alkyl halides even if using reactive n-alkyl iodides like methyl or ethyl iodide, yields are only moderate, longer reaction time are needed. However could obtain more than 80% yields with longer n-alkyl halides (chiral and racemic 3,7-dimethyl-octylbromide, 2-Ethylhexyl-bromide).



**Scheme 6:** Two step synthetic route to hexaalkoxytricycloquinazolines

In a typical procedure, powdered KOH (24 mmol) was mixed with DMSO (5 ml) and stirred at room temperature for 10 min. 1 mmol of hexaacetoxytricycloquinazoline **16** (scheme 6) was added, followed by the alkyl bromide (24 mmol). The reaction mixture was stirred for 24 h at 55<sup>0</sup>C, and then the work-up was done by addition of water and extraction with diethyl ether. The crude product was purified by column chromatography over silica gel eluting with hexane-ethyl acetate. Products were characterized by <sup>1</sup>H NMR-spectroscopy (see experimental part).

All the products (scheme 6) with longer alkyl chains **17a-d** are highly fluorescent, as exemplified by typical absorption and emission spectra of **17a**, presented in figure 20 and figure 21. Compounds **17a-b** and **17d** (scheme 6) were found to be mesogenic showing a discotic mesophase in a very broad

temperature range. The nature of these LC phases were studied by differential scanning calorimetry (DSC) and by optical microscopy with crossed polarizers (chapter 3.2).

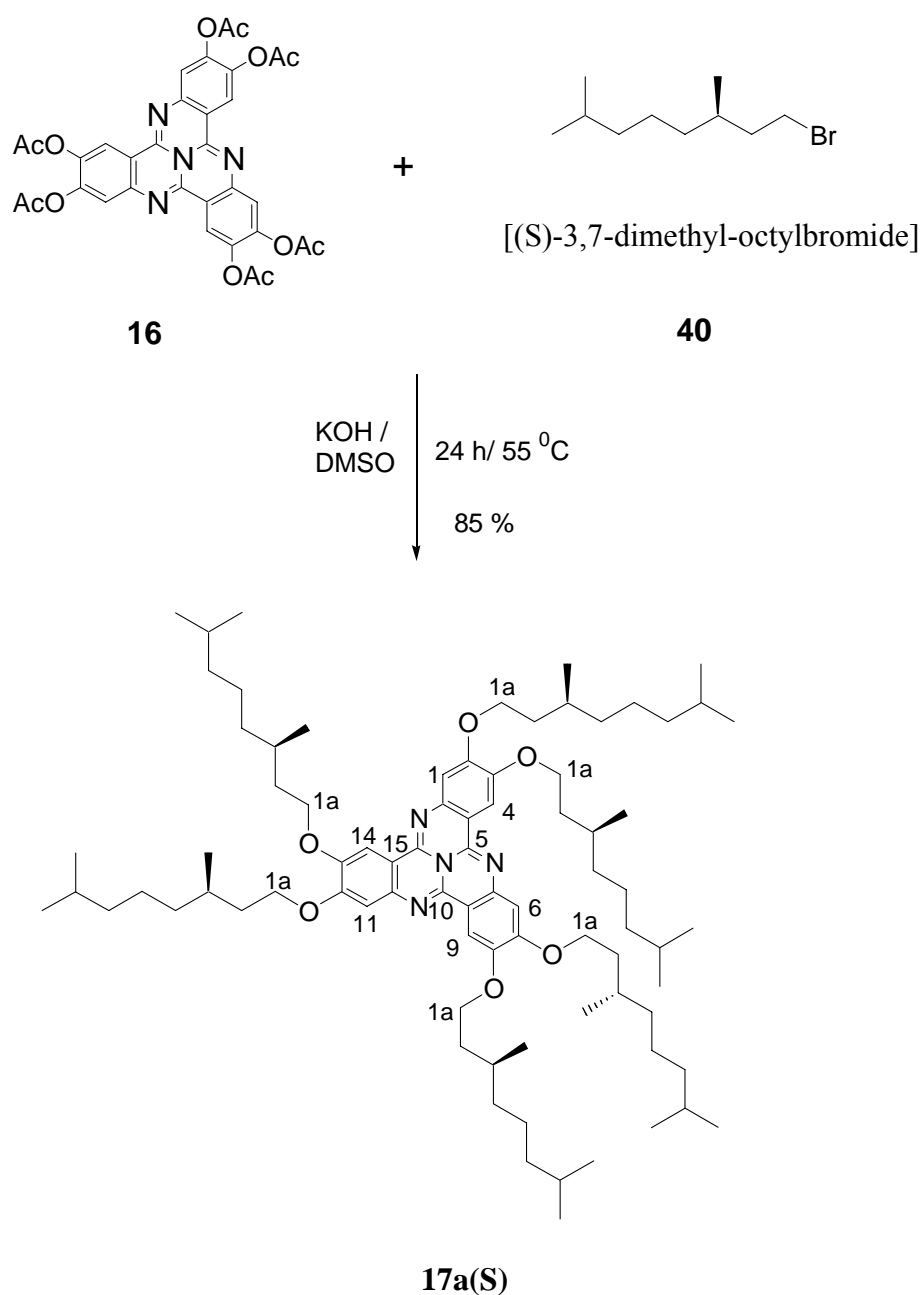
#### **Racemic and chiral hexa(3,7-dimethyloctyloxy) tricycloquinazoline(TCQ)**

Chirality has become one of the most important and complex topics of research in science today. The assembly and aggregation of molecules towards superstructures such as the double helix arrangement in DNA is one of the origins of life. Chirality in liquid crystals has been a focus point of interest<sup>[90]</sup> since their first discovery by *Reinitzer*<sup>[11]</sup> in 1888, where he discovered two derivatives of cholesterol, which have asymmetric molecular structures, and are therefore optically active and chiral<sup>[46]</sup>. They form chiral nematic mesophases, *i.e.* they can selectively reflect light.

Chiral LC molecules allow the study of the LC phases formed by circular dichroism (CD) spectroscopy. Our aim was the generation of a chiral TCQ derivative and the subsequent characterization of its LC phases by absorption and CD spectroscopy.

Chiral TCQ **17a(S)** was synthesized using the procedure outlined before (scheme 7)<sup>[39]</sup>.

In a typical procedure (scheme 6) powdered KOH (24 mmol) was mixed with 5 ml DMSO and stirred at room temperature for 10 min. One mmol of hexaacetoxytricycloquinazoline **16** was added followed by (S)-3,7-dimethyloctyl bromide (24 mmol). The reaction mixture was stirred for 24 h at 55°C and then work up was done by addition of water and extraction with diethyl ether. The crude product was purified by column chromatography over silica gel eluting with hexane-ethyl acetate (8:2). Products were characterized by <sup>1</sup>H NMR and <sup>13</sup>C NMR-spectroscopy (yield 80%).



**Scheme 7:** Synthesis of chiral hexaalkoxy tricycloquinazoline

The chiral hexaalkoxy tricycloquinazoline **17a (S)** was characterized by  $^1\text{H}$  NMR and  $^{13}\text{C}$  NMR-spectroscopy.

The  $^1\text{H}$  NMR-spectrum shows a singlet signal at 7.72 ppm for aromatic protons H1, H6 and H11 which are somewhat downfield compared to the aromatic protons H4, H9 and H14 which shows a singlet signal at 6.91 ppm. Triplet signal at 4.17 ppm accounting for the 12 protons (H1a,  $\alpha$  CH<sub>2</sub>) of the alkyl

chains. **17a(S)** also shows multiplet signals at 2.0-1.2 ppm, 0.98 ppm and 0.88 ppm for rest of the alkyl protons.

$^{13}\text{C}$ -NMR spectroscopy shows 7 signals of non-equivalent carbons in the aromatic region at ( $\delta$ : 165.1, 150.3, 147.1, 143.9, 119.7, 113.2, 108.7 ppm). Other signals of aliphatic carbons are 70.1, 39.7, 37.5, 28.5, 28.3 25.1, 22.3 (two equivalent carbons), 20.1 ppm.

The CD spectrum of the chiral-hexaalkoxy TCQ **17a(S)** is discussed in chapter 3.2 together with the optical properties of TCQs **17a(S)**, **17b**, **17c** and **17d**.

The experimental details and reaction conditions towards the tricycloquinazoline (TCQ) derivative with racemic 3,7-dimethyloctyl side chains are similar to those described for the chiral hexalkoxy TCQ **17a(S)**. NMR spectroscopy and mass spectroscopy revealed identical data and demonstrate the same high purity of the racemic TCQ **17** as for the chiral derivative **17a(S)**. As expected racemic TCQ **17b** shows no CD signal. **17b** shows resemblance with literature characterization data [39].

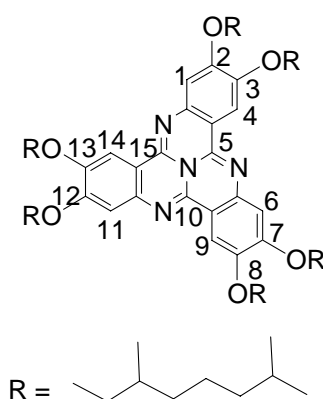


**Fig. 11:** Molecular structure of racemic hexaalkoxy TCQ **17b**

Racemic hexaalkoxy TCQ **17c** and **17d** with 2-ethylhexyl and 3,7,11-trimethyldodecyl side chains were synthesized by identical synthetic routes as **17a(S)**. The yields were between 80-85 % (after purification).

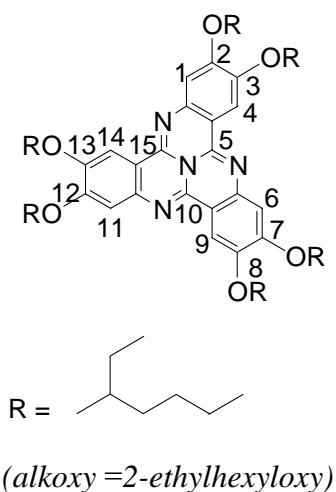


**Fig. 12:** Molecular structure of hexaalkoxy TCQ 17c

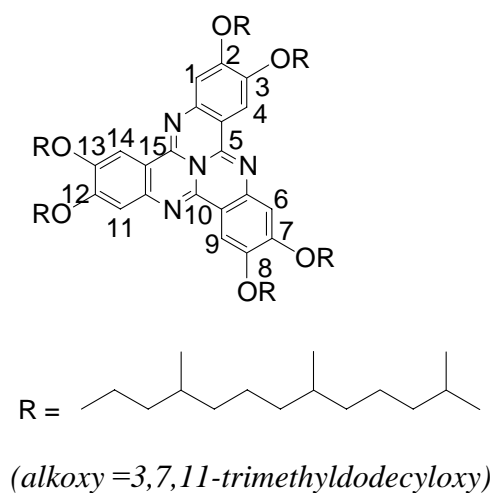


**Fig. 13:** Molecular structure of hexaalkoxy TCQ 17d

Discotic hexaalkoxy TCQ **17c** and **17d** shows very similar  $^1\text{H}$  NMR and  $^{13}\text{C}$  NMR-spectroscopic data in the aromatic region as in the case of chiral and racemic hexa(3,7-dimethyloctyloxy) substituted TCQ **17a** (**S**) and **17b**.



### 3.2 Characterization of TCQ based discotic molecules

The phase transition temperatures of chiral and racemic TCQ i.e. **17a (S)** & **17b** were determined by differential scanning calorimetry (DSC) and optical microscopy.

Racemic TCQ **17b** shows in the DSC a crystal to Col<sub>h</sub> transition at about 117.9 and is clear at 190.8°C, i.e. the Col<sub>h</sub> to isotropic melt transition occurs at 190.8°C [40]. Upon cooling the mesophase texture reappears at 185.9°C, not much different from the transition temperatures in TCQs with linear alkoxy substituents [34,35]. The assignment of the columnar mesophase as Col<sub>h</sub> phase was done in relation to the literature data [40].

The following table shows the thermal transitions of chiral hexaalkoxy TCQ **17a (S)** and racemic hexaalkoxy TCQ **17b** [40]

(alkoxy :3,7-dimethyloctyloxy)

| Compound       | Thermal transitions °C   |  |
|----------------|--|--|
|                | Heating scan   | Cooling scan   |
| <b>17a (S)</b> | Cr 118.1 Col <sub>x</sub> 178.7 Col <sub>h</sub><br>192.8 Iso. | Iso 190.2 Col <sub>x</sub> 175.6 Col <sub>h</sub><br>111.4 Cr. |
| <b>17b</b>     | Cr 117.9 Col <sub>h</sub> 190.8 Iso.                           | Iso 185.9 Col <sub>h</sub> 99.5 Cr.                            |

**Table 1:** Phase transition temperatures (peak temperatures) of TCQ derivatives according to DSC. **17a (S)** & **17b**. Cr = crystal, Col<sub>h</sub> = hexagonal columnar liquid crystalline phase, Col<sub>x</sub> = unknown columnar phase, Iso = isotropic melt.

Figure 14 gives the DSC curves for the chiral hexaalkoxy TCQ **17a (S)**. In contrast to the racemic **17b** we have observed an extra LC-LC transition both in the heating and cooling scan. Figure 14 shows a crystal to Col<sub>x</sub> transition at 118.1, a Col<sub>x</sub> to Col<sub>h</sub> at 178.7 and Col<sub>h</sub> to isotropic melt transition at 190.5°C. The Col<sub>h</sub>-Col<sub>x</sub> transition is observed at 175.6°C. We have assigned the second

columnar phase ( $Col_x$ ) to a higher ordered columnar phase,  $Col_h$  is the hexagonal columnar LC phase which is also present in **17b**. However, a full assignment of the two different columnar mesophases need some further X-ray characterization.

From literature <sup>[40]</sup>, compound **17c** with an 2-ethylhexyl side chain is described to be non-liquid crystalline. It shows a crystal to isotropic transition at 152.8°C (melting point) on heating and crystallises back at 145.7°C on cooling. The non-liquid crystalline nature of this compound could be due to the steric bulk of the ethyl branch close to the aromatic core. In contrast, **17d** with long 3,7,11-trimethyl dodecyl side group shows a sharp mesophase to isotropic transition at 142.1°C (peak temperature). The transition reappears on the cooling cycle at 141°C. The LC mesophase exists down to -50°C, the lowest temperature to which the sample was cooled. No melting /crystallization was observed for **17d**.

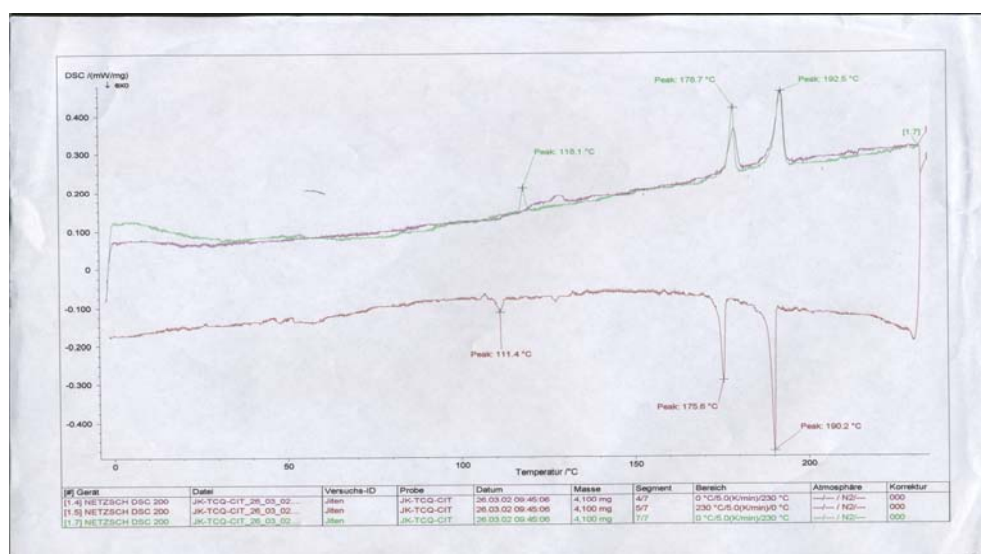


**Fig. 14:** DSC traces for compound **17a(S)** on heating and cooling

Optical microscopy with crossed polarizers suggest that compounds **17a(S)** and **17b** form hexagonal discotic mesophases with similar textures. At room temperature the sample of the chiral hexaalkoxy TCQ **17a(S)** forms orange-yellow crystals. Upon heating these crystals show a crystal to  $Col_x$  transition

(in the microscope at around 120°C, hot stage temperature). Around 160°C the LC film is converted into a viscous birefringent mass under partial dewetting. On further heating the sample becomes fluid and optically isotropic above 205°C. Upon slow cooling (2°C/min) the mesophase textures reappear. Figure 15 show a representative example of such a polarizing microscopic picture of **17a(S)** obtained on rapid cooling from the isotropic liquid into the liquid crystalline state recorded at 70°C in the frozen, glassy LC state. The mosaic textures, resembling reflections on steel cylinders, are characteristic of an unordered, hexagonal columnar phase ( $Col_h$ ), and are very similar to those reported by Billard et al. for 2,3,6,7,10,11-hexaalkoxytriphenylenes<sup>[42]</sup>.

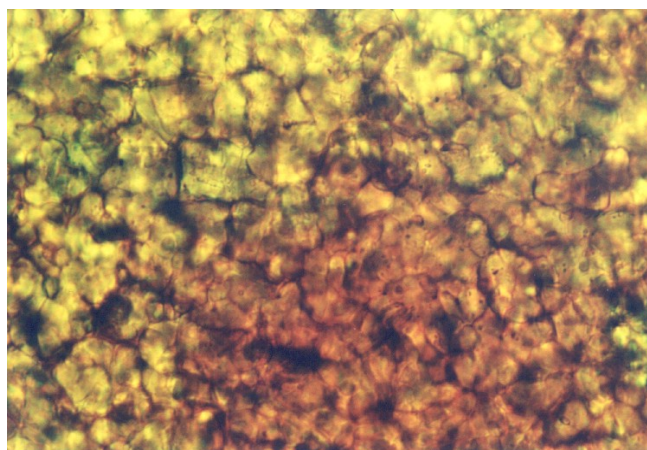


**Fig. 15:** *Optical texture of chiral hexaalkoxy TCQ 17a (S) (recorded at 70°C after cooling from the isotropic melt )*

#### **X-ray scattering experiments**

X-ray scattering is a powerful technique for the study of crystal and liquid crystal structures. When monochromatic X-ray beam hits the crystal or LC phase, the scattered electromagnetic waves from the regularly placed atoms interfere with each other, giving strong diffraction signals in particular directions if the inter-atomic distances are of the same order as the X-ray wavelength (typically 0.05-0.2 nm). The often used Cu-K $\alpha$  radiation has the wavelength of 0.154 nm = 1.542 Å.

For diffraction the path difference between waves scattered from successive planes of atoms in the crystal must equal an integral number of the wavelength,  $n$  ( $n= 1,2,3,\dots$ ). This condition is expressed by the *Bragg* equation [55].

$$n\lambda = 2d \sin\theta$$

where  $d$  is the distance separating successive planes in the crystal and  $\theta$  is the angle of the incident beam with the planes.

The polarizing microscopical texture of the liquid crystalline state suggested a hexagonal columnar mesophase, but to enable definite assignment X-ray scattering experiments were performed at different temperatures for chiral TCQ derivative **17a** (**S**). The overall features observed are consistent with the structure of a  $\text{Col}_h$  phase [47], the derived one-dimensional intensity vs  $2\theta$  profile was obtained by integrating over the entire  $\chi$  (0-360°C) range. Three sharp peaks (figure **16 right**), one very strong and two weaker reflections are seen in the low angle region. The  $2\theta$  values for the three sharp peaks at low angles conform to a two-dimensional hexagonal lattice spacing of ca. 29 Å. In the wide angle region two diffuse reflections are seen. The broad one centered on 4.67 Å corresponds to some ordering of the aliphatic chains. The high angle peak is due to the stacking of the rigid cores within a column giving a core-core separation of ca 3.4 Å. A model of the packing is given in (figure **16 left**).

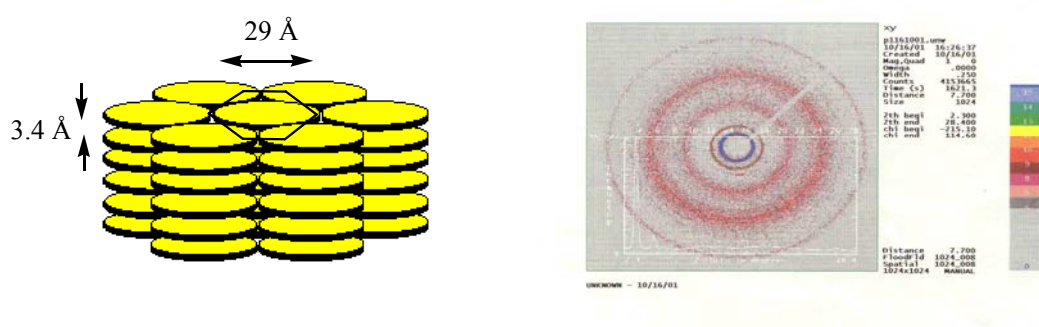


**Fig. 16:** X-Ray scattering pattern of TCQ derivative **17a** (**S**) in the discotic state. (edge-on view, shearing direction is top to bottom)(right) and the real space representation of the columnar mesophase (left).

### Absorption properties

The absorption spectrum of TCQ **17a(S)** consists of two distinct bands. The absorption properties of discotic TCQ **17a(S)** have been measured in chloroform at room temperature (figure 17). The spectrum shows a strong absorption feature centered at  $\lambda_{\text{max}}$  of 282 nm and another around 400 and 422 nm. The long wavelength band represents the  $\pi$ - $\pi^*$  transition of the delocalized  $\pi$ -electron system of TCQ.

The absorption properties are similar for discotic TCQs **17b**, **17c** and **17d** <sup>[40]</sup>.

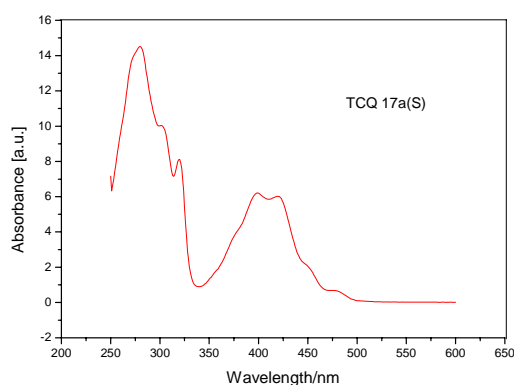


**Fig. 17:** UV/Vis spectrum of discotic TCQ **17a(S)** in chloroform solution at room temperature.

### Fluorescence Properties

For discotic TCQ **17a(S)** an optical excitation at  $\lambda_{\text{max}} = 422$  nm gives a strong yellow fluorescence in the range of 525 to 700 nm with maxima at  $\lambda_{\text{max}} = 572$  and 610 nm. The fluorescence characteristics are very similar to the discotic TCQs **17b**, **17c**, **17d** <sup>[40]</sup> and 2,3,7,8,12,13-hexakis(thioalkoxy)tricycloquinazoline derivatives <sup>[44]</sup>. Figure 18 shows the fluorescence spectrum of discotic TCQ **17a(S)** in chloroform solution.

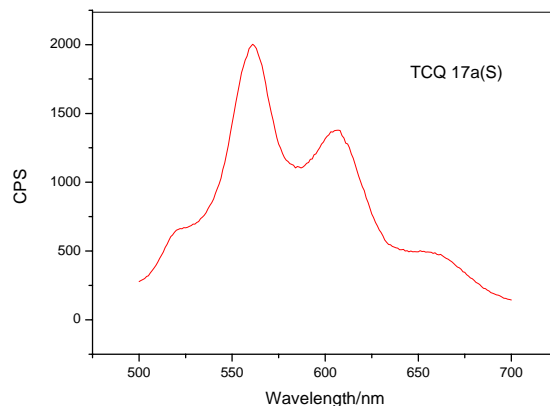


**Fig. 18:** Fluorescence spectrum of discotic TCQ 17a(S) in chloroform solution at room temperature.

### Circular dichroism (CD)

Circular Dichroism (CD) and Optical Rotatory Dispersion (ORD) are special variations of absorption spectroscopy<sup>[56]</sup>. The basic principle of the two methods is the interaction of linearly and circularly polarized light with optically active substances. If a linearly polarized light wave passes through an optically active substance, the direction of the polarization will change, which is wavelength dependent. This phenomenon is called optical rotatory dispersion (ORD). Linearly polarized light waves can be described as a superimposition of two circularly polarized light waves. If a substance absorbs these two circularly polarized components to a different extent, i.e. if the absorption coefficient for the right handed circularly polarized component of the polarized light is different from the absorption of the left handed circularly polarized light, this difference is described as circular dichroism (CD). CD spectroscopy measures this difference  $\Delta\epsilon$  in the absorption coefficient of left and right handed circularly polarized light.

Here, circular dichroism (CD) spectroscopy is used to gain information related to the chiroptical properties in solutions (dispersions) containing aggregated chromophores. Discotic TCQ **17a(S)** shows no CD signal in chloroform solution, indicating the lack of chiral induction in single (isolated) molecules. But a strong CD signal was observed in chloroform /methanol (5/95) as solvent/non-solvent mixture. The chiral TCQ **17a (S)** derivative shows a strong

bisignated CD-signal between 250 and 325 nm, which indicates chiral coupling of chromophores in the aggregated (columnar) mesophase formed and a weak monosignated CD effect in the region of the long wavelength  $\pi$ - $\pi^*$  absorption (400-450 nm). As expected, the racemic TCQ derivative **TCQ 17b** did not show any CD effect in chloroform/methanol.

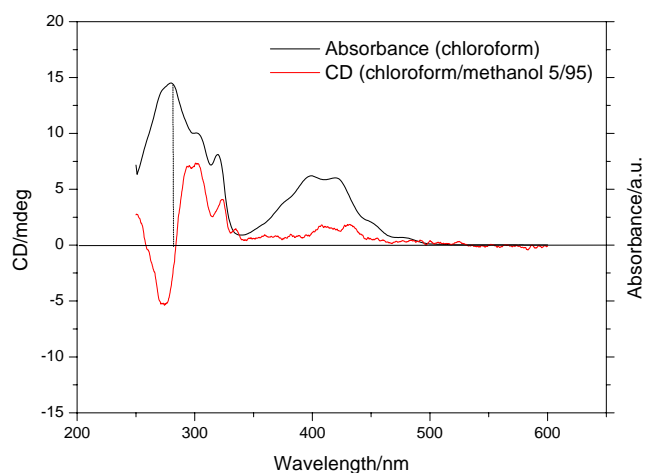


**Fig. 19:** CD spectrum of chiral **TCQ 17a** (*S*) in chloroform/methanol (5/95) at room temperature.

### Ultraviolet photoelectron spectroscopy (UPS)

The valence electronic structure of racemic, discotic **TCQ 17b** has been investigated by means of ultraviolet photoelectron spectroscopy (UPS). The measurements have been made on LB films of the discotic **TCQ 17b**.

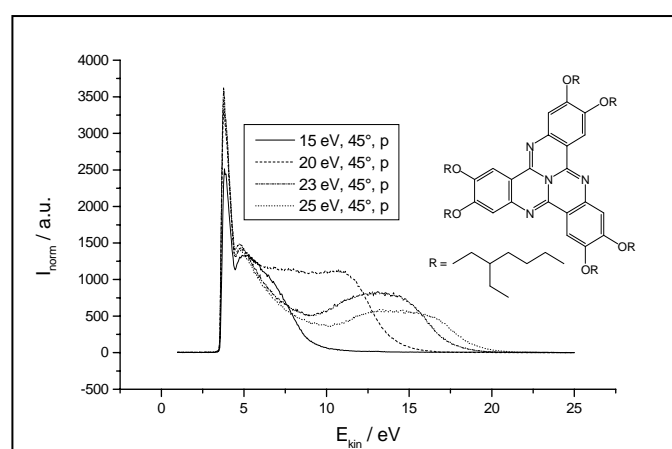


**Fig. 20:** UPS spectra of **TCQ 17b** for various incident photon energies

Figure 20 shows the UPS spectra of a LB-multilayer containing 10 monolayers (ML) of the TCQ derivative **17b** for various incident energies with a polarization direction of the incoming light parallel to the dipping direction of the LB-substrates. The spectra are plotted intensity normalised to the input light intensity versus kinetic energy of the detected photoelectrons. The spectra show an extremely broad peak, which is composed of at least two pronounced bands as can be seen clearly in the spectra detected for 23 and 25 eV photons, respectively.

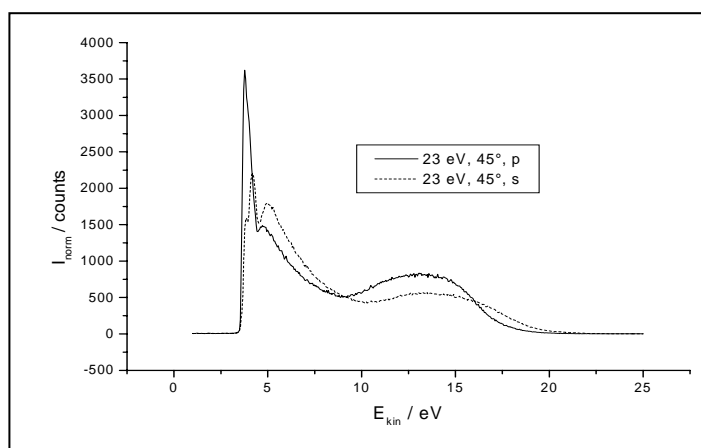


**Fig. 21:** UPS spectra of TCQ **17b** for two polarization directions of the incoming light

From quantum chemical calculations the UPS spectra is expected to be composed of four different peaks resulting mainly from  $\pi$ -electrons and a shoulder at the HOMO position (ca. 3 eV).

Figure 21 represents UPS spectra for the same 10 monolayer (ML) sample at an incident photon energy of 23 eV and an incidence angle of the incoming light and detection angle for the photoelectrons as described above. The polarization direction of the incoming light was either parallel or perpendicular to the dipping direction of the sample. A pronounced anisotropy can be found in the UPS spectra demonstrating a macroscopic alignment of the columnar domains of the discotic material.



### 3.3 Synthesis of indenofluorene and bisfluorenylidene-based conjugated polymers

#### 3.3.1 Low Bandgap Conducting Polymers

From the very early days of the study of conducting polymers, scientists envisioned that there might be a class of these polymers that would have either a zero energy bandgap (a single, continuous band consisting of the valence and conduction bands) or a very low bandgap (figure 22). It was envisioned that these materials might be inherent electronic conductors, that conduct without the need for doping, similar to metals that have overlapping bands. If these materials were indeed like metals, they might show the high electrical conductivity of metals<sup>[75]</sup>.

Conducting polymers were known to be highly colored in the nonconducting state owing to optical transitions of electrons from the valence band to the conduction band. Upon doping, for example oxidatively, new low energy transitions were observed due to the occurrence of polaronic and bipolaronic states, which give rise to two new energy levels within the gap. While electronic transitions involving these energy states increase in intensity with ongoing doping, the original absorptions decrease in intensity (figure 22).

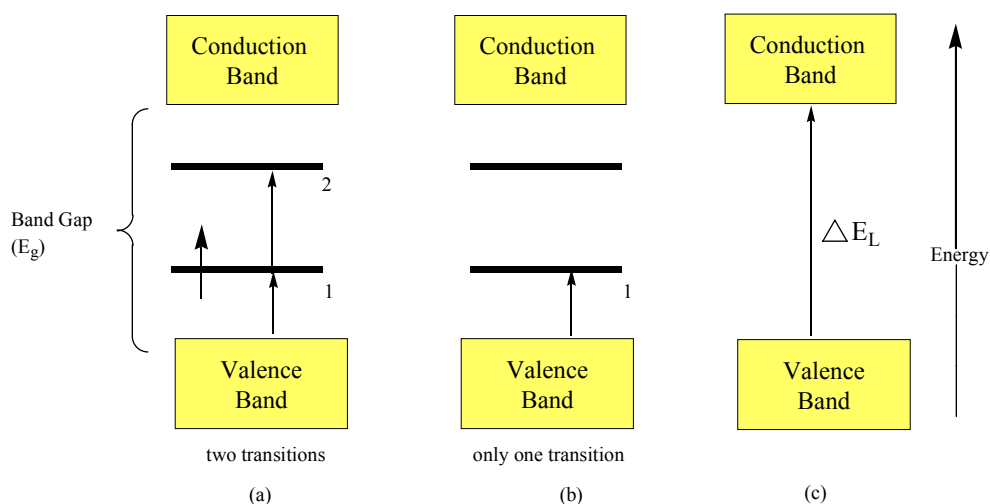


**Fig. 22:** Optical transitions in (a) an undoped (polaronic state) (b) an oxidatively doped (bipolaronic) conducting polymer and (c) neutral.

It was envisioned that a low bandgap polymer might be deeply colored when undoped, with the optical absorption widely shifted to the red when compared to a polymer with a higher bandgap. Since, as indicated above, oxidative doping would produce new absorptions of even lower energy, these new absorptions might be pushed into the near-infrared region of the spectrum. Thus, with the new optical absorptions being in the near-infrared and the original absorptions of the neutral species decreasing in intensity, the doped form of such a polymer might well be very lightly colored and essentially transparent while being highly conductive.

With these objectives in mind, new systems were developed that were designed to have low bandgap energies. Since the initial synthesis of the first truly low bandgap conducting polymer by Wudl and Heeger, namely polyisothianaphthylene, [poly(benzo[*c*]thiophene)]<sup>[76]</sup>, much theoretical and experimental work has been carried out to design and prepare new systems and to understand and predict the properties, including the bandgap energies. Prior to 1984 several systems were prepared that presumably had low bandgap energies, and some quantum-mechanical calculations were also performed on these polymeric molecules<sup>[113, 114]</sup>.

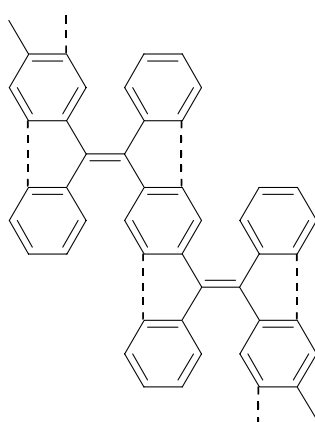
The bandgap energies of most of the well-studied conducting polymers are >2 eV. Thus, for example, that of poly(*p*-phenylene) is ca. 2.7 eV.<sup>[115, 116]</sup>, that of poly(*p*-phenylene vinylene) is ca. 2.4 eV<sup>[117, 118]</sup>, that of polythiophene is 2.0-2.1 eV<sup>[119, 120]</sup>, and that of polypyrrole is ca. 2.2 eV<sup>[121]</sup>. Polyacetylene has a lower bandgap, between 1.5<sup>[122]</sup> and 1.7 eV<sup>[123]</sup>. It was arbitrarily decided to use a bandgap energy of about 1.5 eV as cutoff, a low bandgap conjugated polymer is therefore, one having a band gap of less than 1.5 eV.

A major problem with these low bandgap materials results from the relatively high energy of the electrons in the valence band, such a polymer can be easily oxidized, often already with ambient oxygen. Thus, low bandgap polymers have to be often handled under anaerobic conditions to prevent atmospheric oxidation. Therefore, an important challenge is to design low bandgap materials with high stability under ambient (atmospheric) conditions.

### 3.3.2 Poly(indeno[1,2-*b*]-fluorene) PIF:

In 1977 *Hörhold* first described diphenyl-substituted poly(1,4-phenylene vinylene) DP-PPV <sup>[48]</sup>. DP-PPV and its derivatives represent an intensively investigated class of high-bandgap conjugated polymers with intense solid state fluorescence <sup>[48]</sup>.

The introduction of two additional aryl-aryl bonds (from DP-PPV **9** to PIF **8** see scheme **1**) is accompanied by a dramatic red-shift of the absorption band from  $\lambda_{\max} = 366$  nm (DP-PPV) to  $\lambda_{\max} = 797$  nm (PIF).



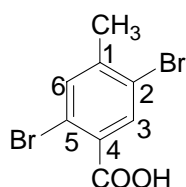
**8**

The geometry of this novel polymer PIF **8** is non-planar <sup>[47]</sup>, since there is a strong steric hindrance at the interring linking positions. 9,9'-Bisfluorenylidene which is a related model system of the interring connection of PIF **8** can form two different conformations, one with a mutual distortion of the planar fluorenylidene building blocks relative to the olefinic double bonds, leading to reduced double-bond character of the BFD molecule and another with a geometric distortion within fluorenylidene subunits under formation of a “butterfly-like” conformation.

Poly(indeno[1,2-b]fluorene) PIF derivatives with their exocyclic double bonds at the 6-and 12-positions represent deeply colored chromophores. PIF **8** forms intensely blue solutions in halogenated hydrocarbons like methylene chloride, chloroform or tetrachloroethane, and in aromatic solvents.

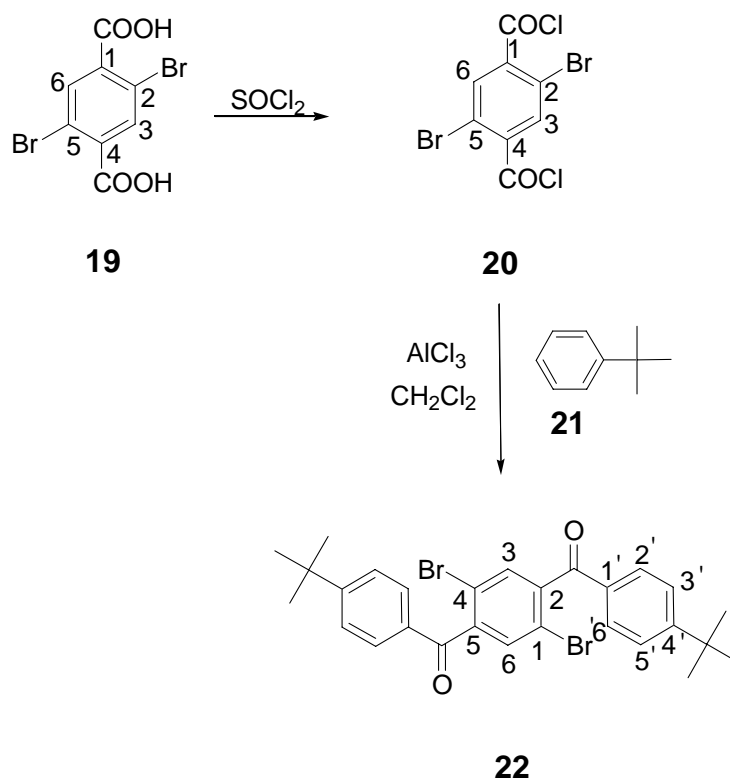
Poly(indeno[1,2-b]fluorene) (PIF) **8** has a main chain structure resembling a picket fence. This polymer has been first described by *Scherf and coworkers* in 1996<sup>[47]</sup>. The unique cross conjugated  $\pi$ -system leads to the widely red-shifted long wavelength absorption band.

The synthesis of poly(indeno[1,2-b]fluorene) PIF starts from commercially available 2,5-dibromo-1,4-xylene, which is converted to 2,5-dibromo-4-methylbenzoic acid **18** by refluxing it in nitric acid and water.



**18**

The second step was the oxidation of 2,5-dibromo-4-methylbenzoic acid **18** to 2,5-dibromoterephthalic acid **19** using  $\text{KMnO}_4$ . This 2,5-dibromoterephthalic acid **19** was then converted to 2,5-dibromoterephthalic dichloride **20**, which was further transformed to 1,4-dibromo-2,5-bis(4-*tert*-butylbenzoyl)benzene by reacting it with *tert*-butylbenzene by *Friedel-Crafts acylation* reaction. (scheme **8**).



**Scheme 8:** Synthesis of the diketo monomer **22**.

The diketone **22** was characterized by  $^1\text{H}$  and  $^{13}\text{C}$  NMR-spectroscopy. The  $^1\text{H}$  NMR-spectrum shows doublet at 7.70 ppm for H3'/H5', a singlet at 7.53 ppm for H3 and H6 and doublet at 7.45 ppm for H2'/H6'. The  $-\text{CH}_3$  protons of the *tert*-butyl group appear at 1.28 ppm (18H).

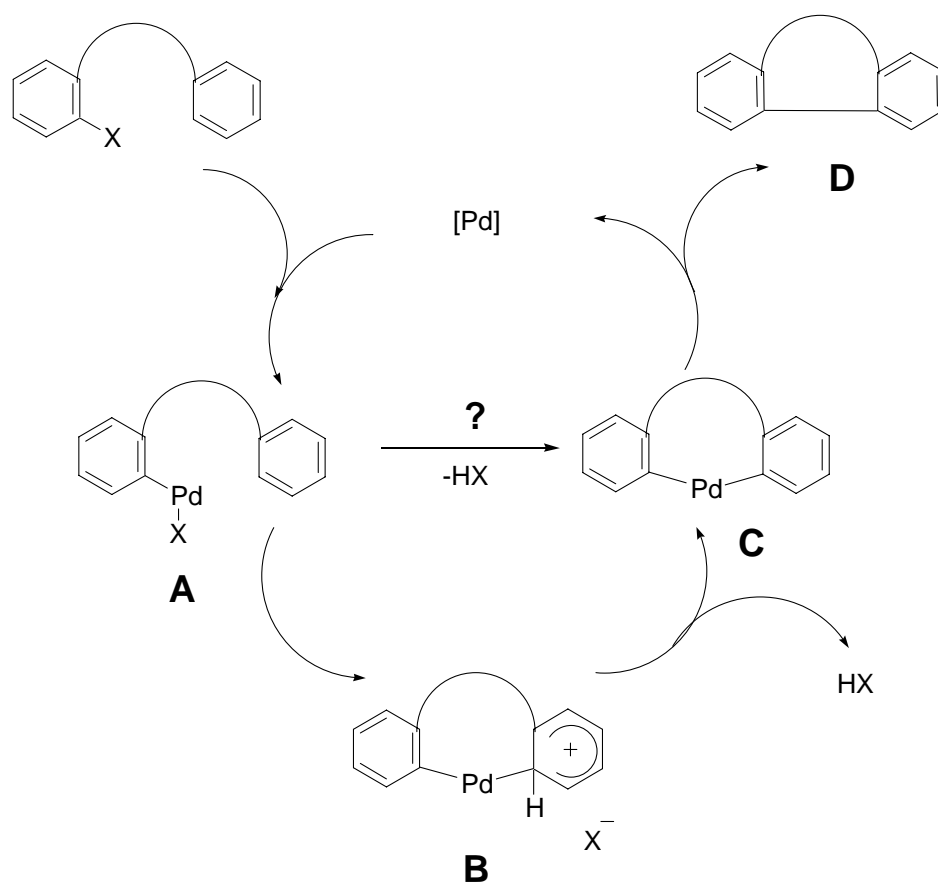
From  $^{13}\text{C}$  NMR-spectroscopy we found seven signals of non-equivalent carbons in the aromatic region ( $\delta$ : 158.9, 143.5, 133.5, 132.8, 130.6, 126.3 and 118.7 ppm). The downfield signal at 193.6 ppm accounts for the carbonyl carbon ( $-\text{C}=\text{O}$ ), while signals at 35.6 and 31.3 ppm stand for the ( $-\text{C}(\text{CH}_3)_3$ ) and  $-\text{CH}_3$  carbons of the *tert*-butyl group.

The next step was to convert **22** to the ring closed 3,9-di-*tert*-butyl-indeno[1,2-*b*]fluorene-6,12-dione **23**. To synthesize the diketone with *tert*-butyl-substituents **23** we used an *intramolecular aryl-aryl cyclisation* of 1,4-dibromo-2,5-bis[4-*tert*-butyl(benzoyl)benzene] **22**. To obtain **23**, this method is superior to older methods as described by *Deuschel and co-workers* <sup>[112]</sup>. Because of the *para*-substitution on the terminal phenyl rings, both hydrogens

in ortho-position to the keto group are equivalent. Thus, the cyclisation to the dione **23** is regioselective without formation of isomers.

We used palladium(II) acetate as effective reagent for the intramolecular cyclisation<sup>[87, 89]</sup>, only catalytic quantities have been used (5 mol%).

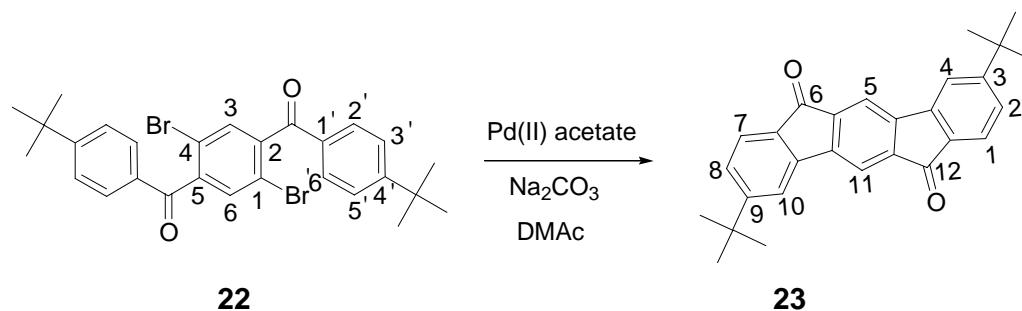
The mechanism of this palladium catalysed aryl-aryl coupling reaction is as for *Suzuki*<sup>[58]</sup> or *Heck* reaction<sup>[88]</sup> not totally known yet. As in the synthesis of palladacycles a cyclic intermediate may occur (scheme 9). In the first step palladium inserts into the C<sub>ar</sub>-Br bond (A) and an arenium complex B is formed by the oxidation addition of the palladium halide to the other aryl ring. Deprotonation yields the palladacycle C, which gives the cyclized product D in a reductive elimination reaction<sup>[55]</sup>.



**Scheme 9:** Proposed mechanism of palladium-catalysed intramolecular dehydrobromination reaction

Using the procedure of *Scherf and coworkers* the cyclisation of 1,4-dibromo-2,5-bis(4-*tert*-butyl-benzoyl)benzene **22** was done using catalytic amounts of

palladium(II) acetate and anhydrous sodium carbonate in dry dimethylacetamide. 1 h reflux gave compound **23** as brick red powder which was recrystallized from DMF to yield 3,9-di-*tert*-butyl-indeno[1,2-*b*]fluorene-6,12-dione in 86% yield.

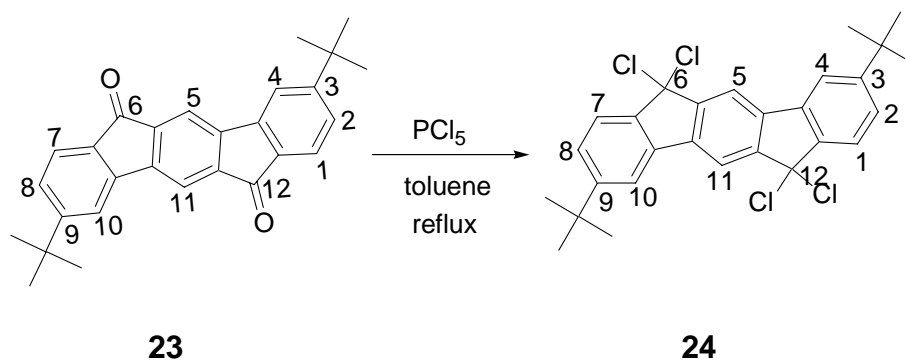


**Scheme 10:** Palladium-catalysed intramolecular dehydrobromination reaction

The corresponding brick red diketone **23** was characterized by  $^1\text{H}$  NMR and  $^{13}\text{C}$  NMR-spectroscopy as well. The  $^1\text{H}$  NMR-spectrum shows a singlet signal at 7.69 ppm for two aromatic protons H5/H11, and a doublet for the two aromatic protons at 7.50 ppm corresponding to H4/H10, another doublet for two aromatic protons H1/H7 at 7.49 ppm and a downfield doublet of doublet signal at 7.26 ppm for the two aromatic protons H2/H8. We can also see upfield singlet signal at 1.30 ppm for 18 protons of *tert*-butyl group.

As expected from the structure of compound **23**  $^{13}\text{C}$  NMR-spectroscopy shows a downfield carbon signal at 191.9 ppm corresponding to carbonyl carbons C6 and C12 and a downfield signal at 159.7 ppm for C3/C9 aromatic carbons, other carbon signals are at  $\delta$ : 151.9, 143.2, 137.3, 135.7, 132.8, 129.4, 130.2 and 123.8 ppm. Signals at 35.1 ppm for (-C(CH<sub>3</sub>)<sub>3</sub>) and 31.5 for (-CH<sub>3</sub>) represent the aliphatic carbons.

The diketone **23** was finally converted to the corresponding “bis-geminal” tetrachloro monomer **24** using phosphorous pentachloride as reagent (Scheme 11). The use of toluene as solvent is therefore very advantageous. The product is poorly soluble in this solvent and precipitates during the conversion. The isolation of pure lemon colored **24** is achieved by simple filtration and washing of the reaction mixture.



**Scheme 11:** Synthesis of “bis-geminal” tetrachloro monomer **24**

Conversion of **23** to **24** was confirmed by  $^{13}\text{C}$ -NMR-spectroscopy. The downfield keto signal at 193 ppm of the cyclic diketone **23** disappears in the  $^{13}\text{C}$  NMR-spectrum of the “bis-geminal” tetrachloro monomer **24**.

From  $^1\text{H}$ -NMR spectroscopy we have a downfield singlet signal for two aromatic protons H5 and H11 at 8.00 ppm, a doublet signal at 7.72 ppm for H1/H7, and a doublet signal at 7.68 ppm for H4/H10 protons, while the H2/H8 aromatic protons appear at 7.44 ppm (dd). A singlet signal at 1.40 ppm is for the 18 methyl protons.

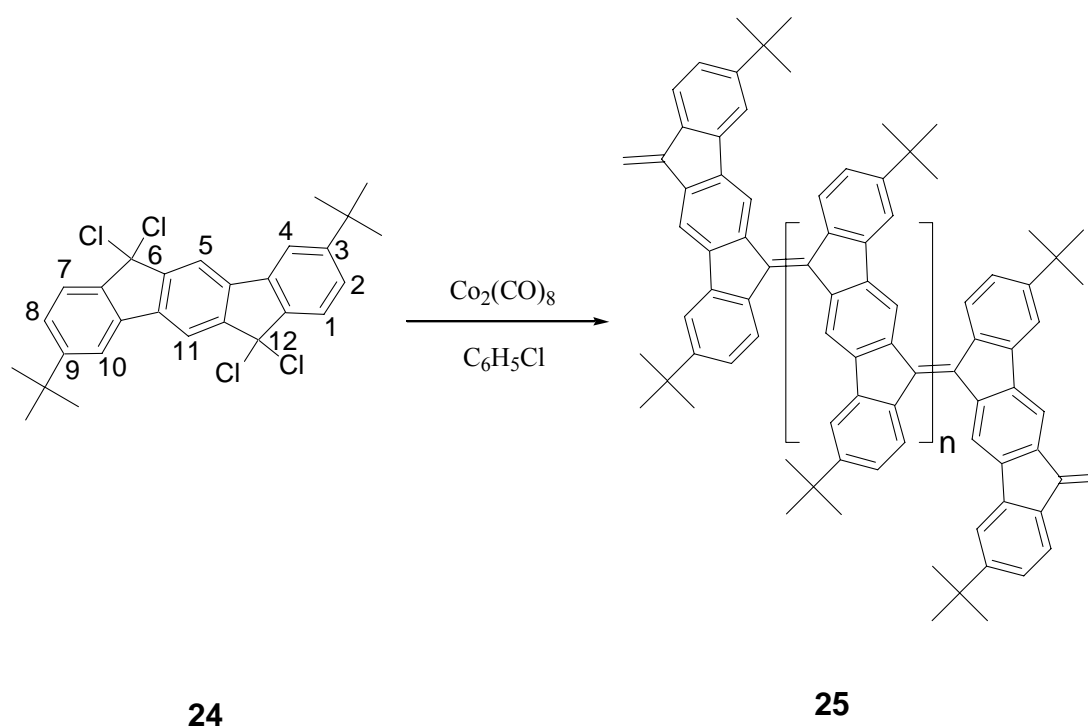
$^{13}\text{C}$  NMR-spectroscopy displays the following signals for the aromatic carbons  $\delta$ : 155.3 ppm for C3/C9, 150.2, 144.4, 138.4, 135.7, 127.1, 124.5, 117.5, 116.6 ppm. The signals at 82.7 ppm ( $-\text{C}(\text{Cl}_2)_2$ ), 35.4 ( $-\text{C}(\text{CH}_3)_3$ ), and 31.5 ppm ( $-\text{CH}_3$ ) represent the aliphatic carbons.

The reductive coupling (polycondensation) of the tetrachloro monomer **24** to poly(3,9-di-*tert*-butyl-indeno[1,2-*b*]fluorene) was done using dicobalt octacarbonyl  $\text{Co}_2(\text{CO})_8$  at 90°C. The condensation is generally accompanied by a color change. The monomer solutions are of pale yellow color, the polymer solutions are deep bluish-black. Condensation is accompanied by a strong foaming of the mixture (generation of CO). The coupling reaction produces deep purple colored polymer **25** (yield 75%).

Chromium hexacarbonyl  $\text{Cr}(\text{CO})_6$ , the chromium/bis(benzene) complex  $(\text{C}_6\text{H}_6)_2\text{Cr}$ , and nickel bis(triphenylphosphano) dicarbonyl  $[(\text{C}_6\text{H}_5)_3\text{P}]_2\text{Ni}(\text{CO})_2$  can also be used as dechlorinating metallorganic reagents<sup>[47]</sup>, however the best



results have been obtained with dicobalt octacarbonyl  $\text{Co}_2(\text{CO})_8$ . The use of the  $\text{Ni}(\text{COD})_2$  complex and cobalt(I)/tris(triphenylphosphano)chloride as dehalogenating agents did not lead to polymeric products; only oligomers of short chain length are formed. In the case of  $\text{Ni}(\text{COD})_2$ , the allylic hydrogens of the cyclooctadiene ligand may act as a source for a hydrogen transfer, thus limiting the molecular weight of the products <sup>[47]</sup>.



**Scheme 12:** *Synthesis of PIF by dehalogenation polycondensation*

The  $^1\text{H}$  NMR-spectrum of poly(3,9-di-*tert*-butylindeno[1,2-*b*]fluorene) (PIF) **25** displays four broad signals of aromatic/olefinic hydrogens at 8.88, 8.41, 7.64, 7.28-7.20 ppm and one of the *tert*-butyl groups at 1.3-1.5 ppm.

The  $^{13}\text{C}$  NMR-spectrum of poly(3,9-di-*tert*-butylindeno[1,2-*b*]fluorene) (PIF) **25** consists of one signal block in the aromatic/olefinic region, accompanied by the two signals of the *tert*-butyl side groups at 35.2 ppm ( $-\text{C}(\text{CH}_3)_3$ ) and 31.3 ( $-\text{C}(\text{CH}_3)_3$ ). The aromatic/olefinic region of the spectrum exhibits 10 signals of

the 10 non-equivalent aromatic/olefinic carbons of  $\delta$ : 152.4, 141.5, 140.2, 139.6, 136.4, 126.9, 124.7, 123.5, 118.8, 117.1.

Absorption spectra of PIF **25** were measured in chloroform solution. The UV/Vis spectrum of the deeply colored polymer **25** shows the occurrence of a conjugated one-dimensional  $\pi$ -system, indicated by the sharp absorption band at long wavelength ( $\lambda_{\text{max}}=797$  nm). An other absorption band occurs at  $\lambda_{\text{max}}=300-314$  nm, typical of the isolated indenofluorene chromophore.

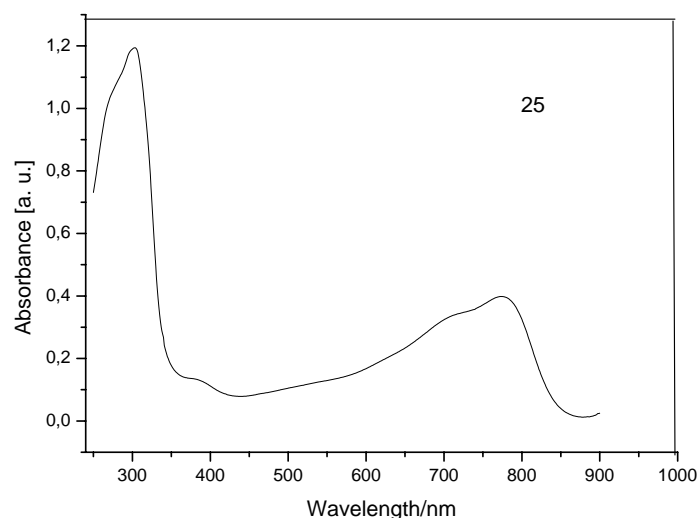


**Fig. 23:** UV/Vis absorption spectrum of PIF **25** in chloroform solution at room temperature

Gel permeation chromatography (PS calibration) provided high number average molecular weights  $M_n$  of up to 12,000 ( $M_w$ : 26.000) corresponding to degree of polymerization of up to 33.

#### 3.3.3 Fluorenylene-encapped poly(indeno[1,2-b]fluorene) PIF

Poly (indeno[1,2-b]fluorene) as a organic semiconductor will be used as charge transport layer in organic field effect transistors (see chapter 3.3.5). However, the stability of the organic semiconductor is a crucial point for OFET applications. To increase the chemical stability of PIF-type polymers the introduction of defined chain-end functions will be a promising way. This can

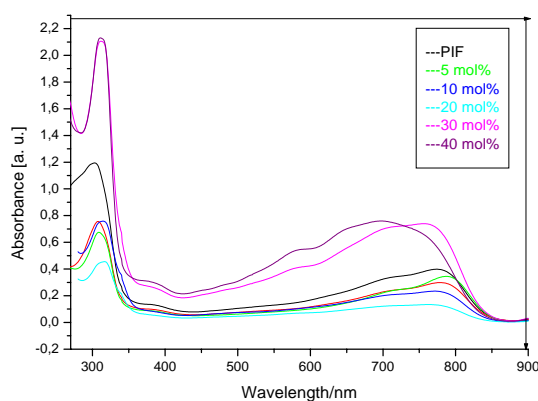


| Molar amounts of endcapping reagent <b>26</b> | $M_n/M_w$ (GPC) <b>27</b> |
|---|---------------------------|
| 5 mol%  | 5,800/10,100              |
| 10 mol%                                       | 2,900/7,400               |
| 20 mol%                                       | 1,900/5,300               |
| 30 mol%                                       | 1,500/2,700               |
| 40 mol%                                       | 1,000/2,000               |

**Table 2:** Molecular weights of **27**

### 3.3.4 Absorption properties of fluorenylene-endcapped poly-(indeno[1,2-*b*]fluorene)

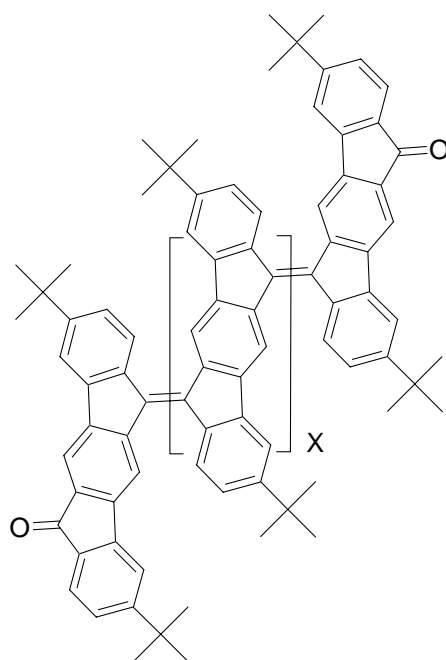
UV/Vis absorption of fluorenylene-endcapped poly(indeno[1,2-*b*]fluorene) **27** was measured in chloroform solution. The UV/Vis absorption spectra of the fluorenylene-endcapped poly(indeno[1,2-*b*]fluorenes) (figure **24**) show that the increase in the amount of endcapping reagent **26** leads to a blue-shift of the absorption band.



**Fig. 24:** UV/Vis absorption spectra of fluorenylene-endcapped PIFs **27** in chloroform solution at room temperature

As already mentioned, the molecular weights gradually decrease with increasing amounts of the endcapper. The product **27** represents mixture of oligomers. The average length of the molecule is reduced with increasing amounts of endcapper. This is now reflected in the UV/Vis spectrum. More and more absorption bands of shorter oligomers becomes visible.

We have compared our results with a series of indenofluorene oligomers which have been made by *H. Reisch* (figure **25**)<sup>[55]</sup>. Figure **26** shows the UV/Vis absorption spectra of this indenofluorene model oligomers. It is clear from figure **26** that with the increase of the oligomer length the long wavelength absorption maximum is gradually red-shifted. Poly(indeno[1,2-b]fluorene) PIF shows a sharp band at  $\lambda_{\text{max}} = 797$  nm, but with decrease of the oligomer length the  $\lambda_{\text{max}}$  blue shifts up to a value of ca  $\lambda_{\text{max}} = 530$  nm for the dimer.

**28****Fig. 25:** PIF-diketo model oligomers<sup>[55]</sup>

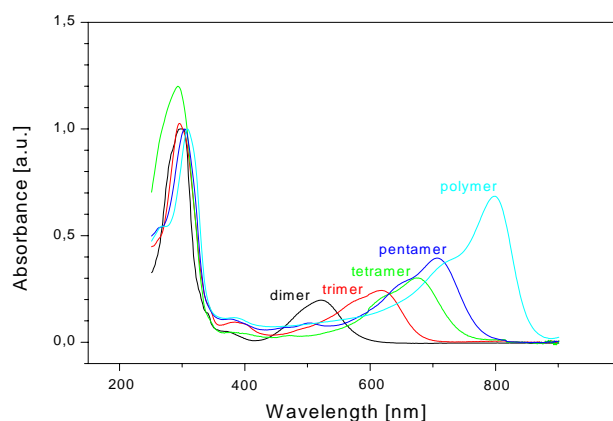


**Fig. 26:** UV/Vis spectra of PIF-diketo model oligomers <sup>[55]</sup>

### 3.3.5 Fluorenylene-encapped PIF as active layer in ambipolar organic field effect transistors and inverters

Fluorenylene-encapped PIF **27** material was used as active layer in organic FETs. Experiments were carried out by *Eduard Meijer* in the group of *Prof. Dr. de Leeuw* at Philips Research Laboratories, Eindhoven, the Netherlands. Ambipolar charge transport is an intrinsic property of pure undoped organic semiconductors. We could show that ambipolar transport is observed experimentally upon reduction of the injection barriers by using low bandgap materials<sup>[84]</sup>.

The main difficulty in achieving ambipolar transistor operation is the injection of both holes and electrons into a single semiconductor material from the same electrode. This electrode needs to have a work function that allows injection of both holes in the highest occupied molecular orbital (HOMO) of the semiconductor and the injection of electrons in the lowest unoccupied molecular orbital (LUMO).

Polymer electronics up to now is typically based on unipolar logic, mainly because of the choice of electrodes in combination with a large band gap semiconductor. For the operation of light emitting diodes and solar cells based on organic semiconductors it is essential that both electrons and holes can flow through the semiconductor layer under an applied electric field, and that they

can be collected in or emitted from the electrodes. This poses requirements on the choice of semiconductor layer in combination with the electrode materials used for the anode and the cathode.

In organic solar cells, typically a blend of an electron-transporting and hole-transporting semiconductor is used. Upon illumination, excitons are formed in the blend, which can be separated in electron and holes by means of an applied electric field. The electron transport and the hole transport provide a conduction path for the electrons and holes to the electrodes, thus converting light into electric current. In polymeric light emitting diodes a high work function with the highest occupied molecular orbital (HOMO) of the organic semiconductor, and a low work function alignment with the lowest occupied molecular orbital (LUMO) of the organic semiconductor. Due to the typically large bandgap ( $>2$  eV) of the polymers used in light emitting diodes, which is required for light emission in the visible range of the spectrum, the anode will be a blocking contact with injection barrier for electrons, and the cathode a blocking contact for injection of holes. Upon application of an electric field across the polymeric semiconductor, electrons and holes flow towards each other and form excitons, which can recombine under emission of light.

To fabricate ambipolar organic transistors, which operate as either n-channel or p-channel transistors, the concepts of the light emitting diode and solar cell are useful, and in this context was demonstrated that a blend of suitable chosen n-type and p-type semiconductors, deposited from solution, in combination with Au electrodes results in ambipolar transistor operation <sup>[97]</sup>. In that case two materials were used where one has its HOMO level aligned with the Au work function and the other its LUMO level.

Operation of an ambipolar transistor requires to inject both holes and electrons from the same electrode. A good contact for one polarity of charge typically results in an injection barrier for their other polarity charge. However, using a material with a smaller energy gap can reduce this injection barrier. Furthermore, the width of an injection barrier can be narrowed by applying a large source to drain field, or by accumulation of high charge carrier densities in the semiconductor film by means of field effect <sup>[98]</sup>. For sufficiently high

amounts of accumulated charge, the injection barrier becomes small enough to allow tunneling from the electrode into the semiconductor. Next to the requirements of a small bandgap also the semiconductor purity is of importance in order to minimize trapping effects.

As mentioned earlier fluorenylene-encapped poly(3,9-di-*tert*-butyl-indeno [1,2-*b*]fluorene) **27** has been used as a novel low bandgap organic semiconductor in ambipolar transistors. The material has a bandgap energy of ca. of 1.55 eV. Gold, with a work function of 5.1 eV, is used for the source and drain injecting contacts. Heavily doped Si wafers have been used as the gate electrode, with a 200-nm-thick-layer of thermally oxidized SiO<sub>2</sub> as the gate-insulating layer. Using conventional lithography, the gold source and drain interdigitated contacts are defined with a channel width  $W$  of 2 cm and length  $L$  of 10 μm. The SiO<sub>2</sub> layer is treated with the primer hexamethyldisilazane. The transistors are completed by spinning a solution of 1 wt% PIF **27** in chloroform onto the substrate. The molecular structure of PIF **27** and a schematic cross-section of the transistor geometry are given in figure **27**. The measurements are performed in a vacuum of 10<sup>-4</sup> mbar at room temperature, after annealing the sample for an hour at 90°C.

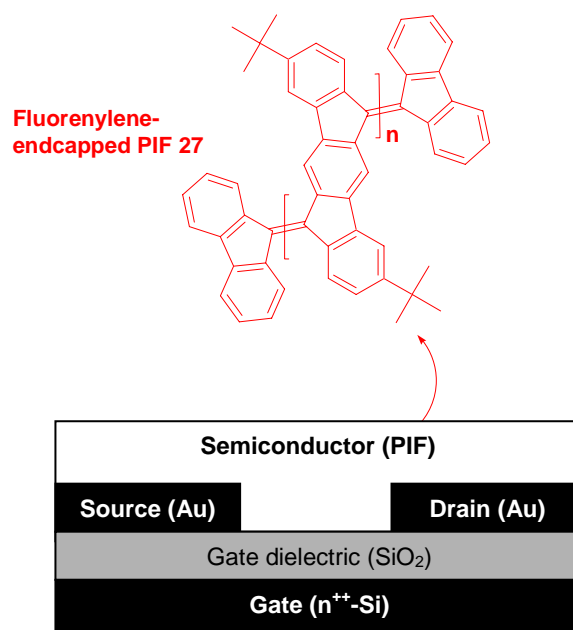


**Fig. 27:** Schematic cross-section of the OFET device.



The source/drain current ( $I_{ds}$ ) versus source/drain voltage ( $V_{ds}$ ) curves for different gate voltages ( $V_g$ ) of the PIF-based organic field-effect transistors (figure 28) demonstrate that the transistor operates both in the hole-enhancement and electron-enhancement mode. For high negative gate voltages  $V_g$  the transistor is in the hole accumulation mode (figure 28a) with a small injection barrier for holes, which is visible via the non-linear output characteristics at low  $V_{ds}$ . At high positive  $V_g$  electrons are accumulated in the semiconductor at the semiconductor-insulator interface (figure 28b). Also for the electrons, a small injection barrier from gold to PIF 27 was observed. From the transfer characteristics in the linear operating regimes of the transistor (figure 29) following field-effect mobilities have been found:

For holes (at  $V_g = -30$  V)  $4 \cdot 10^{-5}$  cm<sup>2</sup>/Vs and for electrons (at  $V_g = 30$  V)  $5 \cdot 10^{-5}$  cm<sup>2</sup>/Vs, respectively. In the present transistor the onset of the field-effect for the electron accumulation was at  $V_g = 10$  V, and for the hole accumulation at  $V_g = -15$  V (figure 29).

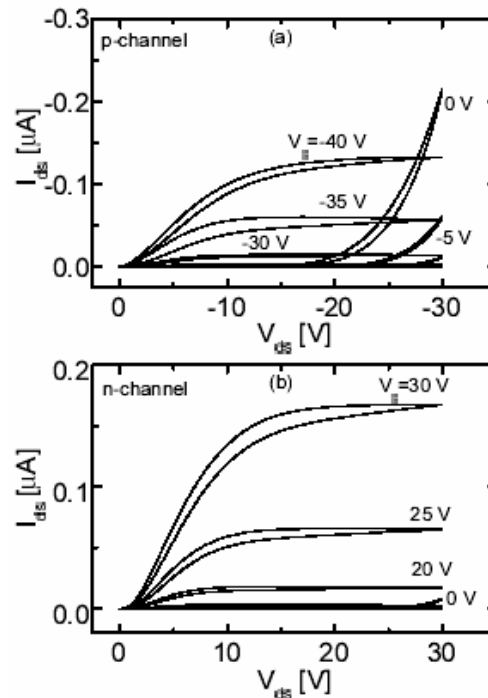


**Fig. 28:** The output characteristics of a PIF-based ambipolar transistor, operating in a) hole-enhancement, and in b) electron-enhancement mode

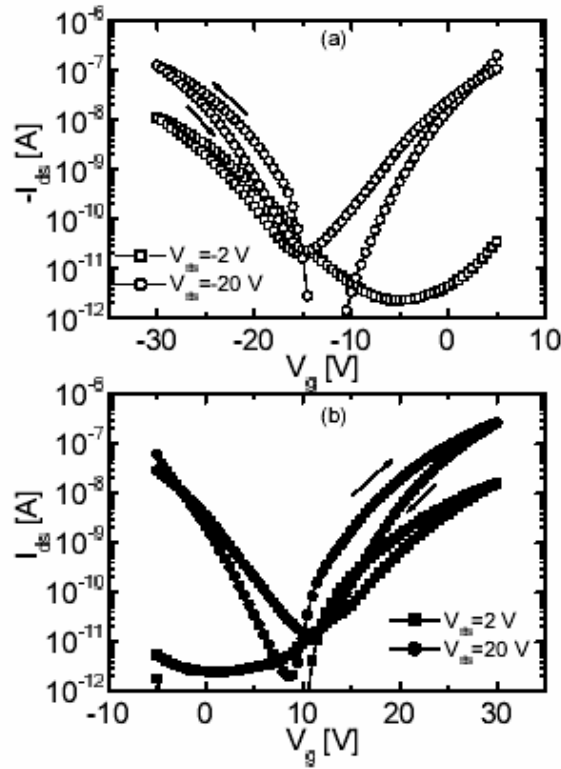


**Fig. 29:** The transfer characteristics of the PIF-based ambipolar transistor. (a) For  $V_g < -15$  V only the hole contribution is observed in the current, whereas for  $V_g > -15$  V the electron current is seen. (b) For  $V_g > 10$  V only the electron contribution to the current is observed. The hole current-contribution is observed for  $V_g < 10$  V

The combination of a single material for source and drain electrodes and a single material for the semiconductor layer with evenly matched field-effect mobility's for the holes and electrons allows the simplest fabrication of a logic voltage inverter.

Conceptually, the inverter works by turning on switches in a specific order. A low power circuit must be constructed to perform as the control circuitry that drives the high power stage. One such control method is the square-wave inverter. In figure 30, if switches SW1 and SW4 are turned on, the load is subjected to  $+V_s$ . However, if SW2 and SW3 are turned on, the load is subjected to  $-V_s$ .  $V_s$  is a constant DC voltage. Assuming the switches are voltage controlled, the source DC voltage is converted to a square-wave AC voltage<sup>[124]</sup>.

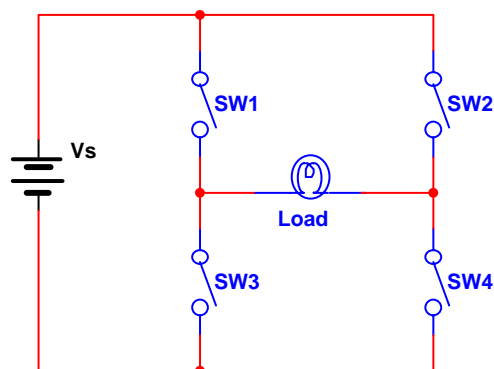


**Fig. 30:** Basic concept diagram for an inverter

Inverter operation is observed for two identical PIF-based ambipolar OFETs connected in accordance with the schematic diagram given in the inset of figure 31. The ambipolar inverter operates in the first and third quadrant, depending on the applied supply voltage,  $V_{DD}$ .

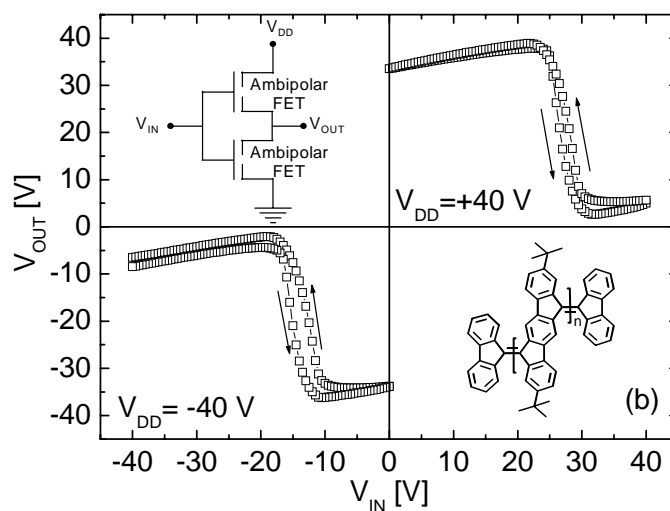
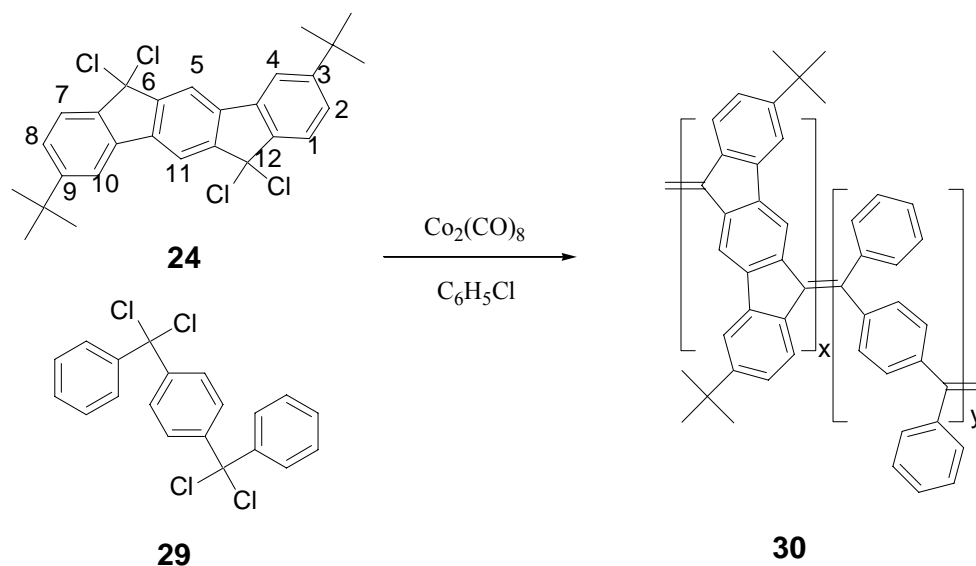


**Fig. 31:** Transfer characteristics of a CMOS (complementary metal-oxide semiconductors) like inverter (see inset) based on two identical ambipolar field-effect transistors based on PIF 27<sup>[69]</sup>. Depending on the polarity of the supply voltage,  $V_{DD}$ , the inverter works in the first or the third quadrant.

### 3.3.6 Synthesis of poly(indeno[1,2-b]fluorene) PIF / poly(*para*-phenylene-diphenylvinylene) DP-PPV statistical copolymers

A poly(*para*-phenylenevinylene) PPV derivative which is substituted at the vinyl subunit with two phenyl groups is poly(*para*-phenylene-diphenylvinylene) DP-PPV which has been first synthesized in 1977 by *Hörhold* represents an intensively investigated high bandgap conjugated polymer of the PPV type with intense solid state fluorescence<sup>[48]</sup>. In contrast, PIF which has been first reported by *Scherf and coworkers* in 1996<sup>[47]</sup> represents a low bandgap conjugated polymer. It was interesting to check the optical and electronic properties of statistical copolymers containing both phenylene diphenylvinylene and indenofluorene moieties. Such copolymers can be synthesized by a similar procedure as for PIF **25**, by dehalogenation with the low valent transition metal compound  $\text{Co}_2(\text{CO})_8$  when adding different amounts of the “non-cyclised” tetrachloro monomer **29**. The “cyclised” tetrachloro monomer **24** and tetrachloro monomer **29** have been used in the molar ratios 0:100, 20:80, 30:70, 40:60, 50:50, 60:40, 80:20, and 100:0.



**Scheme 14:** Synthesis of statistical copolymers **30**

The statistical copolymer **30** shows  $^1\text{H}$  NMR- and  $^{13}\text{C}$  NMR-spectra with many signals (see experimental part), due to the presence of different building blocks and structural sequences.

Molecular weights of these PIF/DP-PPV copolymers **30** have been determined in toluene solution (GPC, PS calibration). The number average molecular weights  $M_n$  have been found between 4,000 and 9,000, the weight average molecular weights  $M_w$  between 8,500 and 18,000 without a systematic dependence from the monomer ratio 25/29.

### 3.3.7 Absorption properties of PIF/DP-PPV statistical copolymer

Absorption properties of the **PIF/DP-PPV** statistical copolymer **30** have been measured in chloroform solution at room temperature. UV/Vis spectra of PIF/DP-PPV copolymers **30** are depicted in figure 32.

The spectra indicate that the length of oligo indenofluorene segments is decreasing with an increase of the length of oligo phenylene-diphenylvinylene segments. The absorption maximum of the oligo indenofluorene segments gradually blue-shifts with increasing molar amounts of the phenylene-vinylene comonomer. More and more well resolved signals of shorter indenofluorene segments become visible (pentamer at ca. 700 nm, tetramer at ca. 650 nm trimer at ca. 550 nm).

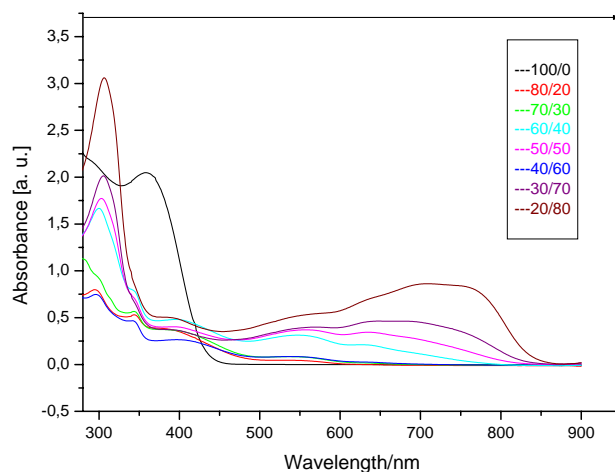
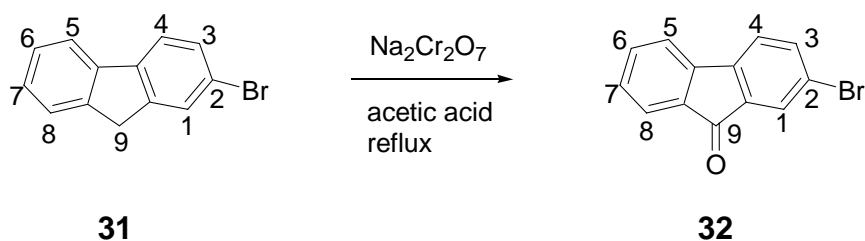


**Fig. 32:** UV/Vis spectra of PIF/DP-PPV **30** statistical copolymers in toluene solution at room temperature

### 3.3.8 Novel conjugated polymers with the bisfluorenylidene (BFD) unit

As said earlier in the introduction chapter (page 14) 9,9'-bisfluorenylidene is a central building block of poly(indeno[1,2-b]fluorene). 9,9'-bisfluorenylidene BFD is a highly overcrowded olefin, is electron deficient and can be easily reduced. It was therefore interesting to synthesize also other conjugated polymers with the 9,9'-bisfluorenylidene (BFD) unit.

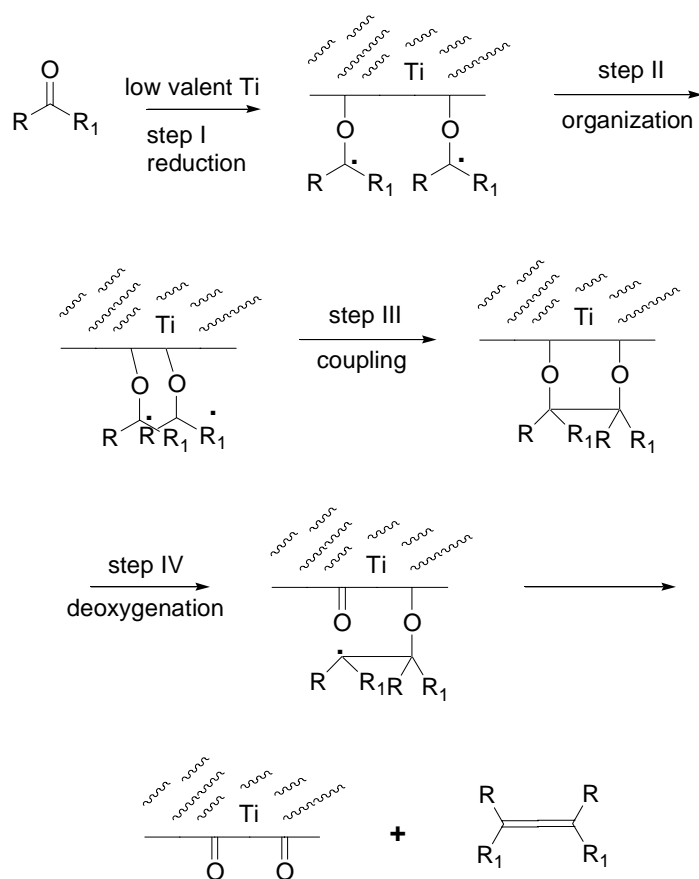
Our key monomer for novel conjugated polymers with the BFD unit is 2,2'-dibromo-9,9'-bisfluorenylidene derivative. Its synthesis of such monomer begins with the oxidation of commercially available 2-bromofluorene to 2-bromo-9-fluorenone in ca. 99% yield using  $\text{Na}_2\text{Cr}_2\text{O}_7$  as oxidizing agent.



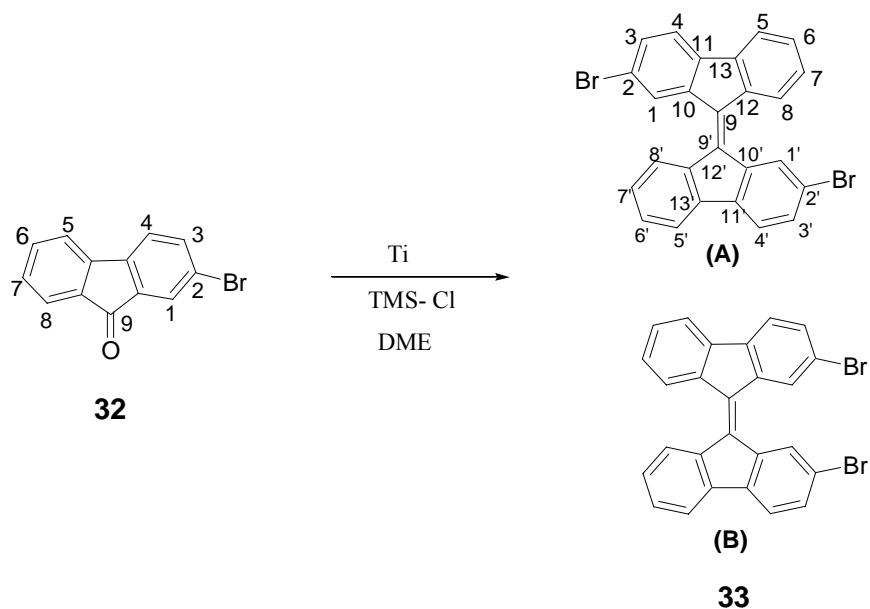
**Scheme 15:** Oxidation of 2-bromofluorene

Confirmation of oxidation at C-9 position of the compound **31** was done by both  $^1\text{H}$  NMR and  $^{13}\text{C}$  NMR-spectroscopy. The signal of the hydrogen in 9-position of **31** at 4.01 ppm disappears in the  $^1\text{H}$  NMR-spectrum of **32**. We can see now a new carbonyl carbon signal at 187.3 ppm in the  $^{13}\text{C}$  NMR-spectrum which is not present in the starting compound **31**.

The next step is the dimerization of **32** with commercially available titanium powder<sup>[52]</sup>. This is a type of *McMurry* alkene synthesis<sup>[94]</sup>. Scheme **16** depicts the generally accepted mechanism of the reaction, which involves four discrete steps after the formation of the active reagent, namely (I) reduction to form surface bound ketyl radicals; (II) organization of two ketyl radicals on the metal surface in near proximity; (III) coupling; and (IV) reductive deoxygenation of the pinacole under olefin formation.



**Scheme 16:** Mechanism of McMurry reaction



**Scheme 17:** McMurry type coupling of 2-bromo-9-fluorenone

2,2'-dibromo-9,9'-bisfluorenylidene **33** was synthesized by a synthetic protocol developed by *Alois Fürstner and co-workers* for this McMurry-type coupling using titanium powder <sup>[52]</sup>. The initial step is an activation of the titanium powder with trimethylsilyl chloride (TMS-Cl), followed by the addition of 2-bromo-9-fluorenone to the active reagent.

The resulting product 2,2'-dibromo-9,9'-bisfluorenylidene **33** forms orange-red crystals which were obtained after column chromatography using hexane as an eluent. The compound **33** is a mixture of *cis* and *trans* isomers. It was not possible to separate these isomers by column chromatography on a preparative scale.

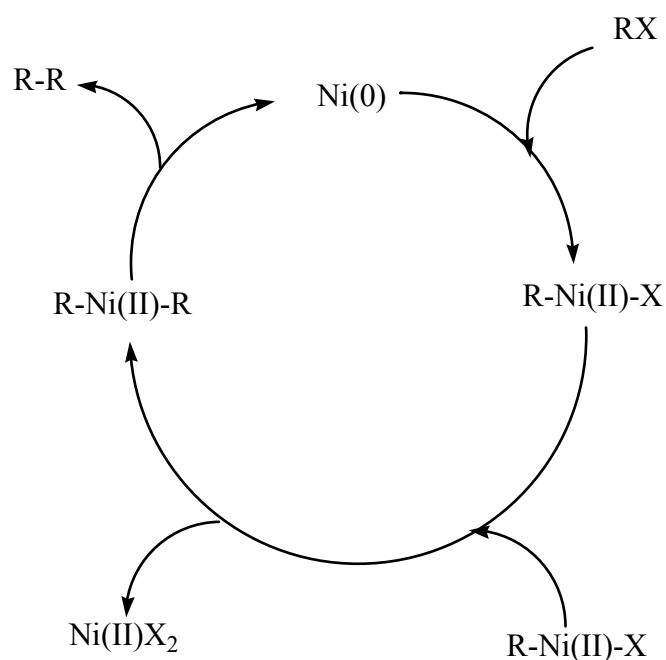
Chromatographic columns are classified to their dimensions and their application areas: a) analytical columns, b) preparative columns and, c) pre-columns or guard columns. The separation of compound **33**, i.e. the mixture of *cis* and *trans* isomers was possible on an analytic scale by HPLC. An octyl modified reversed phase column (Merk RP8) was conditioned with a mobile phase of water-THF and compound **33** was injected (0.1-0.8 mg/100 mL, injection volume: 10  $\mu$ L, column temperature: 25  $^{\circ}$ C). The analytical HPLC runs lead to a separation of *cis* and *trans*-isomers, two fractions with identical UV/Vis-spectra ( $\lambda_{\max}$  = 460 nm) have been isolated at retention times of 18.5 and 19.5 minutes. All attempts to do a preparative scale separation failed.

Isomeric mixture **33** was characterized by  $^1\text{H}$  NMR and  $^{13}\text{C}$  NMR-spectroscopy. The  $^1\text{H}$  NMR-spectrum shows multiplet signals at 7.20-7.70 ppm. A downfield signal at 8.28 ppm is assigned to the H1/1' protons of the *cis*-isomer. Another downfield doublet signal at 8.32 ppm with  $J = 8$  Hz belongs to two protons H1/H1' of the *trans*-isomer. This assignment was supported by *NOE* experiments.

Since the separation of *cis/trans*-isomers was difficult the isomeric mixture of 2,2'-dibromo-9,9'-bisfluorenylidene **33** was further used as precursor for polymerization reactions.

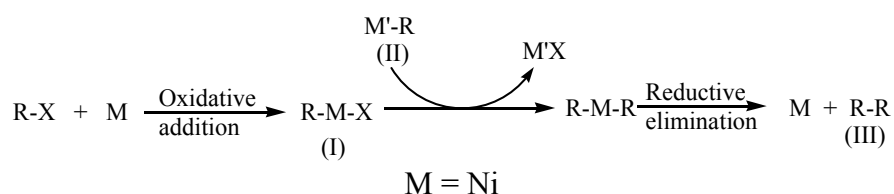


The homocoupling product of **33**, poly(9,9'-bisfluorenylidene-2,2'-diyl) **34** was obtained as an orange-red powder by a *Yamamoto*-type coupling reaction of **33** using the Ni(COD)<sub>2</sub> complex. Reaction time was 5 days under argon at 80°C. Detailed reaction procedure is described in experimental part (see scheme **18** and **19**) with the mechanism of the Ni(0)-catalysed *Yamamoto*-type coupling reaction).

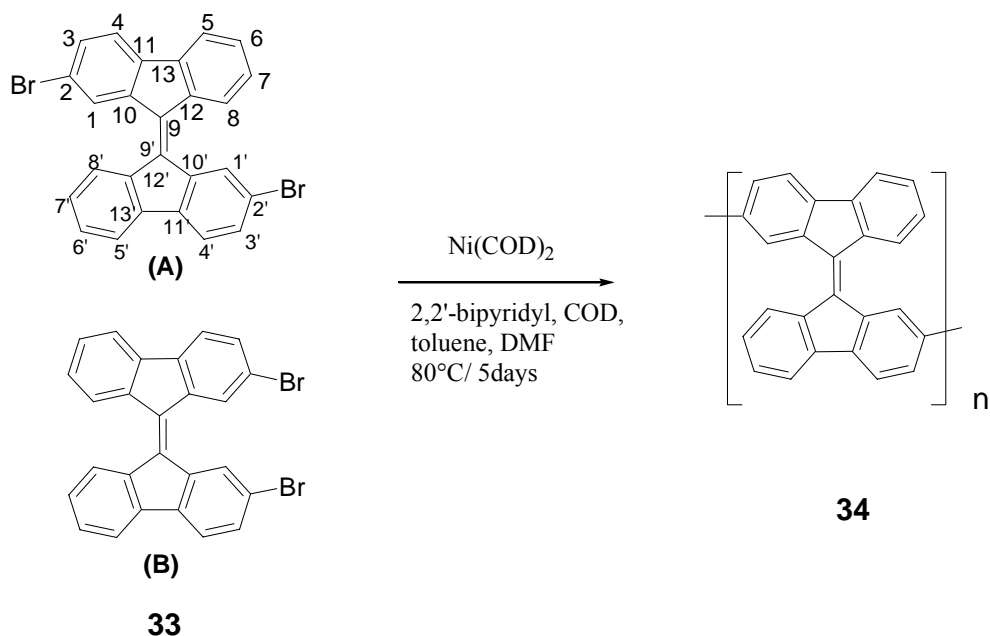


**Scheme 18:** Mechanism of the *Yamamoto*-type coupling reaction

The *Yamamoto*-type aryl-aryl-coupling uses stoichiometric amounts of Ni(COD)<sub>2</sub> [65]. A general catalytic cycle proceeds through the following cycle mediated by organonickel species.



In the reaction cycle oxidative addition of halides to the transition metal complex, e.g. Ni(0), occurs followed by transmetalation, and subsequent reductive elimination to give the coupling product. However this mechanism is not fully accepted.



**Scheme 19:** Yamamoto-type coupling reaction of **33** to polymer **34**

$^1\text{H}$  NMR-spectroscopy shows broad signals typical for polymers in the aromatic/olefinic region between 8.42-8.28 ppm 7.20-7.70 ppm (multiplet). The  $^{13}\text{C}$  NMR-spectrum of poly(9,9'-bisfluorenylidene-2,2'-diyl) **34** consists of one group of 12 signals in the aromatic/olefinic region.

Gel permeation chromatography (GPC) for poly(9,9'-bisfluorenylidene-2,2'-diyl) **34** was measured in toluene (PS calibration):  $M_n/M_w = 4,600/11,000 \text{ gmol}^{-1}$ . UV/Vis absorption spectra for poly(9,9'-bisfluorenylidene-2,2'-diyl) **34** was measured in chloroform. The spectrum shows a strong absorption feature peaking at  $\lambda_{\text{max}} = 310$  and 460 nm. The peak at 460 nm corresponds to the  $\pi$ - $\pi^*$  transition of the conjugated system of **34**. In comparison to the 9,9'-bisfluorenylidene monomer **33** ( $\lambda_{\text{max}} = 460$  nm) the absorption of **34** is red-shifted by 320 nm due to conjugative interactions between the BFD units.

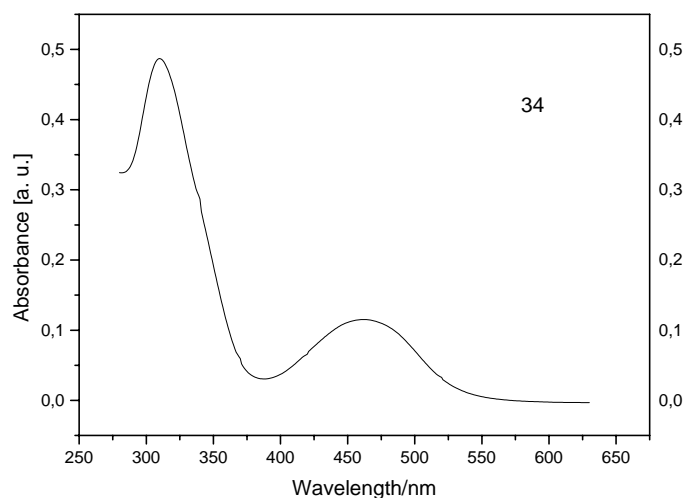
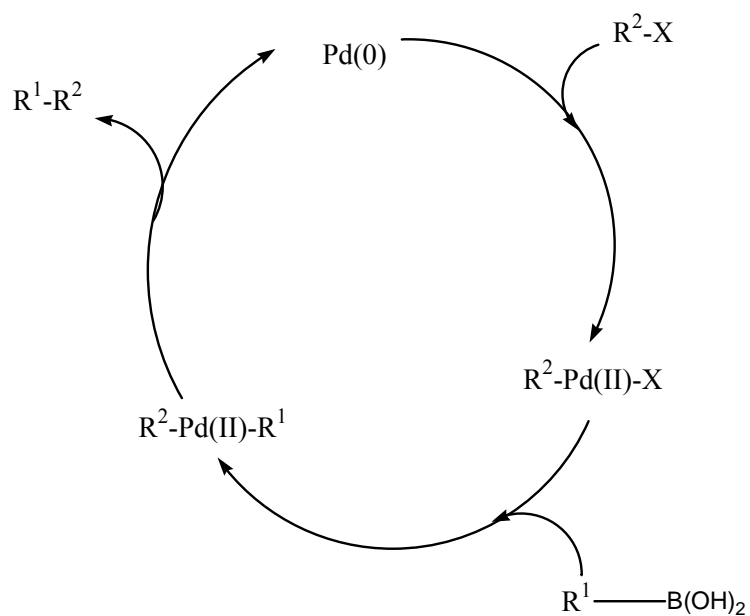


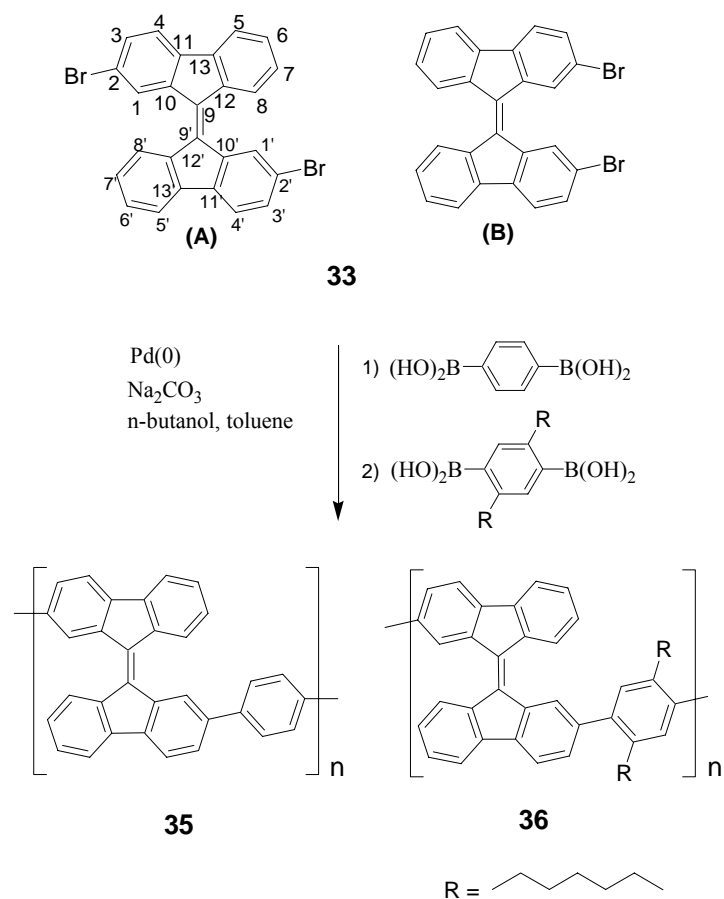
**Fig. 33:** UV/Vis absorption spectrum of **34** in chloroform at room temperature.

The polymer synthesized by the *Yamamoto-type* coupling reaction was of relatively poor solubility (only in halogenated solvents). To get polymers with better solubility, alternating copolymers with additional 1,4-phenylene building blocks (alkylated/non-alkylated) were synthesized by a *Suzuki-type coupling reaction* using a palladium catalyst. Monomers are the *cis/trans* mixture of 2,2'-dibromo-9,9'-bisfluorenylidene **33** and 1,4-phenylene-bisboronic acids in a 1:1 molar ratio. 5 mol% of  $\text{PdCl}_2(\text{PPh}_3)_2$  catalyst and toluene as solvent were used (scheme **21**).

A general catalytic cycle for the *Suzuki-type* <sup>[53]</sup> cross-coupling reaction involves oxidative addition, transmetalation and subsequent elimination (scheme **20**). Oxidative addition is often the rate determining step in the catalytic cycle. An electron withdrawing group on the aryl halide increases the reactivity towards palladium catalysts. Normally the transmetalation between organopalladium(II) halide and organoboron compounds does not occur readily due to the moderate nucleophilicity of organic group on boron atom. However, the reaction is carried out under basic condition so that the nucleophilicity of boron atom can be enhanced by forming a so-called “ate” complex with negatively charged base. Such “ate” complexes undergo a clean transmetalation reaction with the aryl halide.



**Scheme 20:** A general catalytic cycle for the cross-coupling reaction after Suzuki



**Scheme 21:** Suzuki-type cross coupling reaction of **33** with 1,4-phenylene diboronic acids to copolymers **35** and **36**

The bisfluorenylidene-phenylene alternating copolymers were synthesized with unsubstituted 1,4-phenylene and dialkylsubstituted 2,5-dialkyl-1,4-phenylene units.  $^1\text{H}$  NMR- and  $^{13}\text{C}$  NMR data of copolymers **35** and **36** are given in the experimental section. The GPC analysis for copolymers **35** and **36** were done in toluene solution (PS calibration), providing a  $M_n/M_w = 5,600/9,200$  for polymer **35**, and  $M_n/M_w = 1,900/4,500 \text{ gmol}^{-1}$  for polymer **36**. The reason for the low molecular weights for copolymer **36** may be the steric hindrance during the coupling due to the presence of the additional alkyl substituents.

UV/Vis absorption spectra for poly(1,4-phenylene-*co*-9,9'-bisfluorenylidene-2,2'-diyl) **35** and poly(2,5-dialkyl-1,4-phenylene-*co*-9,9'-bisfluorenylidene-2,2'-diyl) **36** were measured in chloroform solution at room temperature. Figure **34** shows the UV/Vis absorption spectras for copolymers **35** and **36** in chloroform.

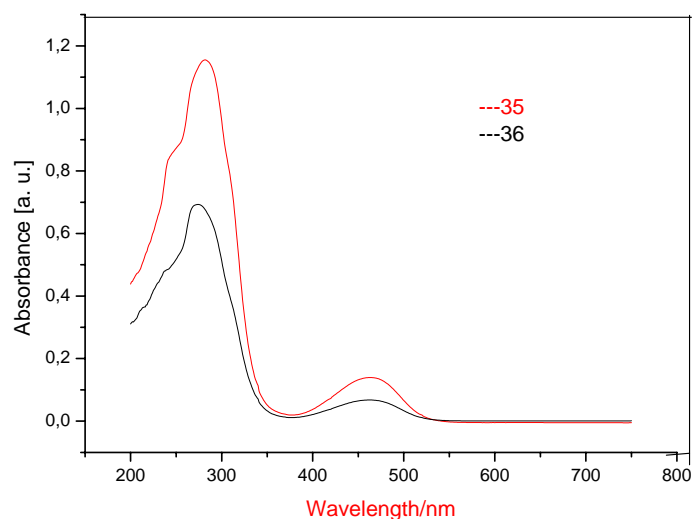


**Fig. 34:** UV/Vis absorption spectrum of **35** and **36** in chloroform solution at room temperature.

Poly(1,4-phenylene-*co*-9,9-bisfluorenylidene-2,2-diyl) **35**, and poly(2,5-dialkyl-1,4-phenylene-*co*-9,9-bisfluorenylidene-2,2'-diyl) **36** show nearly identical absorption spectra with two absorption bands at  $\lambda_{\text{max}} = 290$  and at 460 nm. The long wavelength band is typical for the BFD unit ( $\lambda_{\text{max}} = 460$  nm). Due to a conjugative interaction of the 9,9'-bisfluorenylidene and phenylene building

blocks within the conjugated main chain of **35** and **36**, the long wavelength absorption maximum of the copolymers is red-shifted by 320 nm with respect to the monomeric BFD **33**.

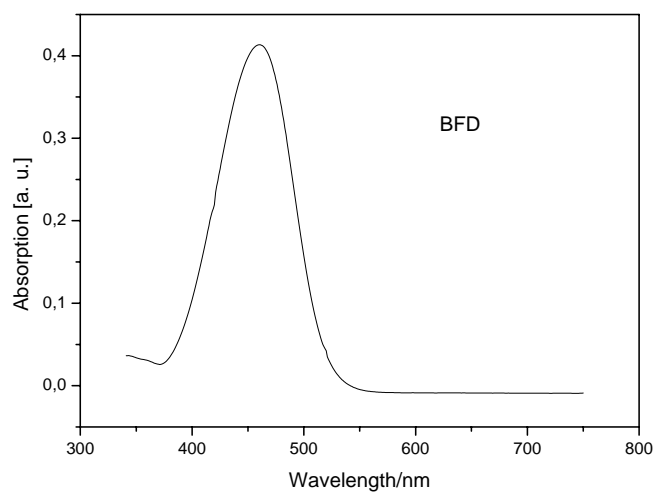


**Fig. 35:** *UV/Vis-absorption spectrum of 2,2'-dibromo-9,9'-bisfluorenylidene 33 in chloroform at room temperature*

## **4 Experimental**

---

### **4.1 Instrumental Details**

#### **Circular dichroism**

Circular dichroism measurements were carried out with JASCO CD spectrometer (Model J-715) using a cylindrical quartz cell (0.1 mL). Spectra were recorded at room temperature with scanning speed of 20 nm/min. CD solution spectra was measured in methanol/chloroform (95/5) solution with concentration of 0.2 mg/ml.

#### **Differential scanning calorimetry**

Differential scanning calorimetry (DSC) was measured on a Mettler DSC 30 with heating and cooling rates of 10 K/min. First order transition temperatures were reported as the minima of their endothermic peaks during heating, or as maxima of the exothermic peaks during the cooling cycle.

#### **Fluorescence spectrometer**

Fluorescence spectra were measured at room temperature in chloroform solution on Hitachi F-2500 Fluorescence Spectrophotometer.

#### **Gel permeation chromatography (GPC)**

Gel permeation chromatography measurements were carried out using a Thermo Separation Products (TSP) setup with RI-(Shodex RI-71) and UV-detector (TSP UV 1000). Linear columns, toluene as a solvent and PS calibration.

#### **IR-Spectroscopy**

Infrared spectroscopy measurements were performed on a Nicolet, Model Impact 400 spectrophotometer. Samples were prepared as KBr pellets and measured in the 400 to 4000  $\text{cm}^{-1}$  region.

#### **Melting Point**

Melting points were determined on a Büchi hot stage apparatus and are uncorrected.

### **Mass Spectroscopy**

Mass spectra were obtained on VG Instrument ZAB 2-SE-FPD by using FD ionization..

### **Elemental analysis**

Elemental analysis were carried out on a Foss Heraeus Vario EL.

### **NMR-Spectroscopy**

<sup>1</sup>H-NMR and <sup>13</sup>C-NMR spectra are recorded in CD<sub>2</sub>Cl<sub>2</sub>, CDCl<sub>3</sub>, C<sub>2</sub>D<sub>2</sub>Cl<sub>4</sub>, or THF on a Bruker DPX 250, Bruker AMX 300 and Bruker DRX 500 with use of the solvent proton or carbon signal as internal standard.

### **Polarizing Light Microscopy**

Polarizing Light microscopy was carried out using a Microscope Olympus (model BX50). Images were taken on a digital camera directly connected to the microscope.

### **UV/Vis absorption spectroscopy**

UV/Vis spectras were recorded at room temperature on Perkin-Elmer Lambda 9 or Perkin-Elmer Lambda 5 spectrometers.

### **X-Ray diffraction- wide angle x-ray scattering (WAXS)**

X-ray diffractograms of powdered compounds were obtained using Bruker wide angle powder diffractometer model D8 operating in the Bragg configuration using *Cu-K<sub>α</sub>* radiation ( $\lambda = 1.542 \text{ \AA}$ ). As additional components at the primary side a 6-cm long “Global Mirror” with the monochromator angle of  $1.28^\circ 2\theta$  was used as well as “Solar slot” or “Solar diaphragm” between the sample and detector in the path of X-rays. The intensity of X-ray reflections depending on the angle was measured by means of a scintillation counter.

### **Materials**

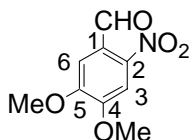
(*S*)-1-Bromo-3,7-dimethyloctane was synthesized according to standard literature procedure<sup>[89]</sup> using commercially available 3(*S*)-3,7-dimethyl-6-octene-1-ylbromide from Aldrich. 325 mesh, Titanium powder was used as



received from Alfa-aesar.  $[\text{PdCl}_2(\text{dppf})]$  and  $\text{Pd}(\text{PPh}_3)_4$  were used as received from Strem.

### 4.2 Monomers and Polymers

#### 4.2.1 2-Nitro-4,5-dimethoxybenzaldehyde **12**



#### **12**

Nitric acid (70%, 10 mL) was cooled to 0°C, vertraldehyde, (2.0 g, 12 mmol) was added with stirring, and the mixture was warmed to room temperature over 1 h and then poured into ice water (100 mL). The resulting yellow solid was collected by filtration, washed with cold water and cold ethanol, dried, and recrystallized from 95% ethanol, affording **12** (2.3 g, 90%) in the form of yellow needles, mp 132°C<sup>[45]</sup>.

#### <sup>1</sup>H NMR-spectrum (300 MHz, CDCl<sub>3</sub>):

$\delta(^1\text{H})$  [ppm]: 10.43 (s, 1H, -CHO), 7.60 (s, 1H, H3), 7.41 (s, 1H, H6), 4.01 (s, 6H, -OMe).

#### <sup>13</sup>C NMR-spectrum (75 MHz, CDCl<sub>3</sub>)

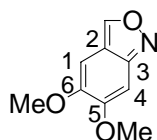
$\delta(^{13}\text{C})$  [ppm]: 190 (-CHO), 154.3 (C4), 154.2 (C5), 142.2 (C2), 125.7 (C1), 117.8 (C6), 110.5 (C3), 56.7 (C-OMe)

**IR:** 2930 (w), 1685 (s), 1600 (s), 1570 (s), 1505, 1460, 1395, 1332 (s), 1280 (s), 1160, 1060, 880 cm<sup>-1</sup>.

**MS** (rel int) m/z: 211.039 (M<sup>+</sup>, 21.6), 164.061 (18.8), 162.007 (17.0), 151.017 (13.3), 150.007 (14.9), 138.037 (23.4), 137.025 (15.5), 136.052 (53.6), 135.013 (14), 125.060 (49.0), 113.002 (23.8), 110.035 (46), 96.987 (34.7), 78.971 (38.9).

UV/Vis (chloroform):  $\lambda_{\text{max abs}} = 264, 350 \text{ nm}$ .

#### 4.2.2 5,6-Dimethoxyanthranil **13**



#### **13**

Tin foil (1.30 g, 11 mmol) was added in small pieces to stirred solution of **12** (500 mg, 2.37 mmol) in glacial acetic acid (15 mL), and the mixture was stirred at room temperature for 20 h and then extracted with diethylether. The organic layer was dried over anhydrous sodium sulfate, solvent was removed under reduced pressure and the residue was purified by column chromatography (silica gel, hexane-ethylacetate (8:2) followed by recrystallization from hexane-ethyl acetate, affording 5,6-dimethoxyanthranil **13** (230 mg, 54%) in the form of white needles, mp 110°C<sup>[45]</sup>.

#### <sup>1</sup>H NMR-spectrum (300 MHz, CDCl<sub>3</sub>):

$\delta(^1\text{H})$  [ppm] : 8.79 (s, 1H, -CHO), 6.76 (s, 1H, H4), 6.62 (s, 1H, H6), 3.94 (s, 3H, -OMe), 3.88 (s, 3H, OMe).

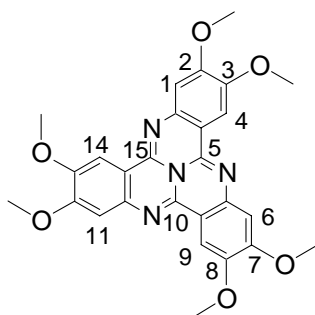
#### <sup>13</sup>C NMR-spectrum (75 MHz, CDCl<sub>3</sub>)

$\delta(^{13}\text{C})$  [ppm] : 158.9 (-CHO), 150.2 (C3), 147.6 (C5), 147.6 (C6), 115.6 (C4), 115.7 (C1), 100.5 (C2), 56.7 (C-OMe)

IR: 2930, 2840, 1700 (s), 1568, 14951 (s), 1460 (s), 1365 (s), 1300 (s), 1270(s), 1160 (s), 1105(s), 1010 (s), 840 (s) cm<sup>-1</sup>.

MS (rel int): Positive Desorption Chemical Ionisation (DCI), 180.0 (M<sup>+</sup>, H), negative DCI, 179.2 (M<sup>-</sup>)

UV/Vis (chloroform):  $\lambda_{\text{max abs}} = 282, 292 \text{ nm}$ .

4.2.3 2,3,7,8,12,13-Hexamethoxytricycloquinazoline **14****14**

Dimethoxyanthranil **13** (200 mg, 1.12 mmol) and ammonium acetate (600 mg, 7.79 mmol) were added to a mixture of sulfolane (5 mL) and acetic acid (2 mL). The mixture was refluxed for 72 h and cooled to room temperature, water (15-20 mL) was added, and the resulting greenish yellow solid was collected by filtration, washed with water and then with methanol, and dried to give 2,3,7,8,12,13-hexamethoxytricycloquinazoline **14** (50 mg, 26.8 %).

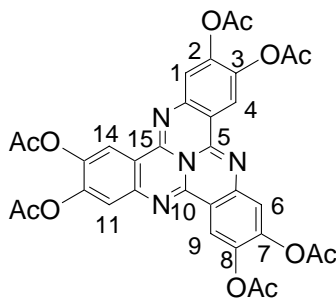
**<sup>1</sup>H NMR-spectrum (300 MHz, CDCl<sub>3</sub>):**

$\delta(^1\text{H})$  [ppm] : 7.61 (s, 3H, H4, H9, H14), 6.82 (s, 3H, H1, H6, H11), 3.99 (s, 9H -OMe), 3.96 (s, 9H, OMe).

**<sup>13</sup>C NMR-spectrum (75 MHz, CDCl<sub>3</sub>)**

$\delta(^{13}\text{C})$  [ppm]: 164.4, 150.7, 147.6, 143.9 119.7 113.4, 108.7 and 58.1 (-OMe)

**MS** (rel int): Positive DCI, 501.3 ( $\text{M}^+$ , H), negative DCI 500.2 ( $\text{M}^-$ )

4.2.4 2,3,7,8,12,13-Hexaacetoxytricycloquinazoline **16****16**

## 4. Experimental

Concentrated HCl (22 mL) was added to pyridine (20 mL) with rapid stirring and the mixture was heated to 220°C to remove water. The resultant molten salt was cooled to 140°C, 2,3,7,8,12,13-Hexamethoxytricycloquinazoline **14** (1 g, 2 mmol) was added and the reaction mixture was heated to 230 °C for 3 h, and then cooled to 100°C. An excess of dry pyridine (10 mL) followed by acetic anhydride (5 mL) was added and the reaction mixture was left at room temperature for 48 h under inert condition. Ice water was added and the resultant dark green precipitate was collected by filtration, washed with water and with excess of methanol, and dried under vacuum to yield **16** (1.2 g, 90%).

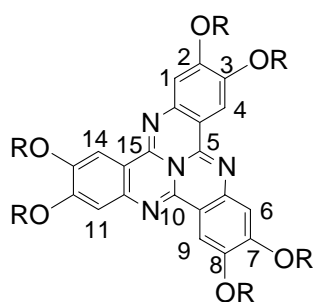
### <sup>1</sup>H NMR-spectrum (300 MHz, CDCl<sub>3</sub>):

$\delta(^1\text{H})$  [ppm]: 8.21 (s, 3H, H4, H9, H14), 7.35 (s, 3H, H1, H6, H11), 2.34 (s, 18H, -OCOCH<sub>3</sub>).

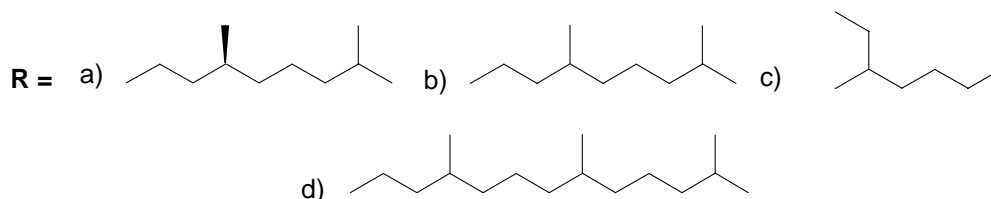
### <sup>13</sup>C NMR-spectrum (75 MHz, CDCl<sub>3</sub>)

$\delta(^{13}\text{C})$  [ppm]: 168.3 (C=O), 165.7, 151.2, 146.5, 141.9, 123.7, 121.1, 115.7, 17.8 (6 Me carbons)

### 4.2.5 2,3,7,8,12,13-Hexaalkoxytricycloquinazolines **17a-d**

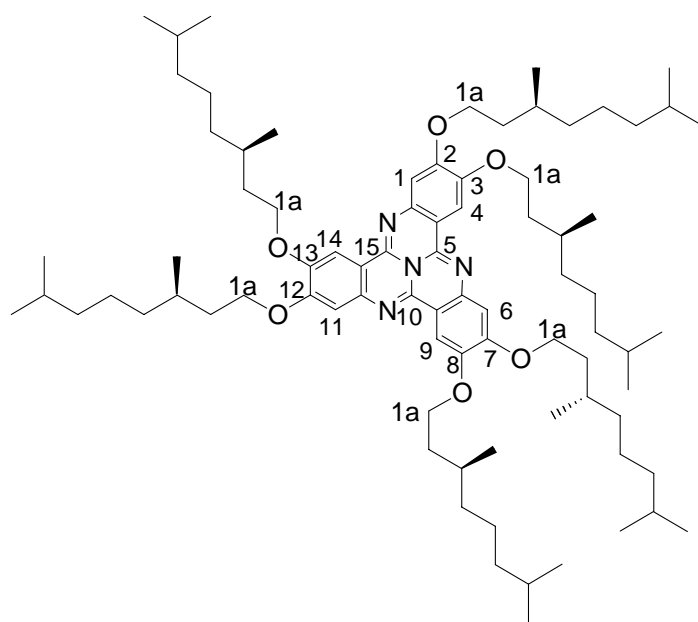


**17**



**General Procedure:**

Powdered KOH (135 mg, 2.4 mmol) was mixed with DMSO (2mL) at room temperature and stirred for 10 minutes. 2,3,7,8,12,13-Hexaacetoxytricycloquinazoline **16** (66.8 mg, 0.1 mmol) followed by appropriate alkyl bromide (2.4 mmol) was added and the reaction mixture was stirred at 55°C for 24 h. Then, work up was done by addition of ice water and extraction with diethyl ether. The crude product was purified by column chromatography (silica gel, hexane-ethyl acetate 8:2) and crystallized or precipitated with ether-acetone to afford **17** yellow crystals in about 80% yield.

**4.2.6 2,3,7,8,12,13-hexa-[(S)-3,7-dimethyloctyloxy]tricycloquinazoline  
17a (S)****TCQ-17a (S)****<sup>1</sup>H NMR-spectrum (300 MHz, CDCl<sub>3</sub>):**

$\delta(^1\text{H})$  [ppm]: 7.69 (s, 3H, H1, H6), 6.91 (s, 3H, H4, H9, H14), 4.02 (t, 12H,  $J=6.2$ , H1a,  $\alpha$ -CH<sub>2</sub>), 1.85 (m, 6H), 1.6-1.3 (m, 48H), 0.96 (m, 36H).

**<sup>13</sup>C NMR-spectrum (75 MHz, CDCl<sub>3</sub>)**

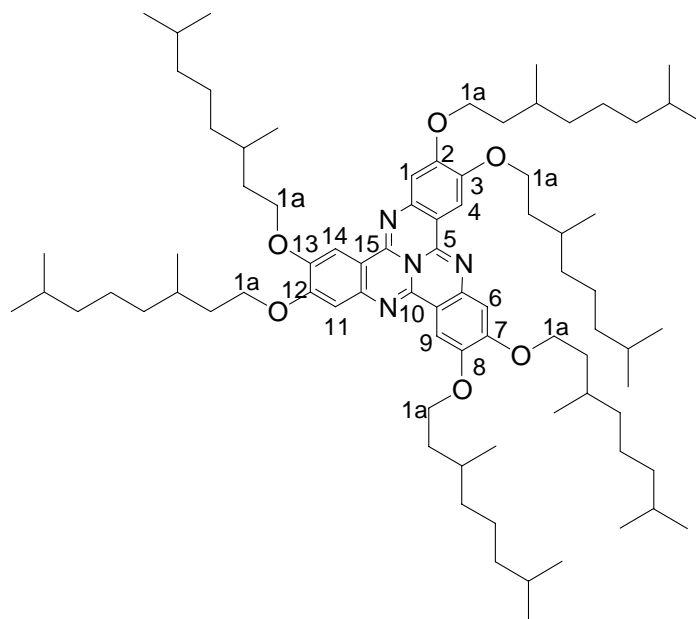
## 4. Experimental

$\delta(^{13}\text{C})$  [ppm]: 165.1, 150.3, 147.1, 143.9 119.7, 113.2, 108.7, 70.1, 39.7, 37.5, 28.5, 28.3, 25.1, 22.3, 20.1 (alkyl chain carbons)

UV/Vis (chloroform):  $\lambda_{\text{max abs}}$ =282, 322, 400, 422, 450 and 482 nm

IR : 3660, 2990, 2855, 1625, 1485, 1465, 1385, 1290, 1100, 1000, 870  $\text{cm}^{-1}$ .

### 4.2.7 Racemic 2,3,7,8,12,13-Hexaalkoxytricycloquinazolines TCQ 17b



**17b**

$^1\text{H}$  NMR-spectrum (300 MHz,  $\text{CDCl}_3$ ):

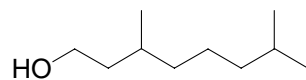
$\delta(^1\text{H})$  [ppm]: 7.69 (s, 3H, H1, H6), 6.91 (s, 3H, H4, H9, H14), 4.02 (t, 12H,  $J=6.2$ , H1a  $\alpha\text{-CH}_2$ ), 1.85 (m, 6H), 1.6-1.3 (m, 48H), 0.96 (m, 36H alkyl).

$^{13}\text{C}$ -NMR spectrum (75 MHz,  $\text{CDCl}_3$ )

$\delta(^{13}\text{C})$  [ppm]: 165.1, 150.3, 147.1, 143.9 119.7, 113.2, 108.7, 70.1, 39.7, 37.5, 28.5, 28.3, 25.1, 22.3, 20.1 (alkyl chain carbons)

UV/Vis (chloroform):  $\lambda_{\text{max abs}}$  = 282, 322, 400, 422, 450 and 482 nm

IR : 3660, 2990, 2855, 1625, 1485, 1465, 1385, 1290, 1100, 1000, 870  $\text{cm}^{-1}$ .

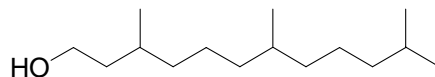
**4.2.8 3,7-Dimethyl-1-octanol 37****37**

Citronellol (39.00 g 0.25 mol) in ethyl acetate (500 mL) was hydrogenated over Adams catalyst (200 mg) under magnetical stirring. It was then filtered off over silica gel to get rid of catalyst and solvent evaporated in vacuum; yield 39.1 g (99 %) of liquid 3,7 dimethyl-1-octanol.

**<sup>1</sup>H NMR-spectrum (300 MHz, CDCl<sub>3</sub>):**

**δ(<sup>1</sup>H) [ppm]:** 0.90 (9H, d, CH<sub>3</sub>), 1.23 (8H, s, CH<sub>2</sub>), 1.50 (2H, m, CH), 1.85 (1H, s, OH), 3.65 (2H, t, OCH<sub>2</sub>).

**FD-MS (m/z):** 157 (M<sup>+</sup> - H), 140 (M<sup>+</sup> - H<sub>2</sub>O).

**4.2.9 3,7,11-trimethyl-1-dodecanol 38****38**

Farnesol (55.00 g 0.25 mol) in ethyl acetate (500 ml) was hydrogenated over Adams catalyst (200 mg) under magnetical stirring using the same procedure as for **37**. 3,7,11-trimethyl-1-dodecanol **38** was obtained as a yellow liquid in 55.6 g (99%).

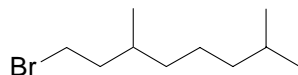
**<sup>1</sup>H NMR-spectrum (300 MHz, CDCl<sub>3</sub>):**

**δ(<sup>1</sup>H) [ppm]:** 0.87 (t, 6H, <sup>3</sup>J = 8.0 Hz), 0.90 (12H, d, CH<sub>3</sub>), 1.23 (14H, s, CH<sub>2</sub>), 1.50 (3H, m, CH, <sup>3</sup>J = 8.0 Hz, -CH(CH<sub>3</sub>)<sub>2</sub>), 2.62 (1H, s, OH), 3.65 (2H, t, OCH<sub>2</sub>).

**$^{13}\text{C}$  NMR-spectrum (75 MHz,  $\text{CDCl}_3$ )**

$\delta(^{13}\text{C})$  [ppm]: 61.2, 40.1, 39.9, 39.3, 37.4, 29.5, 27.9, 24.3, 22.7, 22.6, 19.7, 19.6.

**FD-MS** (m/z): 227 ( $\text{M}^+ - \text{H}$ ), 210 ( $\text{M}^+ - \text{H}_2\text{O}$ ).

**4.2.10 1-Bromo-3,7-dimethyloctane 39****39**

To a solution of (60 g 0.38 mol) 3,7-dimethyl-1-octanol **37** and 109.5 g (0.42 mol) of triphenylphosphine in 200 ml dichloromethane 71 g (0.40 mol) of N-bromosuccinimide was added in portions, with occasional ice-bath cooling, keeping the temperature below 30°C. After stirring for 16 h at room temperature, the solvent was removed in vacuum. The residue was extracted with 500 ml hexane and filtered off. After evaporation of the solvent, distillation (37°C, 0.005 nm Hg) gave 71.8 g (86 %) of a colorless liquid.

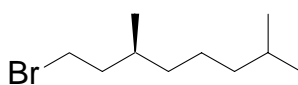
 **$^1\text{H}$  NMR spectrum (300 MHz,  $\text{CDCl}_3$ ):**

$\delta(^1\text{H})$  [ppm]: 3.42 (t, 2H,  $\text{BrCH}_2$ ) 1.52 (m, 2H, CH), 1.24 (s, 8H,  $\text{CH}_2$ ), 0.89 (d, 9H,  $\text{CH}_3$ ).

 **$^{13}\text{C}$  NMR spectrum (75 MHz,  $\text{CDCl}_3$ )**

$\delta(^{13}\text{C})$  [ppm]: 40.1, 39.3, 36.7, 27.9, 24.3, 22.7, 19.7.

**FD-MS** (m/z): 221 ( $\text{M}^+$ ),

**4.2.11 (S)-3,7-dimethyloctylbromide 40****40**



Commercially available (S)-1-bromo-3,7-dimethyl-oct-2-ene (54.7g 0.25 mol) in ethyl acetate (500 mL) was hydrogenated over Adams catalyst (200 mg) under magnetical stirring using the same procedure as for **37**. (S)-3,7-dimethyloctylbromide (54.9 g 99%) **40** was obtained as a yellow liquid.

**<sup>1</sup>H NMR-spectrum (300 MHz, CDCl<sub>3</sub>):**

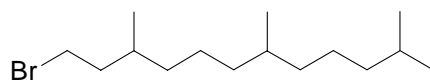
$\delta(^1\text{H})$  [ppm]: 3.42 (t, 2H, BrCH<sub>2</sub>) 1.52 (m, 2H, CH), 1.24 (s, 8H, CH<sub>2</sub>), 0.89 (d, 9H, CH<sub>3</sub>).

**<sup>13</sup>C NMR-spectrum (75 MHz, CDCl<sub>3</sub>)**

$\delta(^{13}\text{C})$  [ppm]: 40.1, 39.3, 36.7, 27.9, 24.3, 22.7, 19.7.

**FD-MS (m/z):** 157 (M<sup>+</sup> - H), 140 (M<sup>+</sup> - H<sub>2</sub>O).

#### 4.2.12 1-Bromo-3,7,11-trimethyldodecane **41**



**41**

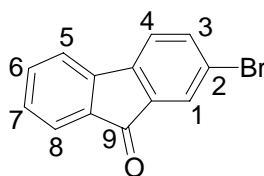
To a solution of 3,7,11-trimethyl-1-dodecanol **38** (86.64 g, 0.38 mol) and 109.50 g (0.42 mol) of triphenylphosphine in 200 ml dichloromethane, 71.00 g (0.40 mol) of N-bromosuccinimide, were added in portions, followed by the same reaction procedure as for **39**. 1-Bromo-3,7,11-trimethyldodecane **41** (103.7 g, 89%) was obtained as a colorless liquid.

**<sup>1</sup>H NMR-spectrum (300 MHz, CDCl<sub>3</sub>):**

$\delta(^1\text{H})$  [ppm]: 0.90 (12H, d, CH<sub>3</sub>), 0.78 (t, 6H, <sup>3</sup>J = 6.59 Hz, -CH<sub>3</sub>), 0.76 (t, 6H, <sup>3</sup>J = 6.59 Hz, -CH<sub>3</sub>), 1.25 (14H, s, CH<sub>2</sub>), 1.65 (3H, m, CH), 3.45 (2H, t, BrCH<sub>2</sub>).

**<sup>13</sup>C NMR-spectrum (75 MHz, CDCl<sub>3</sub>)**

$\delta(^{13}\text{C})$  [ppm]: 41.2, 39.9, 39.3, 37.4, 29.5, 27.9, 24.3, 22.7, 22.6, 19.7, 19.6.

**4.2.13 2-Bromo-9-fluorenone 32****32**

2-Bromofluorene (20 g, 77.22 mmol) and sodium dichromate (40 g, 152.67 mmol) were dissolved in 240 ml of acetic acid under argon atmosphere and heated to reflux for 6 hours. It was then allowed to cool to room temperature. Water was added to the reaction mixture, the mixture was stirred again for another 10-15 min. The solid was filtered through the Buechner funnel. The residue was washed several times with water to get a yellow solid. It was recrystallised from 600 ml of ethanol. The yellow crystals formed were filtered off through a funnel to get 15.4 g of 2-bromo-9-fluorenone **32** (73.12%).

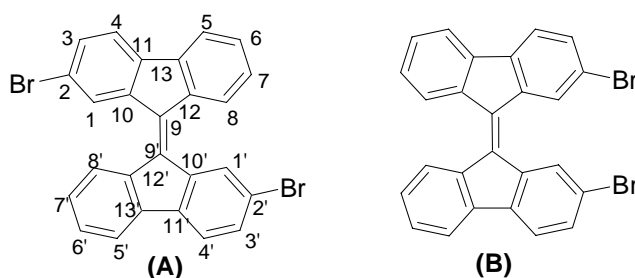
**<sup>1</sup>H NMR spectrum (300 MHz, CDCl<sub>3</sub>):**

$\delta(^1\text{H})$  [ppm]: 7.68 (s, 1H, H1), 7.93 (d, 1H, H3), 7.47 (d, 1H, H4), 7.58 (d, 1H, H5), 7.51 (m, 1H, H6), 7.32 (m, 1H, H7), 7.76 (m, 1H, H8)

**<sup>13</sup>C-NMR spectrum (75 MHz, CDCl<sub>3</sub>)**

$\delta(^{13}\text{C})$  [ppm]: 187.5 (-C=O), 138.9, 138.2, 137.2, 136.7, 136.3, 133.9, 132.7, 130.6, 129.3, 127.1, 127.1, 121.7.

**FD-MS** (m/z) : 258

4.2.14 2,2'-Dibromo-9,9'-bisfluorenylidene (*cis/trans*-mixture) **33****33**

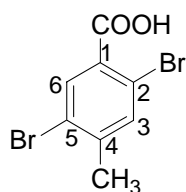
Titanium powder (0.79 g, 16.55 mmol) was suspended in DME (10 mL), TMS-Cl (2.0 mL, 16.6 mmol) was added, and the mixture was refluxed for 67 h under argon. 2-Bromo-9-fluorenone (1.3 g, 5.06 mmol) was added at once to the boiling suspension, and reflux was continued for 4 h. The mixture was allowed to cool to ambient temperature and filtered through a short pad of silica, the insoluble residues were rinsed with THF in several portions (ca. 100 mL), the combined filtrates were evaporated, and the residue was purified by flash chromatography (SiO<sub>2</sub>, hexane-ethyl acetate, 10:1, as eluent), affording 2,2'-dibromo-9,9'-bisfluorenylidene **33** (0.90g, 89%) as orange-red crystals.

**<sup>1</sup>H NMR-spectrum (300 MHz, CDCl<sub>3</sub>):**

$\delta(^1\text{H})$  [ppm]: 8.48 (s, 2H, of E isomer), 8.42 (s, 2H, of Z isomer), 8.32 (d, J = 8 Hz, 2H, Z isomer, no NOE upon irradiation at 8.42), 8.28 (d, J = 8 Hz, 2H, E isomer, 18% NOE upon irradiation at 8.48), 7.20-7.70 (m, 20 H).

**<sup>13</sup>C NMR-spectrum (75 MHz, CDCl<sub>3</sub>)**

$\delta(^{13}\text{C})$  [ppm] : 120.1, 121.2, 126.7, 126.8, 127.4, 127.5, 129.3, 129.5, 129.8, 132.2, 120.7, 137.7, 137.8, 139.6, 139.8, 140.2, 140.7, 140.9

4.2.15 2,5-Dibromo-4-methylbenzoic acid **18****18**

## 4. Experimental

---

In a 1-litre one neck flask fitted with reflux condenser, 75 g (250 mmol) of 2,5-dibromo-p-xylol in a mixture of 200 ml of nitric acid (conc.) and 175 ml of water were refluxed. After 3 days the clear solution was cooled down to room temperature. 2,5-dibromo-4-methyl-benzoic acid **18** was obtained as a white solid. Recrystallization from acetic acid gave a white crystals in 89 % yield (64.0 g), mp 198-200°C.

### <sup>1</sup>H NMR-spectrum (500 MHz, DMSO-d<sub>6</sub>, 373K):

$\delta(^1\text{H})$  [ppm]: 7.89 (s, 1H, H6), 7.67 (s, 1H, H3), 2.37 (s, 3H, CH<sub>3</sub>).

### <sup>13</sup>C NMR-spectrum (125 MHz, DMSO-d<sub>6</sub>, 373 K):

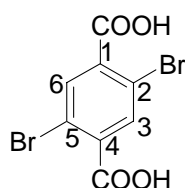
$\delta(^{13}\text{C})$  [ppm] :164.9 (C=O), 142.0, 135.3, 133.3, 132.2, 122.4, 118.7, 21.3 (-CH<sub>3</sub>).

**FT-IR (KBr):** 2964, 2671, 2538, 1677 (C=O), 1588, 1476, 1427, 1336, 1257, 1057, 932 cm<sup>-1</sup>

**FD-MS (m/z) :** 292.4

**Elemental analysis:** found and (calculated) for C<sub>8</sub>H<sub>6</sub>Br<sub>2</sub>O<sub>2</sub> (293.9); C: 32.21 (32.69) H: 2.01 (2.06) Br: 54.41 (54.37)

### 4.2.16 2,5-Dibromo-terephthalic acid **19**



### **19**

2,5-dibromo-4-methylbenzoic acid **18** (20 g, 68.1 mmol) was dissolved in 300 ml of KOH (4M) in 1-litre flask fitted with reflux condenser and addition funnel. The content of the flask were heated to 50°C. Then 24 g of KMnO<sub>4</sub> in 80 ml of water were added via the addition funnel. The reaction mixture was

refluxed for 4 h and then cooled down to room temperature. HCl was added until the reaction mixture was acidic. Excess of  $\text{MnO}_2$  was destroyed with saturated solution of  $\text{Na}_2\text{SO}_3$ . The product was filtered, washed with water, and dried under vacuum to give 18.5g of 2,5-dibromoterephthalic acid **19** (83.74%) as white crystals, mp  $322^\circ\text{C}$ .

**$^1\text{H}$  NMR-spectrum (500 MHz, DMSO- $d_6$ ):**

$\delta(^1\text{H})$  [ppm]: 7.82 (s, 2H)

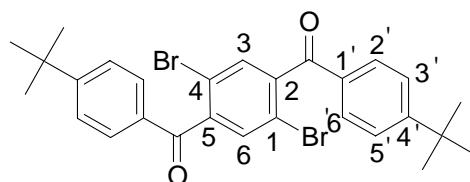
**$^{13}\text{C}$  NMR spectrum (125 MHz, DMSO- $d_6$ ):**

$\delta(^{13}\text{C})$  [ppm] : 172.4 (C=O), 147.1, 135.4, 132.1,

**FD-MS (m/z):** 323.1

**Elemental analysis:** found and (calculated) for  $\text{C}_8\text{H}_4\text{Br}_2\text{O}_4$  (323.9); C: 29.31 (29.66) H: 1.51 (1.24) Br: 49.31 (49.34)

#### 4.2.17 1,4-Dibromo-2,5-bis(4-*tert*-butylbenzoyl)benzene **22**



**22**

A mixture of 2,5-dibromo-terephthalic acid (7.08 g, 22.0 mmol), DMF (2-3 drops) and thionyl chloride (30 mL) was refluxed for 3 h (until a clear solution was obtained). The reaction mixture was then cooled down to room temperature. The excess of thionyl chloride was removed by evaporation and dried well under vacuum to get yellow solid. The product was immediately dissolved in 35 ml of dry dichloromethane, 7.0 g (52.0 mmol) of  $\text{AlCl}_3$  were added to the stirring mixture at  $0^\circ\text{C}$ . Then 13.35 ml (86.0 mmol) of *tert*-butyl benzene in 70 ml dichloromethane, were added dropwise. The reaction

mixture was stirred for 24 h at room temperature. The reaction mixture was quenched with 40 ml of 2N HCl. The organic phase was separated. Aqueous phase was washed three times with dichloromethane. Combined organic phases were washed with water, and dried over MgSO<sub>4</sub>. The solvent was then evaporated. Recrystallization of the crystalline product with acetone afforded yellow crystals of **22** in 77 % yield (9.42 g), mp. 268 °C.

**<sup>1</sup>H NMR-spectrum (500 MHz, C<sub>2</sub>D<sub>2</sub>Cl<sub>4</sub>):**

$\delta(^1\text{H})$  [ppm]: 7.70 (d, <sup>3</sup>J = 8.4 Hz, 4H, H3', H5'), 7.53 (s, 2H, H3, H6), 7.45 (d, <sup>3</sup>J = 8.4 Hz, 4H, H2', H6'), 1.28 (s, 18H, -CH<sub>3</sub>)

**<sup>13</sup>C NMR-spectrum (125 MHz, C<sub>2</sub>D<sub>2</sub>Cl<sub>4</sub>):**

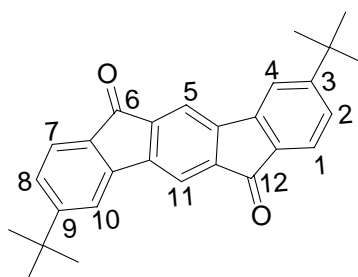
$\delta(^{13}\text{C})$  [ppm] :193.6 (C=O), 158.9, 143.5, 133.3, 132.8, 130.6, 126.3, 118.7, 35.6 (-C(CH<sub>3</sub>)<sub>3</sub>), 31.3 (-CH<sub>3</sub>).

**FT-IR (KBr):** 3082, 3051, 2963, 2932, 2867, 1672 (-C=O), 1602, 1561, 1463, 1408, 1311, 1273, 1108, 1064, 933, 890 cm<sup>-1</sup>

**FD-MS (m/z):** 556.1

**Elemental analysis:** found and (calculated) for C<sub>28</sub>H<sub>28</sub>Br<sub>2</sub>O<sub>2</sub> (556.3); C: 60.45 (60.33) H: 5.07 (5.01) Br: 28.73 (28.34).

**4.2.18 3,9-Di-*tert*-butyl-indeno[1,2-*b*]fluorene-6,12-dion **23****



**23**

1,4-Dibromo-2,5-bis(4-*tert*-butylbenzoyl)benzene **22** (4.7 g, 8.45 mmol), palladium(II) acetate (0.45 g; 2.00 mmol), and anhydrous sodium carbonate (2.60 g, 24.5 mmol) were suspended in 50 mL of dimethylacetamide (DMAc)

and refluxed for 12 h. The mixture was poured in water, and the precipitate formed was washed with 2-propanol until the alcoholic washing solution is colourless. Recrystallization from benzene gives 2.90 g (87.1%) of 3,9-di-*tert*-butyl-indeno[1,2-*b*]fluorene-6,12-dion **23**, mp. 325-327 °C.

**<sup>1</sup>H NMR spectrum (500 MHz, C<sub>2</sub>D<sub>2</sub>Cl<sub>4</sub>):**

$\delta(^1\text{H})$  [ppm]: 7.69 (s, 2H, H5, H11), 7.50 (d, 2H,  $^4J = 1.1$  Hz, H4/H10), 7.49 (d, 2H,  $^3J = 7.9$  Hz H1/H7), 7.26 (dd,  $^3J = 7.9$  Hz,  $^4J = 1.1$  Hz, 2H, H2/H8), 1.30 (s, 18H, -CH<sub>3</sub>)

**<sup>13</sup>C-NMR spectrum (125 MHz, C<sub>2</sub>D<sub>2</sub>Cl<sub>4</sub>):**

$\delta(^{13}\text{C})$  [ppm]: 191.9 (C=O), 159.7, 151.9, 143.2, 137.3, 135.7, 132.8, 129.4, 124.5, 119.9, 112.3, 35.9 (-C(CH<sub>3</sub>)<sub>3</sub>), 31.3 (-CH<sub>3</sub>).

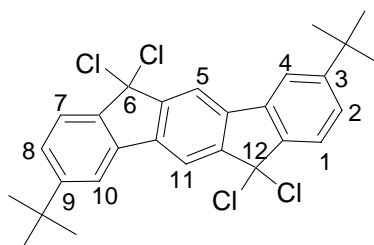
**FT-IR (KBr):** 3056, 2964, 2951, 2901, 2865, 1715, 1705, 1610, 1479, 1431, 1400, 1359, 1187, 1087, 928 cm<sup>-1</sup>

**FD-MS (m/z) :** 394.2

**Elemental analysis:** found and (calculated) for C<sub>28</sub>H<sub>26</sub>O<sub>2</sub> (394.5); C: 85.25 (85.33) H: 6.64 (6.66).

**UV/ Vis (CHCl<sub>3</sub>):**  $\lambda_{\text{max, Abs}}$ : 265, 284, 294, 342, 343, 467nm

**4.2.19 3,9-Di-*tert*-butyl-6,6,12,12-tetrachloro-6,12-dihydro indeno[1,2-*b*]-fluorene **24****



**24**

In a 100 ml single-neck flask fitted with a reflux condenser, a mixture of 3,9-di-*tert*-butyl-indeno[1,2-*b*]fluorene-6,12-dion **23** (830 mg, 2.10 mmol) and

$\text{PCl}_5$  (2.1 g, 10.1 mmol) were suspended in 10 ml of toluene. It was then refluxed for 18 h. After cooling the mixture the lemon coloured product formed was collected by filtration, carefully washed with diethylether, and recrystallized from carbon tetrachloride to give 3,9-di-tert-butyl-6,6,12,12-tetrachloro-6,12-dihydro-indeno[1,2-b]fluorene **24** (780 mg, 86.0 %), mp.  $255^\circ\text{C}$ .

**$^1\text{H}$  NMR-spectrum (500 MHz,  $\text{C}_2\text{D}_2\text{Cl}_4$ ):**

$\delta(^1\text{H})$  [ppm] : 8.00 (s, 2H, H5/H11), 7.72 (d,  $^3J = 8.0$  Hz, 2H, H1/H7), 7.68 (s, 2H, H4/H10), 7.44 (d,  $^3J = 8.0$  Hz, 2H, H2/H8), 1.40 (s, 18H,  $-\text{CH}_3$ )

**$^{13}\text{C}$  NMR-spectrum (125 MHz,  $\text{C}_2\text{D}_2\text{Cl}_4$ ):**

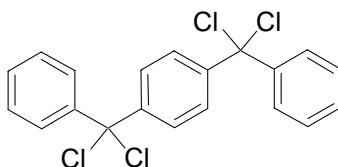
$\delta(^{13}\text{C})$  [ppm]: 155.3, 150.2, 144.4, 138.4, 135.9, 127.1, 124.5, 117.5, 116.6, 82.7 ( $-\text{CCl}_2$ ), 35.4 ( $-\text{C}(\text{CH}_3)_3$ ), 31.3 ( $-\text{CH}_3$ ).

**FT-IR (KBr):** 2960, 2901, 2864, 1615, 1566, 1487, 1475, 1434, 1403, 1391, 1361, 1279, 1254, 1204, 1194, 1155, 1094, 914, 895 884, 789, 757, 700, 678, 417,  $406\text{ cm}^{-1}$

**FD-MS (m/z) :** 504.0

**Elemental analysis:** found and (calculated) for  $\text{C}_{28}\text{H}_{26}\text{Cl}_4$  (504.3); C: 64.93 (66.68) H: 4.95 (5.20) Cl: 27.97 (28.12).

**4.2.20 1,4-Bis(phenyldichloromethyl)benzene 29**



**29**

In a 100 ml single-neck flask fitted with a reflux condenser a mixture of 1,4-dibenzoyl benzene (1.80 g, 6.29 mmol) and  $\text{PCl}_5$  (6.29 g, 30.1 mmol) was



suspended in 25 ml of toluene. The mixture was then refluxed for 5 h. An oily product was formed after cooling down to room temperature. Hexane was then added, the mixture kept overnight in the refrigerator. The solid formed was filtered off and washed with cold hexane until the crystals are white, which was then dried well (Yield 1.72 g, 69 %).

### **$^1\text{H}$ NMR-spectrum (500 MHz, $\text{CDCl}_3$ ):**

$\delta(^1\text{H})$  [ppm] : 7.89 (s, 4H, H1), 7.80 (d, 4H, H1'), 7.40 (dd, 4H, H2'), 7.40 (m, 2H, H3')

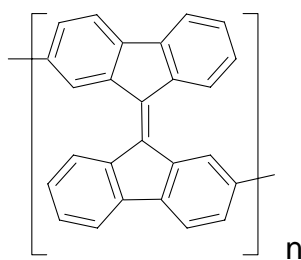
### **$^{13}\text{C}$ NMR spectrum (125 MHz, $\text{CDCl}_3$ ):**

$\delta(^{13}\text{C})$  [ppm] = 143.1, 129.7, 129.2, 128.9, 128.2, 127.5, 91.1 ( $-\text{C}(\text{Cl})_2$ )

**FD-MS** (m/z) : 397

**Elemental analysis:** found and (calculated) for  $\text{C}_{20}\text{H}_{14}\text{Cl}_4$  (397); C: 60.68 (60.14) H: 3.56 (3.53) Cl: 35.80 (34.95).

### **4.2.21 Poly[9,9'-bisfluorenylidene-2,2'-diyl] 34**



**34**

#### a) Synthesis (Yamamoto-type coupling) <sup>[65]</sup>.

Two Schlenk tubes sealed with rubber stoppers were taken. They were evacuated and dried thoroughly with a heat gun. One schlenk tube was flushed with argon and filled with the monomer under a light stream of argon. It was sealed with a rubber stopper and dry toluene (45 mL) was added using a

syringe. The monomer was completely dissolved using an ultrasonic bath. The first schlenk tube was transferred into a glove box and flushed with argon. The tube was filled with Ni(COD)<sub>2</sub> and 2,2'-bipyridyl and sealed again with a new rubber stopper. Once outside the glovebox, dry DMF (15 mL) and dry toluene (15 mL) were added to the schlenk tube using a syringe. The solution turned deep blue (almost black) after a while. The tube was put in an ultrasonic bath for one minute and wrapped completely with aluminium foil to exclude light. The tube was transferred into an oil bath (80° C) and vigorously stirred. 1,5-Cyclooctadiene (COD) was added with a syringe, and the tube was kept at that temperature for 35-40 minutes. Next, the monomer was transferred from the second schlenk tube into the reaction mixture using a syringe. The reaction was carried out at 80° C for 7 days.

b) Isolation: The reaction was stopped by adding 10 mL of a 4M solution of HCl in dioxane. After addition HCl the mixture was stirred for 15 minutes. The tube was then filled with trichloromethane, stirred for another 15 minutes at 80 °C and finally shaken well. The complete mixture was transferred into a extraction funnel and 2N HCl (100 mL) and trichloromethane (200 mL) were added. The phases were separated, the organic phase was treated once again with aqueous 2N HCl. The organic phase was then treated with saturated aqueous Na<sub>2</sub>-EDTA solution and washed with saturated aqueous NaHCO<sub>3</sub> solution and treated once again with the aqueous Na<sub>2</sub>-EDTA solution. The organic phase was passed through a short column with a filter plate of high porosity and a small layer of celite 545 (Aldrich 45,993-1), a considerable amount of silica gel and a thin layer of sand. Afterwards, the solvent was evaporated until the solution becomes viscous. Then, the polymer was precipitated into methanol, acetone and conc. hydrochloric acid (1:1:1) using a pasteur pipette. The polymer was collected by filtration and dried under vacuum.

c) Purification: The polymer was transferred into a glass fiber thimble and extracted with ethyl acetate in a soxhlet extractor for 5 days (it is noticed that

## 4. Experimental

---

one day was sufficient in most cases). The resulting solution containing a considerable amount of low molecular weight polymer may be used for other purposes. The high molecular weight polymer was taken out of the thimble and dried briefly. The product was dissolved in trichloromethane (spectroscopic grade) and washed with aqueous Na<sub>2</sub>-EDTA solution. The organic solution was dried over MgSO<sub>4</sub> and evaporated until the solution becomes viscous. The polymer was precipitated into methanol and acetone (2:1) (both HPLC grade), using a pasteur pipette. The polymer was finally collected and dried under high vacuum.

| Compound   | Amount   | Mol. wt. | mmol | Equivalent |
|--|----------|----------|------|------------|
| 2'2'-dibromo-9,9'-bisfluorenylidene<br>( <i>cis/trans</i> mixture) | 0.9727 g | 486      | 2.0  | 2.0        |
| Ni (COD) <sub>2</sub>  | 1.3      | 275.08   | 4.6  | 4.6        |
| 2,2' Bipyridyl   | 0.72     | 156.18   | 4.6  | 4.6        |
| COD  | 0.30     | 108.18   | 2.9  |            |

Solvents : 15 mL of toluene for monomer and 15 ml DMF + 45 ml toluene to dissolved Ni (COD)<sub>2</sub> / 2,2'- Bipyridyl

**<sup>1</sup>H NMR-spectrum (300 MHz, C<sub>2</sub>D<sub>2</sub>Cl<sub>4</sub>):**

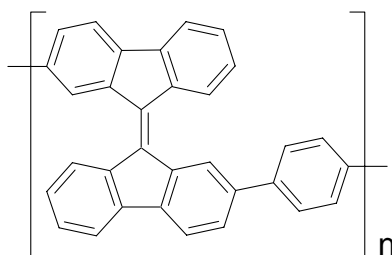
**δ(<sup>1</sup>H) [ppm]** : 8.48-8.12 (ar-H), 7.20-7.70 (ar-H)

**<sup>13</sup>C NMR spectrum (75 MHz, C<sub>2</sub>D<sub>2</sub>Cl<sub>4</sub>):**

**δ(<sup>13</sup>C) [ppm]** = 144.1, 143.2, 141.5, 141.7, 140.1, 135.7, 133.5, 126.4, 123.2, 121.1, 120.3, 120.2.

**GPC (toluene)** : M<sub>n</sub> = 4,600, M<sub>w</sub> = 11,000 gmol<sup>-1</sup>

**UV/ Vis (CHCl<sub>3</sub>)** : λ<sub>max, abs</sub>: 310, 460 nm

**4.2.22 Poly(1,4-phenylene-co-9,9'-bifluorenylidene-2,2'-diyl) 35****35**

In a dry flask a mixture of 2,2'-dibromo-9,9'-bisfluorenylidene as cis/trans isomeric mixture (1mmol) and the corresponding diboronic acid (1 mmol) in 15 mL of dry toluene was filled. 2 g of Na<sub>2</sub>SO<sub>4</sub> in 10 mL of water were added to the stirred reaction mixture. The flask was well evacuated and flushed with argon several times. 35-40 mg of the palladium catalyst [PdCl<sub>2</sub>(PPh<sub>3</sub>)<sub>2</sub>] and 6 mL of n-butanol were added in the absence of light. The reaction mixture was refluxed for 3-5 days under argon. The organic phase were separated and diluted with dichloromethane and washed three times with aqueous 2N HCl and water. The organic solution was finally dried over MgSO<sub>4</sub>. The solvent was evaporated to get a viscous oil. The polymer was precipitated into 1.5l of methanol (1 L) and acetone (0.5 L) using a Pasteur pipette. The polymer was finally collected and dried under high vacuum at ambient or elevated temperature.

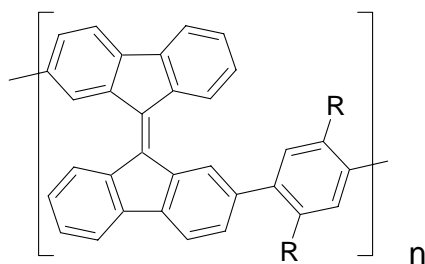
Yield- 380 mg (62%)

**<sup>1</sup>H NMR spectrum (300 MHz, C<sub>2</sub>D<sub>2</sub>Cl<sub>4</sub>):**

**δ(<sup>1</sup>H) [ppm] :** 8.05-7.35 ( ar-H)

**GPC (toluene) :** M<sub>n</sub> = 5,600 ; M<sub>w</sub> = 9,200 gmol<sup>-1</sup>

**UV/ Vis (CHCl<sub>3</sub>):** λ<sub>max, Abs</sub>: 290nm; 460nm

**4.2.23 Poly(2,5-dihexyl-1,4-phenylene-co-9,9'-bifluorenylidene-2,2'-diyl) 36****36**

R = Hexyl

In a dry flask was taken 2,2'-dibromo-9,9'-bisfluorenylidene as mixture of cis/trans isomers (1mmol) and the corresponding 2,5-dihexyl-1,4-bisboronic acid (1 mmol) in dry toluene were placed. 2 g of Na<sub>2</sub>SO<sub>4</sub> in 10 mL of water was added to the stirred reaction mixture, and then followed the procedure as for **36**

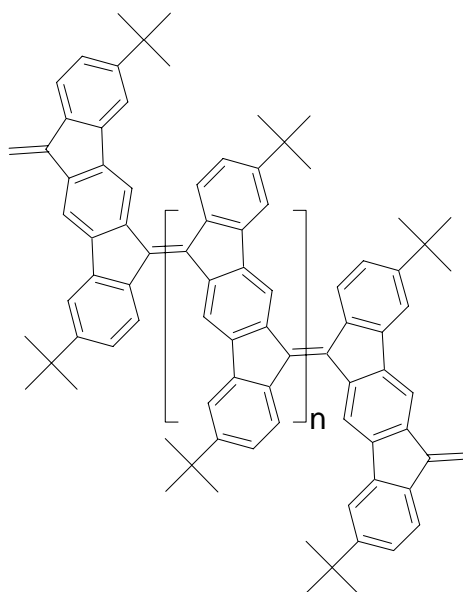
Yield- 410 mg (68 %)

**<sup>1</sup>H-NMR spectrum (300 MHz, C<sub>2</sub>D<sub>2</sub>Cl<sub>4</sub>):**

**δ(<sup>1</sup>H) [ppm] :** 8.05-7.35 (ar-H), 2.40-1.8 (α-CH<sub>2</sub>), 1.10-0.35 (alkyl chain)

**GPC (toluene) :** M<sub>n</sub> = 2,600; M<sub>w</sub> = 5,500 gmol<sup>-1</sup>

**UV/ Vis (CHCl<sub>3</sub>):** λ<sub>max, Abs</sub>: 290nm; 460nm

**4.2.24 Poly(3,9-di-*tert*-butylindeno[1,2-b]fluorene) 25****25**

3,9-Di-*tert*-butyl-6,6,12,12-tetrachloro-6,12-dihydro-indeno[1,2-b]fluorene **24** (560 mg, 1.13 mmol) was suspended in 30 ml of chlorobenzene. The resulting suspension was stirred under an argon atmosphere at 90°C. After it reached this temperature, the coupling reagent dicobalt octacarbonyl  $\text{Co}_2(\text{CO})_8$  (1.03 g, 3.0 mmol) was added in one portion. Formation of foam in 2-3 minutes indicate the onset of the reaction.

After 20 minutes the mixture was poured into 300 ml of methanol, the precipitate formed collected by filtration, washed carefully with methanol, water, 2N hydrochloric acid and again with methanol, until the filtrate was colorless. Remaining metal traces were removed by column filtration with thermally activated, neutral aluminium oxide (eluent: methylene chloride).

**$^1\text{H}$  NMR-spectrum (500 MHz,  $\text{C}_2\text{D}_2\text{Cl}_4$ ):**

$\delta(^1\text{H})$  [ppm] : 8.76 (bs, ar-H), 8.41 (ar-H), 7.28-7.20 (ar-H), 1.37-1.19 (- $\text{C}(\text{CH}_3)_3$ ).

**$^{13}\text{C}$  NMR-spectrum (125 MHz,  $\text{C}_2\text{D}_2\text{Cl}_4$ ):**

$\delta(^{13}\text{C})$  [ppm]: 152.4, 141.5, 140.2, 139.6, 136.4, 126.9, 124.7, 123.5, 118.6, 117.1, 35.3, 31.6.

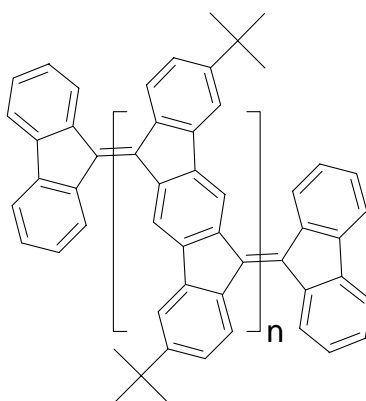
**FT-IR (KBr):** 3075, 2956, 2864, 1712, 1615, 1566, 1487, 1475, 1434, 1391, 1361, 1279, 1254, 1204, 1194, 1155, 1094, 914, 820, 643  $\text{cm}^{-1}$

**Elemental analysis :** found and (calculated) for  $(\text{C}_{28}\text{H}_{26})_n$  (362.5) $_n$ ; C: 90.75 (92.77) H: 6.97 (7.23) Cl: 0.37.

**GPC (toluene):**  $M_n$  : 17,000;  $M_w$  : 40,000  $\text{g mol}^{-1}$ ;

**UV / Vis ( $\text{CHCl}_3$ ):**  $\lambda_{\text{max, absop.}}$  = 309, 385, 731, 797 nm.

**4.2.25 Fluorenylene-end-capped poly(indeno[1,2-b]fluorene) PIF 27**



**27**

3,9-Di-tert-butyl-6,6,12,12-tetrachloro-6,12-dihydro-indeno[1,2-b]fluorene **24** (560 mg, 1.13 mmol) and 9,9'-dichlorofluorene (in different ratios) were suspended in 30 ml of chlorobenzene. The resulting suspension was stirred under an argon atmosphere at 90  $^{\circ}\text{C}$ . After it reached this temperature the coupling reagent dicobalt octacarbonyl  $\text{Co}_2(\text{CO})_8$  (1.03 g, 3.0 mmol) was added in one portion and then followed the procedure as for the synthesis of PIF **26**.

Yield: 400-600 mg (60-70%)

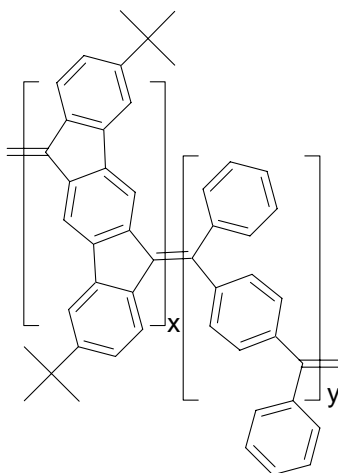
## 4. Experimental

**UV / Vis** ( $\text{CHCl}_3$ ):  $\lambda_{\text{max, Absop}} = 309, 385, 731, 797$ .

**GPC** (toluene):

| Amount of endcapper <b>26</b> | $M_n/M_w$ (GPC)<br>$\text{g mol}^{-1}$ |
|-------------------------------|--|
| 5 mol%                        | 5,800/10,100                           |
| 10 mol%                       | 2,900/7,400                            |
| 20 mol%                       | 1,900/5,300                            |
| 30 mol%                       | 1,500/2,700                            |
| 40 mol%                       | 1,000/2,000                            |

### 4.2.26 Statistical copolymers PIF/DP-PPV composed of indeno[1,2-b]fluorene and phenylene-diphenylvinylene units **30**



**30**

3,9-Di-tert-butyl-6,6,12,12-tetrachloro-6,12-dihydro-indeno[1,2-b]fluorene **24** (560 mg (1.13 mmol)) and DP-PPV (different ratio) was suspended in 30 ml of chlorobenzene. The resulting suspension was stirred under an argon atmosphere at 90 °C. After it reached this temperature, the coupling agent



#### 4. Experimental

---

dicobalt octacarbonyl  $\text{Co}_2(\text{CO})_8$  (1.03 g, 3.0 mmol) was added in one portion and then followed the same procedure as in the case of synthesis of PIF **25**.

Yield: 560-600 mg (60-70%)

**GPC** (toluene,  $M_n/M_w$ )/ **UV / Vis** ( $\text{CHCl}_3$ ,  $\lambda_{\text{max}}$ ) :

| Monomer <b>24</b> | Monomer <b>29</b> | $M_n/M_w$ (GPC)<br>$\text{g mol}^{-1}$ | UV / Vis<br>( $\text{CHCl}_3$ , $\lambda_{\text{max}}$ ) |
|-------------------|-------------------|--|--|
| 0                 | 100               | 9,000/18,000                           | 310 nm   |
| 20                | 80                | 5,000/11,000                           | 310 nm   |
| 30                | 70                | 4,000/8,500                            | 310, 520 nm  |
| 40                | 60                | 5,000/9,000                            | 320, 570 nm  |
| 50                | 50                | 8,000/16,000                           | 320, 610nm   |
| 60                | 40                | 4,000/9,000                            | 340, 660 nm  |
| 80                | 20                | 5,000/13,000                           | 350, 760 nm  |
| 100               | 0                 | 7,000/13,600                           | 790nm  |

## 5 Summary

The aim of the present work “*Tricycloquinazoline (TCQ) based electron deficient discotics and conjugated polymers with indenofluorene and bisfluorenylidene units*” was

- 1) *Introduction of chiral as well as achiral side chains into the tricycloquinazoline (TCQ) core to obtain soluble and processible TCQ derivatives,*
- 2) *To synthesize fluorenylene end-capped poly(indeno[1,2-b]fluorene) (PIF), and statistical copolymers with indeno[1,2-b]fluorene and 1,4-phenylene-diphenylvinylene units, and*
- 3) *To synthesize novel conjugated polymers with the bisfluorenylidene building block.*

The first goal was achieved by synthesizing achiral hexaalkoxytricycloquinazoline **17b** and chiral hexaalkoxytricycloquinazoline **17a(S)** using the procedure of *S. Kumar and coworkers* (1993). It involves six steps to reach the target molecules.

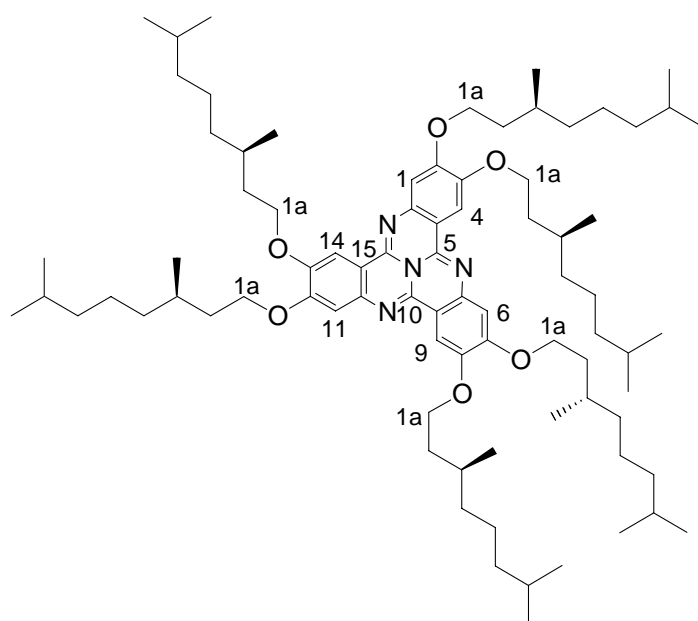


**Fig. 36:** Molecular structure of **17a (S)**

A strong circular dichroism (CD) signal was observed for the chiral hexaalkoxy TCQ **17a (S)** in a chloroform/methanol solvent/non-solvent mixture at

room temperature. It shows a strong bisignated CD signal between 250 and 325 nm, which indicates chiral coupling of chromophores in the columnar mesophase.

Phase transition temperature of chiral hexaalkoxy TCQ **17a(S)** was determined by differential scanning calorimetry (DSC) and optical microscopy. We have observed an second extra LC-LC transition both in the heating and cooling scan for **17a(S)** in contrast to the racemic **17b**. **17a(S)** showed a crystal to Col<sub>x</sub> transition at 118.1, Col<sub>x</sub> to Col<sub>h</sub> at 178.7°C and Col<sub>h</sub> to isotropic melt transition at 190.5°C. The additional transition Col<sub>x</sub> to Col<sub>h</sub> may be related to the occurrence of a columnar hexagonal LC phase of higher degree of order at lower temperatures.

Optical microscopy with crossed polarizer suggested that compound **17a(S)** forms hexagonal discotic mesophases. However additional information concerning the structure of the columnar mesophase came from X-ray scattering experiments. The overall feature observed is consistent with the structure of a Col<sub>h</sub> phase.

The second goal was to synthesize fluorenylene end-capped poly(indeno[1,2-b]fluorene) as novel low bandgap polyhydrocarbons. Statistical copolymers with indeno[1,2-b]fluorene and 1,4-phenylene-diphenylvinylene units (PIF/DP-PPV) were also synthesized and studied. These polymers were synthesized by using the procedure described by *Scherf and co-workers* in 1996. We have used 9,9-dichlorofluorene as an endcapping reagent in different molar ratios (from 5 to 40 mol%).

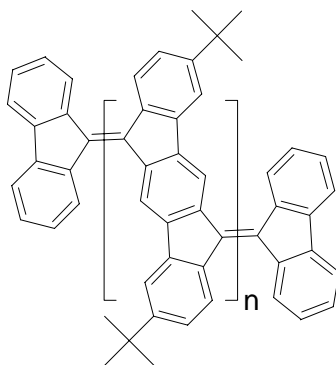


**Fig. 37:** Molecular structure of fluorenylene-end-capped PIF **27**

The aim behind synthesizing fluorenylene end-capped PIFs polymer was to increase the chemical stability and to get an exact molecular weight control it is also possible to to modify the optical and electronic properties. *Eduard Meijer* in the group of *Dr. de Leeuw* at Philips Research Laboratories has used poly(indeno[1,2-b]fluorene) (PIF) and fluorenylene-endcapped poly(indeno[1,2-b]fluorene) as a novel low bandgap organic semiconductor in solution processed ambipolar transistors and inverters (see chapter 3.3.5 for more details).

PIF/DP-PPV statistical copolymers have been also synthesized by the reductive coupling (polycondensation) of tetrachloro monomers (reaction scheme **14**, page 53). The UV/Vis absorption spectra indicate that the extension of the oligoindenofluorene segments is decreasing with increasing molar amount of diphenylvinylene building blocks.

The last topic was to synthesize novel wide bandgap conjugated polymers with the bisfluorenylidene unit. The bisfluorenylidene (BFD) can be easily reduced (n-type character). Several polymers with the BFD units were synthesized by *Yamamoto type aryl-aryl coupling* and *Suzuki-type cross coupling reactions*. UV/Vis absorption spectra of poly(9,9'-bisfluorenylidene-2,2'-diyl) **34**, poly(1,4-phenylene-co-9,9'-bisfluorenylidene-2,2'-diyl) **35**, and poly(2,5-dialkyl-1,4-phenylene-co-9,9'-bisfluorenylidene-2,2'-diyl) **36** showed the characteristic absorption feature of the 9,9'-bisfluorenylidene building block at a  $\lambda_{\max}$  of 460-470 nm.

The incorporation of the BFD unit into the conjugated main chain of **34-36** leads to a small, but significant red shift of  $\lambda_{\max}$  with respect to the monomeric BFD unit (ca. 460 nm).

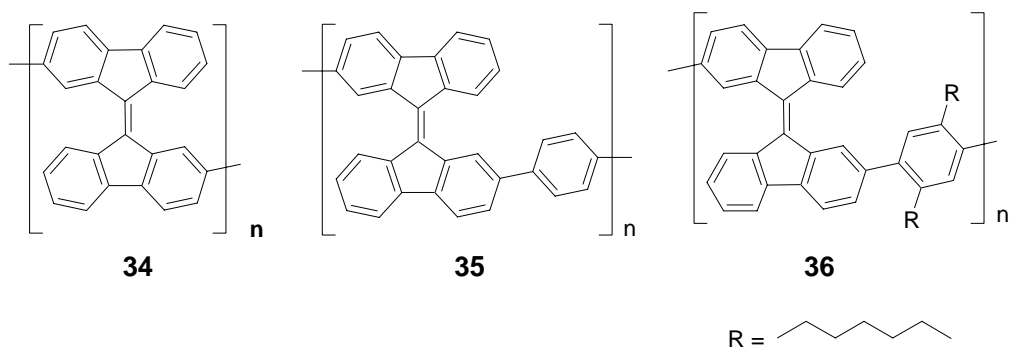
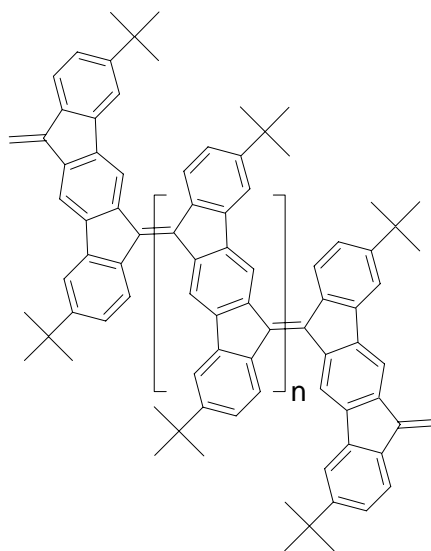


**Fig. 38:** Molecular structures of poly(9,9'-bisfluorenylidene-2,2'-diyl) **34**, poly(1,4-phenylene-co-9,9'-bisfluorenylidene-2,2'-diyl) **35**, and poly(2,5-dialkyl-1,4 phenylene-co-9,9'-bisfluorenylidene-2,2'-diyl) **36**

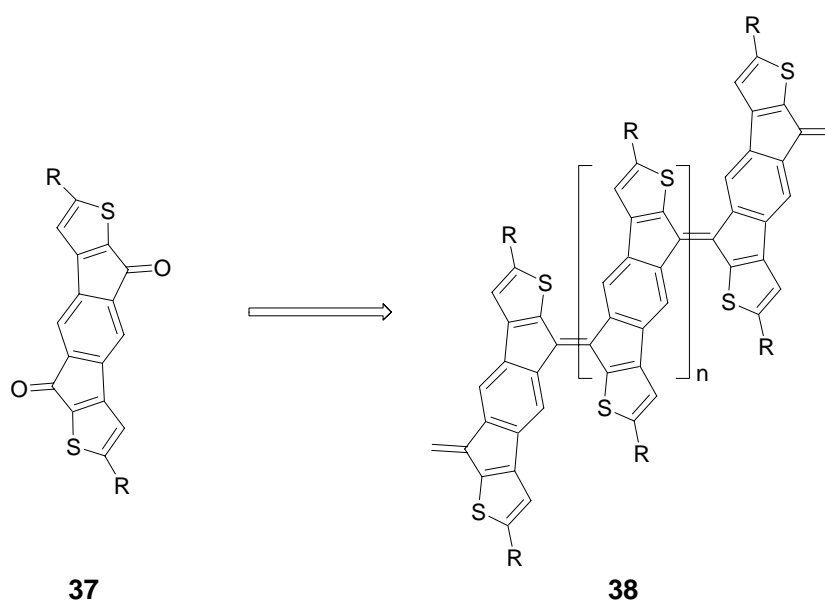
## 6 Future research

Poly(indeno[1,2-b]fluorene) PIF, due to its electron deficient nature can be easily reduced. This material can be therefore used as an ambipolar organic semiconductor in the field effect transistors <sup>[69]</sup>. Besides this, PIF will be also tested as an active component for photovoltaic investigations.



25

This opens the door for other related conjugated polymers with low bandgap energies. Based on the molecular structure of PIF **25** new heteroatomic polymers can be constructed, e.g. **37** and **38**



37

38

R = Alkyl

## 7 Literature

---

- [1] E. Becquerel, *Comptes Rendues* **1839**, 6, 561.
- [2] D. M. Chapin, C. S. Fuller, G. L. Pearson, *J. Appl. Phys.* **1954**, 25, 676.
- [3] J. Bardeen, W. H. Brattain, W. Shockley, *J. Chem. Phys.* **1946**, 14, 714.
- [4] W. H. Brattain, W. Shockley, *Phys. Rev.* **1947**, 72, 345.
- [5] W. Shockley, J. Bardeen, W. H. Brattain, *Science* **1948**, 108, 678.
- [6] M. J. Cohen, J. S. Harris, *IEEE Trans. Electron Devices* **1978**, 25, 1355.
- [7] M. J. Cohen, J. S. Harris, *Appl. Phys. Lett.* **1978**, 33, 812.
- [8] M. J. Cohen, *J. Electrochem. Soc.* **1980**, 127, C83.
- [9] H. Koezuka, A. Tsumura, *Synth. Met.* **1989**, 28, C753.
- [10] J. Paloheimo, E. Punkka, P. Kuivalainen, H. Stubb, P. Ylilahti, *Acta Polytech. Scand.-Electr. Eng. Ser.* **1989**, 178.
- [11] S. Chandrasekhar, S. K. Prasad, *Contemop. Phys.* **1999**, 40, 237.
- [12] A. N. Cammidge, R. J. Busby, in D. Demus, J. W. Goodby, G. W. Gray, H. W. Spiess, *Handbook of Liquid Crystals, Wiley-VCH, Weinheim*, **1998**, Vol.3.
- [13] C. F. van Nostrum, A. W. Bosman, G. H. Gelinck, P. G. Schouten, J. M. Warman, A. P. M. Kentgens, M. A. C. Devillers, A. Meijerink, S. J. Picken, U. Sohling, A. J. Schouten, R. J. M. Nolte, *Chem. Eur. J.* **1995**, 1, 171.
- [14] C. W. Struijk, A. B. Sieval, J. E. J. Dakhorst, M. van Dijk, P. Kimkes R. B. M. Koehorst, H. Donker, T. J. Schaafsma, S. J. Picken, A. M. van de Craats, J. M. Warman, H. Zuilhof, E. J. R. Sudholter, *J. Am. Chem. Soc.* **2000**, 122, 11057.
- [16] G. R. J. Müller, C. Meiners, V. Enkelmann, Y. Geerts, K. Müllen, *J. Mater. Chem.* **1998**, 8, 61.

- [17] A. M. van de Craats, J. M. Warman, P. Schlichting, U. Rohr, Y. Geerts, K. Müllen, *Synth. Met.* **1999**, *102*, 1550.
- [18] H. Eichhorn, *J. Porphy. Phthalc.* **2000**, *4*, 88.
- [19] C. S. Frampton, D. D. MacNicol, S. J. Rowan, *J. Mol. Struct.* **1997**, *405*, 169.
- [20] P. Henderson, H. Ringsdorf, P. Schuhmacher, *Liq. Cryst.* **1995**, *18*, 191.
- [21] O. C. Musgrave, C. J. Webster, *J. Chem. Soc. C* **1971**, 1397.
- [22] T. Yatabe, M. Harbison, J. D. Brand, M. Wagner, K. Müllen, P. Samori, J. P. Rabe, *J. Mater. Chem.* **2000**, *10*, 1519.
- [23] H. Bock, W. Helfrich, *Liq. Cryst.* **1995**, *18*, 387.
- [24] P. Uznanski, S. Marguet, D. Markovitsi, P. Schumacher, H. Ringsdorf, *Mol. Cryst. Liq. Cryst.* **1997**, *293*, 123.
- [25] A. M. van de Craats, J. M. Warman, M. P. de Haas, D. Adam, J. Simmerer, D. Haarer, P. Schuhmacher, *Adv. Mater.* **1996**, *8*, 823.
- [26] A. M. van de Craats, M. P. de Haas, J. M. Warman, *Synth. Met.* **1997**, *86*, 2125.
- [26] A. M. van de Craats, L. D. A. Siebbeles, I. Bleyl, D. Haarer, Y. A. Berlin, A. A. Zharikov, J. M. Warman, *J. Phys. Chem. B* **1998**, *102*, 9625.
- [27] I. C. Sage, in: D. Demus, J. Goodby, G. W. Gray, H.-W. Spiess, *Handbook of Liquid Crystals, Wiley-VCH, Weinheim* , **1998**, *Vol. 1*, Ch. IX
- [28] S. Chandrasekhar, *Liq. Cryst.* **1993**, *14*, 3.
- [29] S. Chandrasekhar S. Kumar, *Surface Sci. Spectra*, **1997**, *8*, 66.
- [30] S. Chandrasekhar, in D. Demus, J. Goodby, G.W. Gray, H.-W. Spiess *Handbook of Liquid Crystals, Wiley-VCH, Weinheim* **1998**, *Vol. 2B*, Ch. VIII; N. Boden and B. Movaghar, *ibid*, Ch IX.
- [31] R. W. Baldwin, K. Butler, F. C. Cooper, M. W. Partridge, *Nature* **1958**, *181*, 838.
- [32] S. C. Pakrashi, *J. Org. Chem.* **1971**, *36*, 642.



- [33] R. W. Baldwin, G. J. Cunningham, M. W. Partridge, *Br. J. Cancer* **1959**, *13*, 94.
- [34] R. W. Baldwin, G. J. Cunningham, M. W. Partridge, H. J. Vipond, *Br. J. Cancer* **1962**, *16*, 275.
- [35] R. W. Baldwin, H. C. Palmer, M. W. Partridge, *Br. J. Cancer* **1962**, *16*, 740;
- [36] R. W. Baldwin, G. J. Cunningham, A. T. Davey, M. W. Partridge, H. J. Vipond, *Br. J. Cancer* **1963**, *17*, 266.
- [37] R. W. Baldwin, G. J. Cunningham, H. G. Dean, M. W. Partridge, S. J. Surtees, H. J. Vipond, *Biochem. Pharmacol* **1965**, *14*, 323.
- [38] D. G. Bloomfield, M. W. Partridge, H. J. Vipond, *J. Chem. Soc. C* **1970**, 2647.
- [39] K. Butler, M. W. Partridge, *J. Chem. Soc.* **1959**, 2396.
- [40] E. Keinan, S. Kumar, S. P. Singh, R. Girlando, E. J. Wachtel, *Liq. Cryst.* **1993**, *11*, 157.
- [41] S. Kumar, E. J. Wachtel, E. Keinan, *J. Org. Chem.*, **1993**, *58*, 3821.
- [42] N. Boden, R. C. Borner, R. J. Bushby, J. Clements, *J. Am. Chem. Soc.* **1994**, *116*, 10807.
- [43] <http://liqcryst.chemie.uni-hamburg.de/>
- [44] Yoneda, F. Mera, A. *Chem. Pharm. Bull.* **1973**, *21*, 1610.
- [45] S. Kumar, D. S. S. Rao, *J. Mater. Chem.* **1999**, *9*, 2751.
- [46] N. Boden, R. C. Borner, R. J. Bushby, J. Clements, *J. Am. Chem. Soc.* **1994**, *116*, 10807.
- [47] K. Ohta, Y. Morizumi, H. Ema, T. Fujimoto, I. Yamamoto, *Mol. Cryst. Liq. Cryst.* **1991**, *208*, 55.
- [48] A. M. Levelut, *J. Chem. Phys.* **1983**, *80*, 149.
- [49] S. Kumar, E. J. Wachtel, *J. Org. Chem.* **1993**, *58*, 3821.
- [50] J. W. Goodby, *J. Mater. Chem.* **1991**, *1*, 307.

- [51] S. Kumar, *Mol. Cryst. Liq. Cryst.* **1996**, 289, 247.
- [52] B. M. Kraszovitskii in *Organic Luminescent Materials* VCH, Weinheim **1988**.
- [53] H. H. Hörhold, M. Helbig, D. Raabe, J. Opfermann, U. Scherf, R. Stockmann, *Z. Chem.* **1987**, 27, 126.
- [54] J. S. Lee, S. C. Nyburg, *Acta Cryst.* **1985**, C-41, 560.
- [55] H. Reisch, *Ph.D. Thesis, Johannes Gutenberg-Universität Mainz*, **2000**.
- [56] O. Kikuchi, K. Matsushita, K. Morihashi, M. Nakayama, *Bull. Chem. Soc. Jpn.* **1986**, 59, 3043.
- [57] A. Frünster, *J. Am. Chem. Soc.* **1995**, 117, 4468.
- [58] M. Miyaura, A. Suzuki, *Chem. Rev.* **1995**, 95, 2457.
- [59] U. Scherf, *Makromol. Chem. Rapid Commun.* **1993**, 14, 575.
- [60] G. Allen et al. *Comprehensive Polymer Science: The Synthesis Characterization, reaction & Applications of Polymers; Vol 1*, Pergamon Press: Oxford, **1989**.
- [61] B. K. Vainshtein et al. *Modern Crystallography 1: Fundamentals of Crystals, symmetry and methods of structural crystallography*, Springer-Verlag, Berlin, Germany **1994**.
- [62] K. Nakanishi, N. Bervo, *Circular Dichroism: Principles & Applications* VCH, New York, USA, **1994**.
- [63] H. Pasch, B. Trathing, *HPLC of Polymers*, Springer-Verlag Berlin, **1998**.
- [64] K. Khurana, *Ind. J. Chemistry.* **1987**, 27, 126.
- [65] H. G. Nothofer, *Ph. D Thesis, Department of Mathematics and Science, University of Potsdam*, **2001**.
- [66] M. Rehahn, A. Schlüter, W. J. Feast, *Synthesis* **1990**, 58, 127.
- [67] H. Finkelmann, *Angew. Chem.* **1987**, 99, 840; *Angew. Chem. Int. Ed. Engl.* **1987**, 26, 816.
- [68] M. Kumada, K. Tamato, *Org. Synt.* **1978**, 58, 127.

- [69] E. Meijer, D. M. de Leeuw, S. Setayesh, E. van Veenendaal, B. –H. Huisman, P. W. M. Blom, J. C. Hummelen, U. Scherf, J. Kadam, T. M. Klapwijk, *Nature Materials* **2003**, *12*, 834.
- [70] E. Peierls, *Quantum Theory of Solids*, Oxford University Press: London **1955**.
- [71] S Karabunarliev, M. Baumgarten, K Müllen, N. Tyutyulkov, *Chem. Phys.* **1994**, *179*, 421.
- [72] W. P. Schrieffer, A. J. Heeger, *Phy. Rev. Lett.* **1979**, *42*, 1698.
- [73] R. Pariser, R. Parr, *J. Chem Phys.* **1953**, *21*, 7676.
- [74] N. Mataga, K. Z. Nihimoto, *Phy. Chem.* **1957**, *13*, 140.
- [75] T. A. Skotheim, R. L. Elsenbaumer, J. R. Reynolds, *Handbook of Conducting Polymers*, Marcel Dekker, INC. New York **1998**, *2*, 277.
- [76] F. Wudl, M. Kobayashi, A. J. Heeger, *J. Org. Chem.* **1984**, *49*, 3382.
- [77] R. S. Mulliken, *J. Chem. Phys.* **1949**, *46*, 675.
- [78] K. Butler, M. W. Partridge, *J. Chem. Soc.* **1959**, 2396.
- [79] B. L. Feringa, R. A. van Delden, N. Koumura, E. M. Geertsema, *Chem. Rev.* **2000**, *100*, 1789.
- [80] J. H. Day, *Chem. Rev.* **1963**, *63*, 65.
- [81] J. Sandström, *Top. Stereochem.* (Eds: N. L. Allinger, E. L. Eliel, S. H. Wilen), Wiley, New York, **1983**, *14*, 83.
- [82] W. Luef, R. Keese, *Top. Stereochem.* **1991**, *20*, 231.
- [83] A. Z. -Q. Khan, J. Sandström, *J. Am. Chem. Soc.* **1988**, *110*, 4843.
- [84] E. J. Meijer, *Ph.D. Thesis, Technical University of Delft*, **2003**.
- [85] S. M. Sze, *Physics of semiconductor devices*, 2<sup>nd</sup> edition, John Wiley & Sons, New York, **1981**.
- [86] D. Monroe, *Phys. Rev. Lett.* **1985**, *54*, 146.
- [87] A. M. Echavarren, J. J. Gonzalez, N. Garcia, B. Gomez-Lor, *J. Org. Chem.* **1997**, *63*, 1286.

- [88] R. F. Heck, *Org. React.* **1982**, 27, 345.
- [89] A. J. Canty in *Comprehensive Organometallic Chemistry Vol. 9* (Hrsg.: E. W. Abel, F. G. A. Stone, G. Wilkinson) Pergamon Press Oxford **1995**.
- [90] T. I. Wallow, B. M. Novak, *J. Am. Chem. Soc.* **1991**, 113, 7411.
- [91] D. Lenoir, *Synthesis* **1989**, 883.
- [92] T. Mukaiyama, T. Sato, J. Hanna, *Chem. Lett.* **1973**, 1041.
- [93] M. Samoc, A. Samoc, B. Luther-Davis, H. Reisch, U. Scherf, *Optics Letters* **1998**, 23, 1295.
- [94] J. E. McMurry, *Chem. Rev.* **1989**, 89, 1513.
- [95] A. Fürstner, D. N. Jumbam, *Chem. Commun.* **1993**, 211.
- [96] A. Fürstner, A. Ernst, *Tetrahedron* **1995**, 51, 773.
- [97] E. J. Meijer, D. M. de Leeuw, S. Setayesh, E. van Veenendaal, P. W. M. Blom, J. C. Hummelen, T. M. Klapwijk, submitted.
- [99] A. Tsumura, H. Koezuka, T. Ando, *Synth. Met.* **1988**, 25, 11.
- [100] J. Badeen, W. H. Brattain, *Phys. Rev.* **1948**, 74, 230.
- [101] W. Shockley, *Bell Syst. Techn. J.* **1949**, 28, 435.
- [102] J. E. Lillienfield, U. S. Patent 1745175, **1930**.
- [103] D. Kahn, M. M. Atalla, *IRE Solid-State Device Research Conference*, Carnegie Institute of Technology, Pitsburg, Pa. **1960**.
- [104] D. F. Barbe, C. R. Westgate, *J. Phys. Chem. Solids* **1970**, 31, 2679.
- [105] H. Shirakawa, E. J. Louis, A. G. MacDiarmid, C. K. Chiang, A. Heeger, *J. Chem. Soc. Chem. Commun.* **1977**, 578.
- [106] F. Ebisawa, T. Kurokawa, S. Nara, *J. Appl. Phys.* **1983**, 54, 3255.
- [107] H. Koezuka, A. Tsumura, T. Ando, *Synth. Met.* **1987**, 18, 699.
- [108] C. Clarisse, M. T. Riou, M. Gauneau, M. Le Contellec, *Electron. Lett.* **1988**, 24, 674.

- [109] G. Horowitz, D. Fichou, X. Z. Peng, Z. G. Xu, F. Garnier, *Solid State Commun.* **1989**, 72, 381.
- [110] E. H. Rodherick, R. H. Williams, *Metal-Semiconductor Contacts*, Oxford University Press, New York **1988**.
- [111] M. Shur, *Physics of Semiconductor devices*, Prentice-Hall, Englewood Cliffs **1990**.
- [112] P. K. Weimer, *Proc. IRE* **1962**, 50, 1462.
- [113] M. -H. Whangbo, R. Hoffmann, R. B. Woodward, *Proc. Rou. Soc. Lond. A* **1979**, 366, 23.
- [114] J. L. Bredas, R.H. Baughman, *J. Polym. Sci., Polym. Lett. Ed.* **1983**, 21, 475.
- [115] G. Grem, G. Leditzky, B. Ullrich, G. Leising, *Synth. Met.* **1992**, 51, 383.
- [116] G. Grem, G. Leditzky, B. Ullrich, G. Leising, *Adv. Mater.* **1992**, 4, 36.
- [117] K. Yoshino, T. Takiguchi, S. Hayashi, D. H. Park, R. -I. Sugimoto, *Jpn. J. Appl. Phys.* **1986**, 25, 881.
- [118] J. Obruzut, F. E. Karasz, *J. Chem. Phys.* **1987**, 87, 2349.
- [119] M. -A. Sato, S. Tanaka, K. Kaeriyama, *Synth. Met.* **1986**, 14, 279.
- [120] T.C. Chung, J. H. Kaufman, A. J. Heeger, F. Wudl, *Phys. Rev. B* **1984**, 30, 702.
- [121] J. -L. Bredas, in *Handbook of Conducting Polymers* (T. A. Skotheim, ed.), Marcel dekker, New York, **1986**, Vol. 2, p. 859.
- [122] A. J. Heeger, in *Handbook of Conducting Polymers* (T. A. Skotheim, ed.), Marcel dekker, New York, **1986**, Vol. 2, p. 729.
- [123] J. H. Burroughes, R. H. Friend, in *Conjugated Polymers: The Novel Science and Tchenology of Highly Conducting and Nonlinear Optically Active Materials* (J. L. Bredas, R. Silbey, eds.), Kluwer Academic, Dordrecht, The Netherlands, **1991**, p. 555.
- [124] <http://austin.onu.edu/~jhurtig/2003webpages/dcac/inverter.htm>.

## 8 List of publications

---

1) "Solution-processed ambipolar organic field-effect transistor and inverters"  
E. J. Meijer, D.M. de Leeuw, S. Setayesh, E. van Veenendaal, B.-H. Huisman ,  
P.W.M. Blom, J.C. Hummelen, U. Scherf, **J. Kadam** & T. M. Klapwijk,

*Nature Materials* **2003**, 2, 12, 834

2) "Ultraviolet photoelectron spectroscopy on the discotic liquid crystal ethylhexyl tricycloquinazoline", S. Schrader, **J. Kadam**, U. Scherf, S. Katholy, J. Reiche, L. Brehmer

*HASY LAB Annual Report 2002*

3) "Induced liquid crystallinity in switchable side-chain discotic molecules"  
**Jitendra Kadam**, Charl FJ Faul, Ulli Scherf,

**Submitted to *Chem. Mater* Feb 2004**

4) "Polymerization in supercritical carbon dioxide: surfactants micelle formation and heterophase polymerization" W.Steffen, U.Scherf, **J. Kadam**, L. Berger, A. Schlewing"; *Supercrit BUCH, Elsevier* **2003**

5) "New chiral discotic liquid crystal: derivative of TCQ having chiral alkyl side chain"; **Jitendra Kadam**, Ullrich Scherf, Sigurd Schrader, *e-polymers* sep. **2002** (poster)

## 9 Curriculum Vitae

---

### JITENDRA S. KADAM

#### PERSONAL DETAILS

Date of birth : 09 July 1974

Place of Birth: Tasgaon, India

Nationality: Indian

Marital Status: Married

#### UNIVERSITY EDUCATION

10/02-01/04

Ph. D. Studies, Prof. Dr. Ullrich Scherf  
Bergische University Wuppertal

03/01-09/02

University of Potsdam

11/99-02/01

Max-Planck Institute for Polymer  
Chemistry, Mainz

#### Topic:

“Tricycloquinazoline (TCQ) based  
electron deficient discotics and  
conjugated polymers with  
indeno fluorene and bisfluorenylidene  
units”

04/98-09/99

Graduate Research Assistant (PA II),  
National Chemical Laboratory, Div. of  
Organic Chemistry, Pune, India

08/95-11/97

M. Sc., University of Pune, India

06/92-04/95

B. Sc., University of Pune, India

#### SCHOOL EDUCATION

06/89-03/92

Science, Pune Board  
Higher Secondary (School) Certificate

06/80-03/89

General, Pune Board  
Secondary School Certificate examination

## 10 Acknowledgement

---

It is indeed a great pleasure for me to pen down a few lines about people to whom my acknowledgements are due.

I acknowledge **Prof. Ullrich Scherf** with a deep sense of gratitude and my heart felt thanks for the encouragement, inspiring guidance and unfailing attention which he gave throughout my work.

I would like to express my thanks to **Michael Forster** for his neverending help and guidance right from the day I stepped in the group.

My thanks go to my colleagues and friends **Roland Güntner** and **Udom Asawapirom**. They contributed by making life more enjoyable at and away from the university. We always enjoyed having spicy food together.

**Bernhard Köhler** was of great help to me for discussions we had, **Christopher Schmitt** also for his help.

I would like to thank **Tony Farrell** for the discussions and helpful suggestions throughout.

I would like to thank my colleague **Satish Patil** for his help. We used to listen to Bollywood music and BBC Asian network while working in the lab or office.

**Askin Bilge** for always showing similarities between our cultures and the sweets made.

**Anke Helfer** and **Sylvia Adamczyk** for the G.P.C measurements. **Ingvid Zenke** for X-ray measurements.

I would like to thank our technicians **Sascha Prentzel**, **Daniel Krüger** and **Edward Preis**.

My thanks also go to **Torsten Bünnagel** for his help when I had some problems in my computer as he is a computer expert in the group, **Frank Galbrecht**, **Benjamin Nehls**, **Bernhard Neumann**.

My heartfelt thanks goes to our secretary **Bianca Enz**. She can make anyone smile with her pleasant nature and a smile on her face. She is the one who was responsible for creating a very good atmosphere in the group.

My thanks are due to **Angeliki Tasina** for her support and encouragement especially to learn German.

I would like to thank my **parents** and **sister** for their support and the interest shown for my research.

Finally, my heartfelt thanks go to my lifepartner, my wife **Swapna** for her patience and understanding during my Ph.D and her help in preparation of this manuscript. Without her support, this work would not have been possible.

Thanks are also due to all my colleagues, I have benefitted immensely from their criticism and encouragement. Apologies to anyone I may have forgotten.